TWO-DIMENSIONAL POTENTIAL FLOW AND BOUNDARY LAYER ANALYSIS OF THE AIRFOIL OF A STOL WING PROPULSION SYSTEM

Thesis for the Degree of Ph. D.

MICHIGAN STATE UNIVERSITY

JAMES ARTHUR ALBERS

1971

This is to certify that the

thesis entitled

TWO-DIMENSIONAL POTENTIAL FLOW AND
BOUNDARY LAYER ANALYSIS OF THE AIRFOIL
OF A STOL WING PROPULSION SYSTEM

presented by

JAMES ARTHUR ALBERS

has been accepted towards fulfillment
of the requirements for

Phd degree in Mech. Eng.

Merle C. Potter
Major professor

Date 5/11/71

TCP-142

ABSTRACT

TWO-DIMENSIONAL POTENTIAL FLOW AND
BOUNDARY LAYER ANALYSIS ON THE AIRFOIL
OF A STOL WING PROPULSION SYSTEM

By

James Arthur Albers

The analysis considers a two-dimensional wing-fan system which consists of an airfoil with flap; the fans which have a distributed suction at their inlet and a jet at their exit; and a jet sheet leaving the flap trailing edge. The solution provides the incompressible potential flow for variable fan or engine mass flow coefficient, the thrust coefficient for the propulsion system exhaust, and the wing and flap angle of attack. This includes the approximate location of the free exhaust jet. This potential flow solution is used as an input to the boundary layer analysis which calculates both laminar and turbulent incompressible boundary layer parameters. In particular, the separation point is determined on the airfoil of a blown flap wing propulsion system at various angles of attack.

The calculated pressure distributions for a particular externally blown flap configuration indicated that the minimum pressure point is near the leading edge (less than 2 percent of chord) of the airfoil with severe adverse pressure gradients at high angles of attack (near 20^{o}). The results of the boundary layer analysis indicated that the

predicted turbulent separation point moved forward from the trailing edge as the angle of attack was increased. Trailing edge separation for the thick wing ($t/c = 0.15$) propulsion system combination considered was verified by experimental data.

TWO-DIMENSIONAL POTENTIAL FLOW AND BOUNDARY LAYER ANALYSIS OF THE AIRFOIL OF A STOL WING PROPULSION SYSTEM

By

James Arthur Albers

A THESIS

Submitted to
Michigan State University
in partial fulfillment of the requirements
for the degree of

DOCTOR OF PHILOSOPHY

Department of Mechanical Engineering

1971

G70195

To my Mother and Father, Theresa, and J. J.

ACKNOWLEDGMENTS

The author wishes to thank his advisor, Dr. Merle C. Potter, for his guidance and assistance throughout this study. His active participation in the project and his willingness to discuss problems as they arose made working with him a rewarding experience. The author also wishes to thank the other members of his guidance committee for their time and interest in this study: Dr. Mahlon C. Smith, Dr. James V. Beck, and Dr. Norman L. Hills.

The author appreciates the assistance and guidance of Roger W. Luidens of NASA Lewis Research Center for his many constructive criticisms during the preparation of this dissertation. I would also like to acknowledge Newell D. Sanders of NASA Lewis Research Center for his continued support throughout the study.

The financial support of NASA Lewis Research Center's Training Office made the continuation of graduate study possible. I would like to give special thanks to Gertrude R. Collins of the NASA Training Office for her assistance throughout the program.

Special appreciation is extended to the author's wife, Theresa Ann, for her encouragement and understanding throughout the study.

TABLE OF CONTENTS

LIST OF FIGURES

SUMMARY

The analysis considers a two-dimensional combined wing and propulsion system which consists of a flapped airfoil with fans located under the wing. The exhaust jet of the fans impacts the flap and is deflected downward.

A numerical method is used which includes the effect of suction at the inlet of the propulsion system and treats the constant thickness exhaust jet as part of the solid body. This method includes the determination of the approximate exhaust jet location. The method provides the potential flow solution for any fan or engine mass flow coefficient, the thrust coefficient for the propulsion system exhaust, the flap deflection angle, and the wing angle of attack. Validity of the numerical solution for a case with suction (but with no jet) was indicated by application of the program to a two-dimensional inlet; excellent agreement was found with experimental results.

The potential flow program was used to obtain the pressure distribution, velocity field, and lift coefficient for a particular externally blown flap, high-lift configuration. The flow field for this configuration indicated high upwash angles (60° to 90°) at the propulsion system inlet and large jet penetrations at high angles of attack. A comparison of two-dimensional lift coefficients obtained by the method of this report with Spence's jet flap theory indicated that

the method of this report yielded lift coefficients that were an average of 10.5 and 12.1 percent higher in the 30° and 60° flap angles, respectively. A comparison of three-dimensional lift coefficients with experimental data for the blown flap indicated good agreement for the 30° flap, with the predicted lift coefficient an average of 11.4 percent higher than experimental data. Calculated pressure distributions showed severe adverse pressure gradients over a large portion of the wing at angles of attack of 20° or greater.

The surface velocity distribution obtained from the potential flow solution was used to determine the boundary layer growth and separation on the upper surface of the airfoil. The boundary layer solution was obtained by reduction of the partial differential equations of motion to a set of ordinary differential equations at each x-location using finite differences for the x derivatives. By an iterative solution to the differential equations, the boundary layer parameters for both laminar and turbulent flow were found. The results indicated that the predicted turbulent separation point moved forward from the trailing edge as the angle of attack is increased. Trailing edge separation for the thick wing ($t/c = 0.15$) propulsion system combination considered was verified by the experimental data.

INTRODUCTION

In recent years there has been much interest in short-takeoff-and-landing (STOL) aircraft for both civil and military applications. A STOL airplane must have the capability for both high lift at takeoff and low drag at cruise. Past experimental work (refs. 1 to 3) demonstrated that the jet flap concept was capable of producing high lift. The jet flap airfoil injects high velocity air over the flap surface from a slot located at the trailing edge of the airfoil, as shown in Figure 1(a). (The jet flap airfoil (Fig. 1(a)) is sometimes referred to as a "jet augmented flap" in the literature.) One way to implement the jet flap concept is to use an externally blown flap. This may be accomplished by using high-bypass-ratio turbofan engines which exhaust into the wing flap system.

A STOL concept under investigation at NASA Lewis Research Center is a multiple-fan externally blown flap (Fig. 1(b)). Important in this design concept is passing some of the fan exhaust through the gaps in the flaps to control the boundary layer over the wing upper surface. Some of the aerodynamic problems associated with this concept are (1) airfoil design for takeoff, cruise, and landing; (2) fan location and orientation; (3) penetration of propulsion system exhaust jet; (4) the slot location and amount of blowing which are necessary for satisfactory boundary layer control. An analytical tool is needed to do detailed design studies of these aerodynamic problems. This tool should have the capability to handle both potential flow and boundary layer flow.

The potential flow analysis is the first step in obtaining an analytical tool to design STOL wing propulsion systems. By shaping the airfoil geometry, the designer can modify the wing pressure distributions to delay separation. Fan location and orientation can be improved by analysis of the velocity and pressure distributions and the flow field obtained from the potential flow solution of the combined wing and propulsion system. A method to handle the slot location and the amount of blowing is discussed in reference 4. This problem is not included in this study. From the potential flow solution, we can determine the maximum attainable lift coefficient for the wing propulsion system. Using the surface velocity distribution as input to a boundary layer analysis, we can determine the separation point for a given engine-wing combination. The development of the potential flow solution was the first phase of this study.

There are many approximate potential flow theories. Some approximate methods for calculating flow over two-dimensional bodies are discussed in references 5 to 7. Most approximate methods assume, for simplification, that the body is slender or that the perturbation velocities caused by the body are small. Another type of approximate solution utilizes a distribution of singularities on or interior to the body surface. Some of the methods, based on a distribution of vorticity over the body surface are discussed in references 8 to 10. The potential flow theory that is often used when considering high-lift wing systems is that of Spence's jet flap theory as discussed in references 11 and 12. This thin airfoil theory considers the effect of a highly idealized jet sheet leaving the trailing edge of the flap, and does not take into account the effect of the propulsion system inlet and the thickness distribution of the lifting system.

The most general and comprehensive two-dimensional incompressible potential flow method and program is the Douglas method as reported in references 13 to 15. This method utilizes a distribution of sources and sinks on the body surface, and does not require bodies to be slender and perturbation velocities to be small. This method has the potential for dealing with distributed suction over part of the surface, and hence can handle the propulsion system inlet airflow. However, the program cannot handle problems for which the location of part of the boundary is unknown. For a combined wing and propulsion system, the shape and location of the jet exhaust of the fan or engine is not known a priori, hence, a method is developed to determine them.

The second phase of this report includes a study of the boundary layer growth and separation on the airfoil of the STOL wing propulsion system. During takeoff and landing the wing operates at high-lift coefficients with adverse pressure gradients over a large portion of the wing. This adverse pressure gradient may cause either laminar and/or turbulent separation. In general, the designer employs the various techniques at his disposal to avoid flow separation and to achieve the desired wing propulsion characteristics. Separation may be delayed by shaping the wing velocity distribution, by modification of airfoil geometry, by engine location and orientation, and with boundary layer control devices. By using the potential flow surface velocity distribution as input to the governing boundary layer equations, we may solve the boundary layer growth and separation characteristics on the airfoil of the wing propulsion system.

Techniques for solving the boundary layer equations can be divided up into two general solution methods. The first includes the explicit-integral methods which require a procedure for solving ordinary differential equations for "integral" properties of the boundary layer. Some of the more commonly used integral methods are discussed in references 16 and 17. A discussion of a computer program based on the above methods is given in reference 18. These integral methods applied to the analysis of two-dimensional airfoils are discussed in reference 19. Integral methods are widely used at the present time for predicting the behavior of both laminar and turbulent boundary layers, but are not applicable for the strong adverse pressure gradients that are encountered on STOL wing propulsion systems at high angles of attack.

The second method of solution of boundary layers is the finite difference methods which provide a procedure for solving the coupled partial differential equations of mass, momentum and energy. One accurate numerical procedure for solving partial differtial equations of the diffusion type was developed by Crank and Nicolson as discussed in reference 20. Numerical methods developed specially for hydrodynamic phenomena are given by Flügge-Lotz and Bradshaw et al. in references 21 and 22. The three finite difference boundary layer methods more commonly used are those of (1) Spalding and Patankar, (2) Cebeci and Smith, and (3) Mellor and Herring and are reported in references 23 to 26. Spalding and Patankar's compressible method obtains a finite-difference equation from the boundary layer partial differential equation by formulating each term in the partial differential equation as an integrated average over a small control volume. Both of the other two methods are incompressible and transform and linearize the partial differential equations by using finite differences for the x derivatives resulting in a series of ordinary differential equations. The ordinary differential equations are then integrated numerically across the boundary layer at each x-location.

Numerical methods, used to solve the partial differential equations for turbulent flow, require as input an empirically based expression for the turbulent effective viscosity. The effective viscosity hypothesis used by Spalding and Patankar is based upon the mixing-length hypothesis of Prandtl and utilizes a Couette-flow relationship for the region close to the wall. Reference 27 indicates that the pressure gradient produced systematic deviations in the predicted heat-transfer rate and that the mixing-length constants should depend on the pressure gradient. Then the mixing length should be increased for adverse and reduced for favorable pressure gradients. The method of Smith, et al., utilizes an eddy viscosity based on Prandtl's mixing-length theory in the inner region. In the outer region a constant eddy viscosity modified by an intermittency factor is used. Mellor and Herring in formulating their effective viscosity hypothesis divide the boundary layer in terms of an inner layer and outer layer and an overlap layer. The value of each region is based on experimental data and is uniquely determined by values of a pressure gradient parameter and displacement thickness Reynolds number. A more detailed discussion of this hypothesis is given in references 28 to 30.

The method of Mellor and Herring was chosen for the prediction method to be used to calculate both laminar and turbulent boundary layer growth because of its accuracy, physical soundness, and adaptability to the particular application problem. Their effective viscosity hypothesis should be applicable to high adverse pressure gradient flows. Also an incompressible boundary layer analysis is sufficient, since here, we are only interested in studying the takeoff and landing flow characteristics of the wing-propulsion system. This corresponds to a free stream Mach number of 0.12 or less.

The purpose of this report is to develop an analysis to solve the potential flow and boundary layer growth of a STOL wing propulsion system. The potential flow solution was obtained by extending the two-dimensional Douglas analysis and computer program to include the effect of suction at the propulsion system inlet, and by the development of a technique for determining the approximate location of the exhaust jet of the propulsion system. The potential analysis was used to obtain the flow field including the surface velocity and pressure distributions, and the lift coefficient. The surface velocity distribution was used to obtain the boundary layer growth and separation on the airfoil of a particular externally blown flap, high-lift configuration.

POTENTIAL FLOW ANALYSIS

Representation of the Wing Propulsion System

While the present development can be used for any two-dimensional configuration, it is helpful in describing the analysis to consider a particular physical system. The high-lift wing propulsion system for STOL applications under investigation at Lewis is a multiple-fan externally blown flap, as shown in Figure 2(a). The wind tunnel model is semispan with a NASA 4415 airfoil section, a 66 centimeter (26 in.) chord and a 165.1-centimeter (65-in.) span. The model has eight propulsion units spaced spanwise with the inlets under the wing and the exhausts ahead of a double slotted flap. The 30° and 60° flap deflections in Figure 1(b) represent typical takeoff and landing configurations.

Since the proposed STOL lifting system utilizes a large number of fans closely spaced spanwise on each wing, it is reasonable to approximate the actual flow with a two-dimensional flow. This approximation should be valid as long as there is a sufficient number of fans for blowing to be uniformly distributed along the wing trailing edge. The representation of the two-dimensional lifting system is shown in Figure 2(b). The equivalent body surface over which the potential flow is calculated consists of the airfoil with flap; the fans, which have a distributed suction at their inlet and a jet at their exit; and the jet sheet leaving the flap trailing edge.

The wing propulsion system combination is idealized by considering it to be one solid body with suction at the fan inlet. The jet stream, as it exits from the propulsion system is at a higher total pressure than the surrounding flow with free stream lines separating this jet from the remaining potential flow. In potential flow the total pressure is everywhere constant; hence, in this study the jet is considered to be part of the solid body. This assumes no mixing of the external free stream and the free jet. The equivalent two-dimensional propulsion system dimensions and jet sheet thickness were determined from the known mass flow rate and thrust of the Lewis propulsion system (Fig. 2(a)). The method used to determine the location of the free jet is discussed in the section, Location of Propulsion System Exhaust Jet.

The potential flow problem for a given wing propulsion system combination becomes one of calculating the velocities on and external to the body surface for any combination of the following variables: (1) free stream velocity V_∞, (2) fan or engine mass flow rate $\dot{m}$ per unit span (3) propulsion system thrust T per unit span, (4) flap angle θ, and (5) wing angle of attack α. The first three variables can be combined into two dimensionless parameters: the fan or engine mass flow coefficient $C_Q = \dot{m}/\rho V_\infty C$ and the thrust coefficient $C_T = T/(1/2\rho V_\infty^2 C)$. The development of the theory to handle this calculation is discussed in the following sections. All symbols used for the potential flow analysis are defined in appendix A.

Basic Equations and Boundary Conditions

The basic potential flow equation is obtained from the incompressible continuity equation together with the condition of irrotationality which gives Laplace's equation

$$\frac{\partial^2\phi}{\partial x^2} + \frac{\partial^2\phi}{\partial y^2} = 0 \tag{1}$$

where ϕ is the velocity potential due to the presence of the body only. To ensure uniqueness of the solution, the regularity condition at infinity is specified as

$$|\nabla\phi|_{\infty} \to 0 \tag{2}$$

The velocity field $\vec{V}$ can be expressed as the sum of the two velocities

$$\vec{V} = \vec{V}_{\infty} + \vec{v} \tag{3}$$

where $\vec{V}_{\infty}$ is the free stream velocity and $\vec{v}$ is the disturbance velocity due to the presence of the body only.

A general method of solving the potential flow for an arbitrary boundary is to use a large number of sources and sinks distributed on the surface of the body. This is the method presented in this report. The boundary condition, illustrated in Figure 3, specifies that the entire normal component of velocity of the fluid at any point p on the surface must be equal to the prescribed normal velocity on the surface. The contribution supplied by the source-sink distribution is $\vec{v}\cdot\vec{n}$ and that supplied by the free stream velocity is $\vec{V}_{\infty}\cdot\vec{n}$. The prescribed normal velocity V_N on the surface is due to suction or blowing. Thus, the boundary condition becomes

$$\vec{V}_\infty \cdot \vec{n}\Big|_P - \vec{v}\cdot\vec{n}\Big|_P = V_N \tag{4}$$

Since $\vec{v}\cdot\vec{n} = \partial\phi/\partial n$, the boundary condition on ϕ is

$$\frac{\partial\phi}{\partial n}\Big|_P = \vec{V}_\infty \cdot \vec{n}\Big|_P - V_N \tag{5}$$

Equations (1), (2), and (5) form the classic Neumann problem of potential theory which is the basic problem we wish to solve. The direct problem as just defined, can be solved exactly by conformal transformation only for a limited class of boundary surfaces. By using a large number of sources and sinks distributed on the surface of the body, the boundary condition can be formulated into an integral equation.

Formulation of the Boundary Condition as an Integral Equation

A simple potential function which satisfies equation (1) is the potential due to a point source. The potential at a point P due to source at q is expressed as

$$d\phi(P) = \frac{\sigma(q)\,dS}{r(P,q)} \tag{6}$$

where $\sigma(q)$ is the local intensity per unit area of the source and $r(P,q)$ is the distance between P and q. Since Laplace's equation is linear, the combined potential due to a distribution of sources is also a solution. By considering a continuous source distribution on the surface S, the potential at point P due to the entire body becomes

$$\phi(P) = \int_S \frac{\sigma(q)}{r(P,q)}\,dS \tag{7}$$

The potential as thus given satisfies equations (1) and (2), but it must also satisfy the boundary condition as given by equation (5). Applying the boundary condition requires evaluating the derivative $\partial\phi/\partial n$ at point p on the boundary surface. The derivative of $1/r(p,q)$ becomes singular at p when p and q coincide so that the principal value of the integral must be extracted. The principal value, according to reference 31, is $-2\pi\sigma(p)$. This is the contribution to the normal velocity at p from the source at p. The contribution of the remainder of the sources to the normal velocity is given by the derivative of the integral of equation (7) evaluated on the boundary. The normal derivative of ϕ becomes

$$\left.\frac{\partial\phi}{\partial n}\right|_p = -\,2\pi\sigma(p) + \int_S \frac{\partial}{\partial n}\left[\frac{1}{r(p,q)}\right]\sigma(q)\;dS \tag{8}$$

Applying the condition of equation (5) to equation (8) results in the integral equation for the source-intensity distribution $\sigma(p)$

$$2\pi\sigma(p) - \int_S \frac{\partial}{\partial n}\left(\frac{1}{r(p,q)}\right)\sigma(q)\;dS = -\vec{V}_\infty\cdot\vec{n} + V_N \tag{9}$$

This equation is a Fredholm integral equation of the second kind whose solution is the central problem of the analysis.

The quantity $-\partial/\partial n[1/r(p,q)]$ is called the kernel of the integral equation and depends only on the geometry of the surface. The first term of equation (9) is the normal velocity induced at p by a source at p. The second term is the combined effect of the sources at other points q on the surface of the body. The specific boundary conditions determine the right-hand side of equation (9). The first term on the right is the normal component of the free-stream velocity at p. The second term on the right is the prescribed normal velocity on the boundary surface at p. The solution of this Fredholm integral equation then requires determining the unknown function σ on the body surface.

Solution of Integral Equation

Since the boundary of the wing propulsion system is completely arbitrary, the integration of equation (9) with respect to S should be done numerically. The boundary is approximated by a large number of surface elements whose characteristic lengths are small compared to the body. It is assumed that the surface element is a flat segment as shown in Figure 4. As the number of elements increase, the assumed model approaches the shape of the body. The value of the source intensity is assumed to be constant over each surface element. By assuming this constant intensity over each element, the problem becomes one of finding a finite number of values of σ, one for each of the surface elements. This gives a number of linear equations equal to the number of unknown values of σ. On each element a control point (the midpoint of the element) is selected where equation (8) is required to hold. Rewriting equation (8) in summation form yields

$$\left.\frac{\partial \phi}{\partial n}\right|_p = -2\pi\sigma(p) + \sum_{p \neq q} \frac{\partial}{\partial n}\left[\frac{1}{r(p,q)}\right] \sigma(q)\ \Delta S \tag{10}$$

The right side of equation (10) now becomes a matrix consisting of the normal velocities induced by a source of intensity σ at the control point of all elements. The normal velocity at the control point of the i^{th} element due to all surface elements is denoted as

$$\left.\frac{\partial\phi}{\partial n}\right|_i = A_{ii}\sigma_i + \sum_{\substack{j=1 \\ j\neq i}}^{N} A_{ij}\sigma_j = \sum_{j=1}^{N} A_{ij}\sigma_j \qquad (11)$$

Thus

$$A_{ij} = \frac{\partial}{\partial n}\left[\frac{1}{r(p,q)}\right]\Delta S$$

where i corresponds to p and j corresponds to q.

The source densities of all the surface elements must be determined in such a way that the normal velocity condition is satisfied at all control points. This results in

$$\sum_{j=1}^{N} A_{ij}\sigma_j = -\vec{V}_\infty\cdot\vec{n}_i + V_{N,i} \qquad (12)$$

This set of linear algebraic equations is an approximation to the integral equation (9). Both $\vec{V}_\infty\cdot\vec{n}$ and the prescribed normal velocity V_N, in general, vary over the body surface. The linear equations are solved by a procedure of successive orthogonalization, as discussed in reference 32. Once the linear equations have been solved, flow velocities may be calculated for points on and off the body surface (see appendix B). The method just described is used to obtain the basic solutions of potential flow.

Basic Solutions

The superposition of any solutions to the integral equation (9) is also a solution since Laplace's equation is linear. Hence, the flow about a body may be thought of as a linear combination of four basic flows illustrated in Figure 5:

(1) Uniform flow at zero angle of attack

(2) Uniform flow at 90° angle of attack

(3) Vortex flow

(4) Flow due to suction or blowing

The uniform flow solutions are solutions due to free stream velocity (rectilinear flow) past the body surface at 0° and 90°, respectively. For these basic solutions, the boundary condition of zero normal velocity on the surface must be satisfied. Then the prescribed velocity normal to the surface must be zero for the basic uniform flow solutions. From equation (5) the boundary condition becomes

$$\left.\frac{\partial \phi}{\partial n}\right|_p = \left.\vec{V}_\infty \cdot \vec{n}\right|_p \tag{13}$$

The solution for the body at any angle of attack may be obtained by a linear combination of the 0° and 90° uniform flow solutions.

For a lifting body the circulation is obtained by placing a vortex at any convenient location within the body. The boundary condition of zero normal velocity on the surface still applies (eq. (5)) except that now $\vec{V}_\infty$ is replaced by the vortex velocity at any point. If $\vec{V}_v$ represents the velocity at any point p on the body caused by the vortex, the boundary condition for the basic vortex solution becomes

$$\left.\frac{\partial\phi}{\partial n}\right|_p = \vec{V}_v \cdot \vec{n}\Big|_p \tag{14}$$

The suction flow solution is obtained by specifying a prescribed normal velocity V_N at the fan face with a zero free stream velocity. This gives the desired mass flow rate for the inlet of the propulsion system. From equation (5) the boundary condition for the basic suction velocity solution becomes

$$\left.\frac{\partial\phi}{\partial n}\right|_p = -V_N \tag{15}$$

For each basic solution, the velocities on the body surface and at prescribed locations in the flow field may be obtained. From the basic solutions the total combined solution may be obtained.

Combination Solution

The total velocity tangent to the body surface can be obtained by adding the tangential velocities of the four basic solutions.

$$V_t = V_{t,0}\cos\alpha + V_{t,90}\sin\alpha + \Gamma\, V_{t,v} + V_{t,s} \tag{16}$$

where α is the angle of attack.

The nondimensional circulation Γ is determined by satisfying the Kutta condition at the trailing edge of the body. This condition stipulates that the flow at the body trailing edge be smooth. Thus, the tangential velocities above and below the trailing edge must be equal in magnitude. If ΔV is defined as $\Delta V = V_{upper} - V_{lower}$, the Kutta condition is satisfied if $\Delta V = 0$ at the body trailing edge. Then from equation (16)

$$\Delta V_{t,0} \cos \alpha + \Delta V_{t,90} \sin \alpha + \Delta V_{t,s} + \Gamma \, \Delta V_{t,v} = 0 \tag{17}$$

Solving for Γ yields

$$\Gamma = - \frac{\Delta V_{t,0} \cos \alpha + \Delta V_{t,90} \sin \alpha + \Delta V_{t,s}}{\Delta V_{t,v}} \tag{18}$$

Once the combined velocities on the body surface are known, the pressure coefficient, the lift coefficient, and the thrust coefficient can be obtained (see appendix C).

For off-body points it is more convenient to combine the basic source intensities rather than the basic velocities. The equation for the combined source intensity is

$$\sigma = \sigma_0 \cos \alpha + \sigma_{90} \sin \alpha + \Gamma \, \sigma_v + \sigma_s \tag{19}$$

Then, the x and y components of velocity are calculated from the combined source intensities (see appendix B). This approach is the same as that used in reference 15, with the addition of the basic suction source intensity being added to the other basic source intensities.

Location of Propulsion System Exhaust Jet

The location of the propulsion system exhaust jet is determined by the following variables: (1) jet angle θ at flap trailing edge, (2) jet penetration H, (3) jet angle θ_1 at trailing edge of jet and (4) total length of the free jet L_T. The representation of these variables is shown in Figure 2(b). It was assumed that the free jet leaves the flap trailing edge at the flap angle θ. The flap angle is defined as the angle between the free stream direction and lower flap surface. After the jet leaves the trailing edge, the free stream velocity turns the jet, which approaches a horizontal asymptote several chord lengths beyond the airfoil leading edge. For typical thrust coefficients C_T corresponding to takeoff and landing conditions, this occurs at approximately four chord lengths from the airfoil leading edge (see ref. 10).

For a reasonable approximation to the jet shape, the lift coefficient is expected to depend principally on the vertical location of the jet asymptote. The problem then becomes one of finding the jet penetration H as shown in Figure 2(b). Initially, the penetration was assumed and a cubic equation used to approximate the shape of the jet sheet. (A cubic equation is the simplest expression that adequately approximates the jet shapes obtained from Spence's jet flap theory of ref. 12.) The correct distance H is that value for which the vertical component of thrust at the flap trailing edge balances the integrated vertical pressure forces on the free jet. Several values of H were assumed until the correct value of H was obtained.

Since the angle of the free jet is not exactly horizontal several chord lengths beyond the wing, a small angle θ_1 (5^o or less) was assumed. The length of the jet L_T was extended until the vertical component of force on the end of the jet (last 5 percent of the jet) was negligible for the chosen angle θ_1. Thus, if the jet is extended beyond this length, it gives no significant contribution to the lift coefficient. Neglecting the vertical component of thrust at the end of the jet for an angle of 5° results in only a 3 percent variation in lift coefficient. Since the body was represented by the wing, flap, and jet, it was assumed to be closed at the jet trailing edge and the Kutta condition applied here.

Potential Flow Computer Program

A general description of the potential flow computer program along with the imputs and outputs of the program is given in appendix D. This appendix also includes a complete program listing.

DISCUSSION AND RESULTS OF POTENTIAL FLOW ANALYSIS

Validity of Analysis

Inlet air suction

To help ensure validity of the analysis, comparisons were made with known existing flow solutions. One existing solution solves the suction problem indirectly. It is also based on the Douglas method, but has application only to inlets and ducts (see ref. 33). This method utilizes three basic solutions, shown in Figure 6, to obtain a combined solution of physical interest. The flow about the inlet is obtained by considering the three basic solutions; $\vec{V}_1$ with inlet duct extension closed, $\vec{V}_2$ with the duct open, and $\vec{V}_3$ the crossflow solution. With these three solutions any combination of free-stream velocity and mass flow through the inlet can be obtained. The duct must be extended far downstream of the region of interest to obtain valid solutions. This method could not be used to get solutions for a wing-engine combination since the body must be closed to consider it a lifting body. To make a comparison between this existing flow solution and the method presented in this report a two-dimensional inlet, shown in Figure 7, was considered. This inlet was chosen because experimental data were available. In the present analysis, mass flow through the inlet was obtained by considering a distributed suction V_N downstream of the inlet (see Fig. 7). Comparison of the nondimensional surface velocities for the two methods are shown in Figures 8(a) and (b). Also shown is experimental data obtained from reference 34. The reference velocity V_{ref} was arbitrarily selected as the average velocity at an x/L of 0.89. Agreement between the two predictions is excellent for both the surface and centerline velocities. Comparison of experimental data with the prediction is quite acceptable for the centerline velocities. There is a slight variation between the experimental and predicted surface velocities. One reason for this variation could be boundary layer effects. The preceding discussion indicates that the combined uniform flow and suction solution is valid.

Exhaust jet shape

For a valid solution of a wing propulsion system there must be a reasonable approximation to the jet shape. The lift coefficients and pressure distributions for a given thrust coefficient depend principally on the flap angle θ and jet penetration H, as outlined in the analysis section, and not on the precise local shape of the jet. This is illustrated in Figure 9, which considers various free jet shapes for a 30° flap. For clarity the jet thickness is not shown. The assumed cubic equation is shown, along with representative upper and lower bounds for the jet shape. For the jet shapes A and C shown, the solution results in only a ±2.5 percent variation in lift coefficient from the assumed cubic shape B. This percent variation is distributed over the entire wing surface, as illustrated by the pressure distributions in Figure 9(b). Figure 9(b) shows only a 3 percent variation in pressure distribution for the jet shapes considered. Thus, the lift coefficients and pressure distributions depend principally on the flap angle and jet penetration and not on the precise local shape of the jet for the present configuration.

As a point of interest, a comparison of the jet shape based on the Spence's theory of reference 12 was made with the jet shape obtained from the present method. Spence of reference 12 assumes that all flow deflections from the free stream are not large and uses vortex distributions that are placed on the x-axis rather than on the airfoil or jet. Thus, a comparison could only be made for relatively small flap deflections (30° or less). A comparison of the nondimensional jet shape predicted from Spence's theory and from the method of this report is shown in Figure 10 for a 30° flap deflection and a thrust coefficient of 3. The basic shapes of the two cases are the same close to the wing. The jet penetration of the present method is larger than Spence's theory at the greater distances, as would be expected. The present method, besides not assuming small angle approximations, includes the wing thickness and camber effect which would increase the lift coefficient and would also result in a greater penetration.

Example Applications

Flow field

Potential flow solutions are adequate representations of the flow around bodies if the surface boundary layers are thin and remain attached. It is assumed that the final design of a high-lift wing propulsion system will be one in which boundary layer separation is prevented at relatively high angles of attack and flap settings. Representative flow fields for an externally blown flap high-lift configuration are shown in Figures 11(a) to (c). The flow fields were obtained by sketching streamlines tangent to the calculated velocity vectors at various points in the flow. The wing propulsion system is shown, along with the shape of the jet exhaust of the propulsion system. For the conditions shown, the upwash angles at the propulsion system inlet are quite large, varying from 60° to 90° depending on flap angles and wing angles of attack. Two stagnation points occur on the lifting body. One occurs ahead of the inlet below the leading edge of the wing, and the other occurs downstream of the inlet on the under surface of the fan. Both stagnation points move further aft as the flap angle and the wing angle are increased. By observation of the flow fields it is seen that the under surface of the wing is in a relatively stagnant region. The jet penetration increases with angle of attack (Figs. 11(a) and (b)). For a flap angle of 60° (Fig. 11(c)) the jet penetration distance is approximately three chord lengths at five chord lengths beyond the wing leading edge. This jet penetration is also important when considering the effect of the ground on lift coefficient.

<u>Pressure distribution</u>

The predicted pressures on the surface of the airfoil are valid only if the boundary layer is very thin and attached to the surface. The potential flow pressure distributions can be used both to calculate the boundary layer growth on the surface of the airfoil and as a design aid for the combined wing and propulsion system. Pressure distributions on the wing upper surface with a 30° blown flap at various angles of attack are presented in Figure 12. The incompressible pressure coefficient, corresponding to the minimum pressure point, ranges from -7.5 to -51 for the 0° and 20° angle of attack, respectively. These extremely high negative pressure coefficients correspond to the very high lift coefficients which are discussed in the following section. The minimum pressure point for all angles of attack occurs very near the leading edge of the airfoil, and severe adverse pressure gradients over a large portion of the wing result at the higher angles of attack. The stagnation point moves further under the leading edge as angle of attack increases, resulting in high velocity gradients about the leading edge.

To illustrate the effect of the inlet airflow of the propulsion system and the effect of the exhaust jet a comparison was made of the pressure distributions for (1) the wing alone, (2) the wing with jet but without inlet air suction, and (3) the wing with inlet air suction and jet. This comparison is presented in Figure 13 for a 30° flap. At the minimum pressure point for the wing alone there exists a pressure coefficient of -4.8 near the wing leading edge, followed by a mild adverse pressure gradient. The wing with jet but without inlet air suction would be representative of a jet flap airfoil shown in Figure 1(a). Jet flap theory does not include the effect of the inlet airflow of the propulsion system. For the wing with jet (without suction) the pressure coefficient is about -18 at the minimum pressure point, and there is a severe adverse pressure gradient over a large portion of the wing upper surface. When the effect of the suction at the propulsion system inlet is included, the magnitude of the pressures is reduced considerably over the wing upper surface, resulting in a minimum pressure coefficient of -7.6, followed by a much milder adverse pressure gradient. It may appear from the upper surface pressure distributions of Figure 13 that the lift with the jet alone is much larger than the lift associated with the jet with suction; but this is not the case if both upper and lower surfaces of the airfoil are considered. The change in pressure distribution between the zero suction case and the suction case is a result of a shift in the stagnation point ($C_p = 1.0$) on the under surface of the wing. For the wing, without suction, one stagnation point occurs just ahead of the inlet of the propulsion system. For the wing with suction this stagnation point moves closer to the wing leading edge and another stagnation point occurs on the under surface of the fan (see Fig. 11(a)). The corresponding shift in the pressure distributions on both the upper and lower surfaces presented in Figure 13 results in less than 5 percent decrease in lift when the effect of inlet suction is included for the selected inlet location. The preceding discussion indicates that the effect of suction resulting from a fan or inlet installed under the wing affects the pressure distribution on the wing upper surface favorably, with only a small effect on total lift coefficient.

Lift coefficients

In order to further indicate the applicability of the present analysis a comparison (Fig. 14) was made between Spence's theory (ref. 12) and the method of this report for two-dimensional lift coefficients for the blown flap configuration (Fig. 1(b)). The lift coefficients predicted by the method of this report for the 30° flap range from 6.5 to 13, while those for the 60° flap range from 15 to 21. The lift coefficients predicted by the present method generally range from 9.1 to 12 percent and from 10.6 to 13.6 percent higher than Spence's theory for the 30° and 60° flap, respectively. This difference exists since Spence's theory does not take into account the effects of the thickness and camber of the wing. The suction effect decreases the lift by approximately 5 percent, as discussed previously. The thickness and camber effect corresponds to approximately 15 percent increase in lift coefficient.

The two-dimensional lift coefficients were used to determine three-dimensional lift coefficients to compare with experimental data of a semispan blown flap model (Fig. 2(a)). The three-dimensional lift coefficient is

$$C_L = fC_l \tag{20}$$

where f is a function of aspect ratio and thrust coefficient (assuming an elliptical lift distribution) and was obtained from reference 35 as

$$f = \frac{AR + \frac{2C_T}{\pi}}{AR + 2 + 0.604(C_T)^{1/2} + 0.87C_T} \tag{21}$$

Calculated three-dimensional lift coefficients along with experimental data obtained from the Lewis test program are presented in Figure 15. The aspect ratio was 5 for the blown flap model. The theoretical lift coefficients range from 4 to 7.5 and from 9 to 13 for the 30° and 60° flap, respectively. There is good agreement between theory and experiment for the 30° flap case, with theory ranging from 10.8 to 12 percent higher than the experimental data. The lift coefficients for the 60° flap range from 28.6 to 28.4 percent greater than the data. The calculated lift coefficient is the maximum attainable lift coefficient for each configuration corresponding to complete boundary layer control and negligible viscous effects. This may indicate that the 60° flap configuration did not have optimum boundary layer control and that improvements could be made in obtaining better experimental coefficients.

BOUNDARY LAYER ANALYSIS

Basic Equations of Motion

Consider the motion of a viscous incompressible fluid along a curved two-dimensional surface. Let x represent the distance measured along the surface of the airfoil from the stagnation point and y represent the distance normal to the airfoil surface, as shown in Figure 16. The time average velocity components in the x and y directions are designated at $\bar{u}$ and $\bar{v}$, respectively. The curvature of the surface is denoted by K, which is a continuous function of x. (All symbols used for the boundary layer analysis are defined in appendix E.) For steady turbulent motion, the Navier-Stokes equations may be written (see ref. 36) as:

$$\frac{1}{1 + Ky} \bar{u} \frac{\partial \bar{u}}{\partial x} + \bar{v} \frac{\partial \bar{u}}{\partial y} + \frac{K\bar{u}\bar{v}}{1 + Ky} = - \frac{1}{\rho(1 + Ky)} \frac{\partial \bar{p}}{\partial x} + \nu_e \left[\frac{1}{(1 + Ky)^2} \frac{\partial^2 \bar{u}}{\partial x^2} + \frac{\partial^2 \bar{u}}{\partial y^2} \right.$$

$$\left. - \frac{y}{(1 + Ky)^3} \frac{\partial K}{\partial x} \frac{\partial \bar{u}}{\partial x} + \frac{K}{1 + Ky} \frac{\partial \bar{u}}{\partial y} - \frac{K^2 \bar{u}}{(1 + Ky)^2} + \frac{2K}{(1 + Ky)^2} \frac{\partial \bar{v}}{\partial x} + \frac{\bar{v}}{(1 + Ky)^3} \frac{\partial K}{\partial x} \right] \tag{22a}$$

$$\frac{1}{1+Ky}\,\overline{u}\,\frac{\partial \overline{v}}{\partial x} + \overline{v}\,\frac{\partial \overline{v}}{\partial y} - \frac{K\overline{u}^2}{1+Ky} = -\frac{1}{\rho}\frac{\partial \overline{p}}{\partial y} + \nu_e\left[\frac{1}{(1+Ky)^2}\frac{\partial^2 \overline{v}}{\partial x^2} + \frac{\partial^2 \overline{v}}{\partial y^2}\right.$$

$$\left. - \frac{y}{(1+Ky)^3}\frac{\partial K}{\partial x}\frac{\partial \overline{v}}{\partial x} + \frac{K}{1+Ky}\frac{\partial \overline{v}}{\partial y} - \frac{K^2\overline{v}}{(1+Ky)^2} - \frac{\overline{u}}{(1+Ky)^3}\frac{\partial K}{\partial x} - \frac{2K}{(1+Ky)^2}\frac{\partial \overline{u}}{\partial x}\right] \qquad (22b)$$

where ν_e is the effective kinematic viscosity which includes the turbulent eddy viscosity. The equation of continuity is

$$(\partial\overline{u}/\partial x) + (\partial/\partial y)[(1+Ky)\overline{v}] = 0 \qquad (23)$$

These exact equations of motion are extremely difficult to solve. However, by means of an order of magnitude analysis (including curvature), we may simplify the equations of motion. The resulting boundary layer equation of motion for surfaces with curvature becomes

$$\frac{1}{1+Ky}\,\overline{u}\,\frac{\partial \overline{u}}{\partial x} + \overline{v}\,\frac{\partial \overline{u}}{\partial y} + \frac{K\,\overline{u}\,\overline{v}}{1+Ky} = -\frac{1}{\rho(1+Ky)}\frac{\partial \overline{p}}{\partial x} + \nu_e\left(\frac{\partial^2 \overline{u}}{\partial y^2} + \frac{K}{(1+Ky)}\frac{\partial \overline{u}}{\partial y} - \frac{K^2\overline{u}}{(1+Ky)^2}\right)$$

$$(24a)$$

$$K\overline{u}^2/(1+Ky) = (1/\rho)(\partial\overline{p}/\partial y) \qquad (24b)$$

The continuity equation remains the same as equation (23).

The curvature terms in the preceding equations of motion would have a negligible effect on the turbulent boundary layer growth (95 percent of the airfoil upper surface), since the surface curvature is small in this region of the airfoil. However, large surface curvature exists on the leading edge of the airfoil (5 percent of the airfoil surface), which is in the laminar portion of the boundary layer. The effect of large surface curvature has some effect on the laminar velocity profiles (see ref. 37). Neglecting the effect of curvature would result in an error in the calculated velocity profile at transition which is used at the start of the turbulent boundary layer calculations. However, a variation of the velocity profile in this region has a negligible effect on the turbulent separation point, since the turbulent separation point is insensitive to the starting profile. This is illustrated in the section, Turbulent Boundary Layer Growth and Separation.

Thus, if one neglects the effects of surface curvature, the preceding equations reduce to the standard Navier-Stokes equations (ref. 38, p. 545). The resulting momentum and continuity equation along the surface of the body are

$$\bar{u}\,\frac{\partial \bar{u}}{\partial x} + \bar{v}\,\frac{\partial \bar{u}}{\partial y} = U\,\frac{dU}{dx} + \frac{\partial\left[\nu_e\,\frac{\partial \bar{u}}{\partial y}\right]}{\partial y} \tag{25}$$

$$\frac{\partial \bar{u}}{\partial x} + \frac{\partial \bar{v}}{\partial y} = 0 \tag{26}$$

The equations apply to both laminar and turbulent flow if the definition of $\nu_e\,\frac{\partial \bar{u}}{\partial y}$ is taken to be:

$$\nu_e\,\frac{\partial \bar{u}}{\partial y} = \bar{\tau}/\rho \tag{27}$$

and

$$\bar{\tau}/\rho = \nu\,\frac{\partial \bar{u}}{\partial y} - \overline{u'v'} \tag{28}$$

where $-\overline{u'v'}$ is the Reynolds shear stress. For laminar flow $\nu_e = \nu$.

The boundary conditions are

$$\bar{u}(x,0) = 0 \tag{29a}$$

$$\overline{v}(x,0) = \overline{v}_w(x) \tag{29b}$$

$$\lim_{y\to\infty} \int_0^y [U(x) - \overline{u}(x,y')]dy' = U(x)\delta^*(x) \tag{29c}$$

Equation (29a) is an obvious wall boundary condition. Equation (29b) is a general wall boundary condition on $\overline{v}$ which includes the effect of wall transpiration velocity $\overline{v}_w$. Equation (29c) requires that $\overline{u} \to U$ as $y \to \infty$, and also requires that the displacement thickness (and the momentum thickness) be finite. This removes a lack of uniqueness of the type encountered by Hartree (ref. 39) in his solution of the laminar equations.

Transformed Equation of Motion

It is convenient for calculation purposes to transform the (x,y) coordinates into (x,η) coordinates through the following equations:

$$f'(x,\eta) = \frac{U(x) - \overline{u}(x,y)}{U(x)}; \quad \eta = \frac{y}{\delta^*(x)} \tag{30a, b}$$

For turbulent flows, the velocity profile can best be represented in a defect formulation as expressed in the preceding equations. The present method uses δ^* with which to scale y so that $\eta = y/\delta^*$ need never exceed an outside value of 10. Also, $f'(x,\eta)$ is a slowly varying function of x so that relatively large increments in x are possible. Making the preceding substitutions in equations (25) and (26), results in the following transformed boundary layer equation for two-dimensional, incompressible flow (see appendix F):

$$(Tf'')' + [Q(\eta - f) - \overline{v}_w/U]f'' + P(f' - 2)f' = \delta^*(1 - f')\frac{\partial f'}{\partial x} = \delta^* f''\frac{\partial f}{\partial x} \tag{31}$$

where

$$Q = \frac{\frac{d}{dx}(\delta^* U)}{U}, \quad P = \frac{\delta^* dU/dx}{U}, \quad \text{and} \quad T = \frac{\nu_e}{U\delta^*}$$

The term T, the nondimensional effective viscosity, is discussed in the following section. The primes on f denote differentiation with respect to η.

Applying the transformations of equations (30a, b) to the boundary conditions (29a, b, c) result in

$$f'(x,0) = 1 \tag{32a}$$

$$f(x,0) = 0 \tag{32b}$$

$$\lim_{\eta\to\infty} f(x,\eta) \to 1 \tag{32c}$$

Effective Viscosity Hypothesis

Mellor and Gibson first formulated for equilibrium turbulent boundary layers an eddy viscosity composed of a linear function of distance from the wall and Clauser's (ref. 40) constant eddy viscosity for the defect region. They later generalized their treatment for flows in which the pressure gradient parameter $\beta = (\delta^*/\tau_w)dp/dx$ varied in the streamwise direction (see ref. 28). This method utilized a family of curves for different values of β as a starting point. Parametric differentiation then yielded an equation containing derivatives of the defect function with respect to β at constant y/δ^* and $d\beta/dx$. Mellor and Gibson refined the analysis by specifying a general formulation of $d\beta/dx$ (ref. 29). For purposes of developing an effective viscosity ν_e, which is composed of an eddy and a molecular viscosity, Mellor divides the boundary layer into a wall layer, overlap layer and a defect layer.

The hypothesis for the form of ν_e has as its basis three assumptions:

1. In the inner, or wall, layer, ν_e depends on only three quantities, ν, y and $\frac{\partial \overline{u}}{\partial y}$, where ν is the molecular viscosity.

2. In the outer, or defect layer, ν_e depends on only three quantities, $(\delta^* U)$, y and $\frac{\partial \overline{u}}{\partial y}$, where $\delta^* \equiv \int_0^\infty \frac{(U - \overline{u})dy}{U}$ is the scale suggested by Clauser (40).

3. In this two layer model, there is a region where the layers overlap and both expressions for ν_e apply simultaneously.

From Prandtl's theory (ref. 38, p. 555)

$$\overline{\tau} = \rho \left[\kappa^2 y^2 \left(\frac{\partial \overline{u}}{\partial y}\right)\right] \left(\frac{\partial \overline{u}}{\partial y}\right) = \rho [\nu_e] \frac{\partial \overline{u}}{\partial y} \tag{33}$$

Then using the first two assumptions it follows that in the wall layer ν_e must have the form

$$\frac{\nu_e}{\nu} = \phi \left(\frac{\kappa^2 y^2}{\nu} \frac{\partial \overline{u}}{\partial y}\right) \tag{34a}$$

and in the defect layer, ν_e must be of the form

$$\frac{\nu_e}{\delta^* U} = \Phi \left(\frac{\kappa^2 y^2}{\delta^* U} \frac{\partial \overline{u}}{\partial y}\right) \tag{34b}$$

where κ is an empirical constant. Mellor makes Prandtl's theory more general so that both the laminar sublayer and logarithmic portions of the turbulent layer are included. It follows from the third assumption that in the overlap region ν_e must have the form

$$\frac{\nu_e}{\nu} = \phi = \frac{\delta^* U}{\nu} \Phi \qquad (35)$$

Thus, in the overlap region ϕ and Φ must be linear functions so that

$$\frac{\nu_e}{\nu} = \frac{\kappa^2 y^2}{\nu} \frac{\partial \overline{u}}{\partial y} \qquad (36)$$

Mellor thus assumes that in the overlap region Prandtl's theory holds exactly. For the hypothesis to predict correctly a viscous sublayer, it is clear that very close to the wall $\phi \to 1$ (because $\nu_e = \nu$).

An alternative functional form equivalent to equation (34) but offering some computational advantage was given by Mellor (41); it may be written as

$$\frac{\nu_e}{U\delta^*} = \Phi(X), \quad X = \frac{\kappa y}{U\delta^*} \sqrt{\overline{\tau}/\rho}; \text{ in the defect layer} \qquad (37a)$$

$$\frac{\nu_e}{\nu} = \phi(\chi), \quad \chi = \frac{\kappa y}{\nu} \sqrt{\overline{\tau}/\rho}; \text{ in the wall layer} \qquad (37b)$$

As before in the overlap layer, we must have

$$\nu_e = \nu\phi = \delta^* U \Phi = \kappa y \sqrt{\overline{\tau}/\rho}$$

Specific functions are determined by comparison of calculated profiles with constant pressure incompressible velocity profiles and are shown in Figure 17. The value $\kappa = 0.41$ is the von Karman constant and is chosen to predict correctly the experimentally observed logarithmic law of the wall (when $\overline{\tau} \simeq \overline{\tau}_w$). The constant 6.9 is chosen to give a best fit to Laufer's data (42) in the viscous sublayer in the manner demonstrated in (29). The function $\Phi(X)$ resembles a suggestion by Clauser (40), the difference being that Clauser used the wall value $\sqrt{\overline{\tau}_w/\rho}$ instead of the local value $\sqrt{\overline{\tau}/\rho}$. It was found by Mellor (29) that Clauser's interpretation could not be correctly applied to boundary layers with strong pressure gradients.

Finally, the relations (37a, b) were proposed for the empirical inner and outer functions for ν_e. Since the knowledge of the differential equation for ν_e is absent, a composite function using the method of Van Dyke (43) can be formed. The composite function is expressed as the sum of the inner and outer functions minus their common asymptote. Thus, the non-dimensional effective viscosity T can be written for turbulent flow for the whole layer as

$$T = \phi(\chi) + Re_{\delta^*}\Phi\left(\frac{\chi}{Re_{\delta^*}}\right) - \chi \tag{38a}$$

$$T = \frac{1}{Re_{\delta^*}}\,\phi(Re_{\delta^*}X) + \Phi(X) - X \tag{38b}$$

where

$$Re_{\delta^*} = \frac{U\delta^*}{\nu}$$

For laminar flow

$$T = 1/Re_{\delta^*} \tag{39}$$

Solution of the Boundary Layer Equation

The first phase of the solution of the boundary layer equation (31) which is a nonlinear partial differential equation, is the reduction to a set of ordinary differential equations using finite differences for the x derivatives. The x derivatives are represented by finite differences in the x-direction according to an adaptation of the Crank-Nicolson scheme (ref. 20). Equation (31) is written in terms of average functions at a point halfway between the x position of the known profile, x_{i-1}, and that of the profile to be calculated x_i as follows:

$$[\overline{Tf''}]' + \left[(\overline{\delta_x^*} + \overline{P})(\eta - \overline{f}) - \frac{\overline{v}_w}{U}\right]\overline{f''} + [\overline{P}(\overline{f'}-2)]\overline{f'}$$

$$= \frac{\overline{\delta^*}}{\Delta x}(1 - \overline{f'})(f_i' - f_{i-1}') + \frac{\overline{\delta^*}}{\Delta x}\overline{f''}(f_i - f_{i-1}) \qquad (40)$$

where

$$\delta_x^* = \frac{d\delta^*}{dx}$$

Then, using the relations

$$\overline{f'} = \frac{1}{2}(f_i' + f_{i-1}'), \text{ etc.}$$

Equation (40) can be written in terms of functions at position x_i as

$$-(Tf'')_i' = -\tau_b' + c_1(f_i'' + f_{i-1}'') + c_2(f_i' + f_{i-1}')$$

$$-c_3(f_i' - f_{i-1}') - c_4(f_i - f_{i-1}) \qquad (41)$$

where

$$c_1 = (\overline{\delta_x^*} + \overline{P})\left[\eta - \frac{1}{2}(f_i + f_{i-1})\right] - (v_{w_i} + v_{w_{i-1}})/(U_i + U_{i-1})$$

(42a)

$$c_2 = \overline{P}\left[\frac{1}{2}(f_i' + f_{i-1}') - 2\right] \tag{42b}$$

$$c_3 = (\delta_i^* + \delta_{i-1}^*)\left[1 - \frac{1}{2}(f_i' + f_{i-1}')\right]/\Delta x \tag{42c}$$

$$c_4 = (\delta_i^* + \delta_{i-1}^*)\,\frac{1}{2}(f_i'' + f_{i-1}'')/\Delta x \tag{42d}$$

$$\tau_b' = -\,[Tf'']_{i-1}' \tag{42e}$$

Finally, the form in which this equation is solved is

$$[b_5 f'']_i' = b_4 + b_3 f_i'' + b_2 f_i' + b_1 f_i \tag{43}$$

where the coefficients are

$$b_1 = -\,c_4 \tag{44a}$$

$$b_2 = c_2 - c_3 \tag{44b}$$

$$b_3 = c_1 \tag{44c}$$

$$b_4 = -\,\tau_b' + c_1 f_{i-1}'' + (c_2 + c_3) f_{i-1}' + c_4 f_{i-1} \tag{44d}$$

$$b_5 = -\,T_i \tag{44e}$$

Since equations (43) is nonlinear, the solution is carried out iteratively for each i value. The coefficients b_1 to b_5 are evaluated using the results at the previous (i-1) step. The resulting linear equation is then solved for f' and f''. δ^* is adjusted so that $f(\infty) = 1$ to some specified accuracy. The parameters P and Q are recalculated and the effective viscosity function, T, is recalculated. Then the cycle begins again and is continued until the desired accuracy is obtained at a particular step.

The second phase of the method is the solution of the ordinary differential equations. Equation (43) is rewritten as a set of first-order differential equations. The Runge-Kutta method is then used for solving the equations. See Hildebrand (ref. 44) and McCracken (ref. 45) for details of this method.

DISCUSSION OF RESULTS OF BOUNDARY LAYER ANALYSIS

Laminar Boundary Layer Growth

By using the surface velocity distribution obtained from the potential flow analysis as input to the boundary layer analysis, we may obtain the boundary layer growth on the airfoil of the wing propulsion system. Velocity distributions used for the boundary layer analysis are shown in Figure 18. The incompressible velocity distributions are illustrated at the start of the stagnation point to the trailing edge of the airfoil. For high angles of attack (15° or greater) the flow becomes compressible over a small (10 percent) portion of airfoil surface from x/L of 0.05 to x/L of 0.15. For typical takeoff and landing conditions the free stream Mach number is 0.12 or less. Since the flow is incompressible for 90 percent of the airfoil surface, the incompressible velocity distributions were used as inputs to the incompressible boundary layer analysis discussed in the previous section. For practical applications we are concerned with angles of attack, 15° or less.

In order to compute a boundary layer solution, it is necessary to prescribe the velocity profile in the boundary layer at the start of the calculation; namely, the stagnation point of the airfoil. The velocity profile resulting from a similarity wedge flow solution for stagnation point flow over a circular cylinder was assumed (see ref. 38). This and other similar profiles could also be generated from a specialization of equation (31). This is described in reference 26.

The boundary layer is laminar in the region of velocity increase (i.e., roughly from the stagnation point to the point of maximum velocity) and becomes turbulent in most cases from that point on and throughout the region of velocity decrease. The velocity profiles of Figure 18 indicate that laminar flow exists only on the first 5 percent of the leading edge of the airfoil surface for an angle of attack of 15°.

Typical parameters for the laminar portion of the flow are shown in Figure 19. The strong accelerated flow results in a large rate of decrease of the local skin friction coefficient ($C_f = \tau_w/\rho U^2/2$). The skin friction coefficient ranged from 0.035 near the stagnation point to 0.0025 at the point of maximum velocity. The shape factor remained a constant value of approximately 2.2 throughout the laminar region, as would be expected (see ref. 19). The displacement thickness Reynolds number increases linearly from the stagnation point to the point of maximum velocity.

Transition

The pressure distribution in the external flow exerts a decisive influence on the position of the transition point. In ranges of decreasing pressure (accelerated flow) the boundary layer generally remains laminar, whereas even a very small pressure increase always brings transition with it. The location of the transition point is generally determined by experiment but may also be predicted by empirical methods. From experimental data, Crabtree (ref. 46) established a curve of momentum thickness Reynolds number and a pressure gradient parameter at transition. When the curve obtained from predicted boundary layer calculations intersect the experimental curve, the location of transition is determined. Michel's method (ref. 47) established an experimental curve of Re_θ and Re_x at transition. Both of these methods are for smooth surfaces with low turbulence. Granville (ref. 48) predicted a method for finding the distance between instability and transition points.

Theoretical investigations into the process of transition from laminar to turbulent flow are based on the acceptance of Reynolds' hypothesis that transition occurs as a consequence of an instability developed by the laminar boundary layer. Thus, the position of the point of maximum velocity of the potential velocity distribution (point of minimum pressure) influences decisively the position of the point of instability and the region of transition. Usually, the chordwise distance over which the transition region extends is relatively small. Thus, the transition region may be considered to take place at a point. A rough guide for the location of the transition point of airfoil shapes is given by Schlichting (ref. 38). According to Schlighting's rule, the point of transition almost coincides with the point of minimum pressure or maximum velocity of the potential flow in the range of Re_x from 10^6 to 10^7. At very large Re_x, the transition may be a short distance ahead of the maximum velocity. At small Re_x, the transition may take place some distance after the maximum velocity. In summary, we can establish the rule that the point of transition lies behind the point of minimum pressure but in front of the point of laminar separation, at all except very large Reynolds numbers. Taking into account the Reynolds number ($6x10^6$) the adverse pressure gradient, and the turbulence intensity usually associated with flow over STOL wing propulsion systems, transition was assumed to take place at the point of minimum pressure.

Turbulent Boundary Layer Growth and Separation

Boundary layer parameters

It is important that the development of the turbulent boundary layer from the transition point be accurately determined to find out whether the turbulent boundary layer would separate and, if so, at what point on the airfoil. The laminar velocity profile at the transition point is used for the initial turbulent boundary layer calculation. It is necessary to know the shape factor, and skin friction coefficient which are indicative of separation. The turbulent boundary layer parameters on the airfoil of a blown flap wing propulsion system at verious angles of attack are illustrated in Figure 20. The parameters are shown up to but just shy of the point of separation on ~~the~~ airfoil. The displacement and momentum thicknesses are nondimensionalized by L, the distance along the airfoil from stagnation point to trailing edge of the airfoil. As angle of attack is increased the displacement thickness, momentum thickness, and displacement thickness Reynolds number increase at a faster rate. Thus, the separation point occurs closer to the leading edge of the airfoil as the angle of attack is increased.

The point of separation is determined by the condition of zero wall shear stress which gives zero skin friction coefficient. Another condition of the point of separation is the increase in shape factor H as the separation point is approached. At zero angle of attack the shape factor remains a relatively constant value (1.45) with a slight increase at the trailing edge of the airfoil. The skin friction coefficient decreases to a value of 0.0018 at the trailing edge. The shape factor increases at a faster rate as the angle of attack is increased and reaches a value of 2.0 or greater at the point of separation. Likewise the skin friction coefficient approaches zero at a faster rate as angle of attack is increased. The above result is caused by the increase in the adverse pressure gradient as angle of attack is increased. For angles of attack 15° and greater, the skin friction coefficient was 0.0001 or smaller just shy of separation. Hence, this point was used as the separation point.

Velocity Profiles

The effect of the starting velocity profile on the turbulent boundary layer separation point is now considered. Three velocity profiles at the start of the turbulent boundary layer growth are illustrated in Figure 21. Curve B is obtained by assuming a similarity wedge flow solution for a circular cylinder at the stagnation point. Curves A and C are arbitrary selected profiles. Using the profiles in Figure 21 and the surface velocity distributions on the airfoil of the wing propulsion system resulted in a negligible effect on the turbulent separation point.

The boundary layer velocity profiles on the airfoil of a wing-propulsion system at various angles of attack are shown in Figure 22. At zero angle of attack there exists a very mild adverse pressure gradient along the surface of the airfoil (Fig. 18). This results in a small change in the velocity profile along the surface of the airfoil (Fig. 22(a)). For angles of attack 15^{o} and greater, the velocity profiles are shown up to the point near separation (Figs. 22(b) to (e)). As the separation point is approached, the boundary layer thickens and results in an inflection point in the velocity profile. These profiles give approximately zero skin friction ($C_f = 0.0001$) and hence are indicative of the profile near separation. The change in the velocity profiles at the various locations along the surface resulted in a cross-over of the velocity profiles in the outer portion of the boundary layer. This occurred at a velocity ratio $\overline{u}/U$ of approximately 0.75. Schlichting (ref. 38, p. 630) reported this cross-over characteristic in velocity profiles for convergent and divergent channels.

Consequences of separation

The separation at high angles of attack as indicated in the previous section results in a loss of lift and the airfoil stalls. Airfoil stall refers to the angle of attack corresponding to the maximum lift coefficient. Typical lift curves illustrating the stall characteristics of airfoils in subsonic flows are shown in Figure 23 (see refs. 49 and 50). Three main classifications of stalling behavior occur, depending on airfoil shape and Reynolds number: (1) trailing-edge stall, where there is a gradual loss of lift at high lift coefficient as the turbulent separation point moves forward from the trailing edge; (2) leading-edge stall, where there is an abrupt loss of lift, as the angle of attack for maximum lift is exceeded, with little or no rounding over of the lift curves; and (3) thin-airfoil stall, where there is a gradual loss of lift at low lift coefficients as the turbulent reattachment point moves rearward. Trailing edge stall is characteristic of most conventional thick airfoils (say $t/c > 12\%$) at moderate to high Reynolds numbers. Leading-edge stall is characteristic of moderate airfoils ($t/c \simeq 9\%$) and is caused by an abrupt separation of the flow near the nose without subsequent reattachment, i.e., short bubble "bursting". The process of laminar boundary layer separation, transition, turbulent reattachment is referred to as a "short bubble". Thin-airfoil stall is characteristic of thin-airfoil sections ($t/c \simeq 6\%$) and is the result of laminar separation near the leading-edge and turbulent reattachment moving progressively rearward with increasing incidence, i.e., a long bubble. The process of laminar boundary layer separation just aft of the leading edge, transition to turbulence, but reattachment not so quickly established is referred to as a "long bubble". The above stall characteristics for airfoils can be used as an aid in the classification of the stall associated with STOL wing propulsion systems.

The experimental lift curve of the blown flap wing propulsion system with airfoil t/c of 15 percent (see Fig. 2(a)) is illustrated in Figure 24(a). The lift curve increases almost linearly to an angle of attack of 20° and then there is a gradual loss in lift coefficient at high angles of attack. This is typical of the trailing edge stall of thick airfoils as shown in curve (a) of Figure 23. Having assumed that the transition point is near the point of minimum pressure resulted in the predicted turbulent separation point to move forward from the trailing edge as angle of attack is increased. This is illustrated in Figure 24(b). At an angle of attack 15° the separation point is near the trailing edge and moves slightly forward at 20°. At the stall angle of attack of 25° (angle of maximum lift coefficient) the separation point moves still further near the leading edge corresponding to an x/L of 0.57. At an angle of attack of 30° the separation point moves considerably forward as would be expected to an x/L of 0.34. The above experimental curve and indicated separation points validate the assumption of the transition point to occur near the point of minimum pressure for the given airfoil shape and fan location. However, boundary layer characteristics could be quite different for other airfoil geometries and fan locations.

CONCLUDING REMARKS

A method was developed to determine the two-dimensional potential flow solution of STOL wing propulsion systems. The Douglas potential flow computer program was extended to include the effect of suction at the propulsion system inlet and to provide a technique for determining the approximate location of the exhaust jet of the propulsion system. The effect of suction was obtained by combining a basic suction solution with the uniform flow solution for a lifting body. The jet exhaust was considered as part of the solid body and its location was determined by balancing the vertical component of thrust at the flap with the integrated vertical pressure forces of the free jet.

The applicability of the potential flow program is illustrated by considering a multiple-fan externally blown flap under high-lift conditions. The results indicated high upwash angles (60° to 90°) at the fan inlet and large jet penetration at high angles of attack. (The predicted two-dimensional lift coefficients for the 30° flap ranged from 6.5 to 13 while for the 60° flap ranged from 15 to 21 (for angles of attack from 0° to 20°). The predicted two-dimensional lift coefficients for a 30° flap were an average of 10.5 percent higher than predicted by Spence's jet flap theory which neglects thickness effects.

The predicted three-dimensional lift coefficients were an average 11.4 percent higher than experimental data for the 30° blown flap high-lift configuration. The calculated pressure distributions indicated that the minimum pressure point is near the leading edge (less than 2 percent of chord) of the airfoil, with severe adverse pressure gradients at high angles of attack. The pressure coefficient, corresponding to the minimum pressure point, ranged from -7.5 to -51 for the 0° and 20° angle of attack, respectively. The effect of suction due to a fan or inlet installed under the wing decreases the magnitude of the upper surface pressure distribution with only a small effect on total lift coefficient (obtained by integration of pressure distribution on both the upper and lower surfaces of the airfoil).

The surface velocity distribution obtained from the potential flow solution was used to determine the boundary layer growth and separation on the upper surface of the airfoil. The boundary layer solution was obtained by reduction of the partial differential equations of motion to a set of ordinary differential equations using finite differences for the x derivatives. By an iterative solution to the differential equations the boundary layer parameters for both laminar and turbulent flow were found. Near separation the shape factor was found to be 2.0 or greater. This corresponded to a skin friction coefficient of approximately 0.0001. The results indicated that the predicted turbulent separation point moved forward from the trailing edge as the angle of attack is increased. Trailing edge separation for a thick wing ($t/c = 0.15$) propulsion system combination considered was

verified by the experimental lift curve. However, this boundary layer characteristic could be quite different for other wing geometries and propulsion system locations.

The ability to predict the potential flow and boundary layer solution makes the analysis in this report extremely useful as a tool in the design of a STOL wing propulsion system. The analysis can be used to design the airfoil and to determine the optimum location and orientation of the propulsion system. From the predicted surface velocity distributions and boundary layer calculations one may minimize the frictional drag for a given wing propulsion system. The potential flow solution can be used to determine the jet penetration - an important quantity when considering ground effect.

The analysis has application not only to wing propulsion systems, but to any lifting or nonlifting body where suction or blowing is applied.

APPENDIX A

SYMBOLS FOR POTENTIAL FLOW ANALYSIS

APPENDIX A

SYMBOLS FOR POTENTIAL FLOW ANALYSIS

A_{ii}	normal velocity of element i caused by a unit source at element i
A_{ij}	normal velocity of element i caused by a unit source at element j
AR	aspect ratio
B_{ij}	tangential velocity of element i due to a unit source at element j
C	chord length
C_l	two-dimensional lift coefficient
C_L	three-dimensional lift coefficient
C_p	pressure coefficient
C_Q	mass flow coefficient
C_T	thrust coefficient
f	correction factor (eq. (21))
F_y	force in vertical direction
H	jet penetration (see Fig. 2(b))
M	number of elements that describe the jet
L	length
L_T	total length of free jet (see Fig. 2(b))
$\dot{m}$	fan or engine mass flow rate per unit span

N	number of elements that describe the body
n	a normal to the body surface
p	static pressure
P	arbitrary point in the flow field off the surface
r	distance between two points
S	surface of body
T	thrust per unit span
v	disturbance velocity
V	velocity
W_{kj}	complex velocity
w	complex potential
X_{jk}	velocity in x direction at point j due to a unit source at element k
x	Cartesian coordinate
y	Cartesian coordinate
Y_{jk}	velocity in y direction at point j due to a unit source at element k
z	Cartesian coordinate
α	angle of attack
α_i	orientation of surface element
Γ	nondimensional circulation
ξ	variable Cartesian coordinate (see Fig. (25))
$\dot{\eta}$	turning efficiency of exhaust jet
η	variable Cartesian coordinate (see Fig. (25))
θ	flap angle (see Fig. 2(b))

θ_1	jet angle at trailing edge of jet (see Fig. (2(b))
σ	surface source intensity per unit area
ρ	density
ζ	variable Cartesian coordinate (see Fig. (25))
ϕ	velocity potential
ψ	stream function

Subscripts

i	control point of i^{th} element
j	control point of j^{th} element
N	normal
p	arbitrary point on the surface
q	a surface point
ref	reference
s	refers to suction flow solution
t	tangential
v	vortex flow solution
∞	free stream
0	flow solution at zero angle of attack
90	flow solution at 90^o angle of attack

Superscripts

$\rightarrow$	vector

APPENDIX B

VELOCITIES IN TERMS OF SOURCE DENSITIES

APPENDIX B

VELOCITIES IN TERMS OF SOURCE DENSITIES

Consider the body illustrated in Figure 25(a), which extends over the range $-\infty \leq z \leq +\infty$. Any point on the body is described by $p(x,y,z)$ the general point being considered. The point $q(\xi,\eta,\zeta)$ is the variable point for which integration is performed. The potential ϕ_p due to a point source at any point p in the region R bounded by $z = -\infty$, $z = +\infty$, $S = S_o$ and $S = S_1$ is

$$\phi_p = \int_R \frac{\sigma dR}{r} \tag{B1}$$

It is evident from Figure 25(a) that if p is the plane $z = 0$

$$r = [(x-\xi)^2 + (y-\eta)^2 + \zeta^2]^{1/2}$$

Hence,

$$\phi_p = 2\int_{S_o}^{S_1}\int_0^{\infty} \frac{\sigma(S)d\zeta dS}{[(x-\xi)^2 + (y-\eta)^2 + \zeta^2]^{1/2}} \tag{B2}$$

Here the upper limit for the ζ variable of integration signifies a large but finite value. The normal and tangential velocities $\partial\phi/\partial n$ and $\partial\phi/\partial s$ can be evaluated in terms of x and y derivatives of the potential from equation (B1)

$$\left(\frac{\partial\phi}{\partial x}\right)_p = -2\int_{S_o}^{S_l}\int_0^\infty \frac{\sigma(S)(x-\xi)d\zeta dS}{[(x-\xi)^2+(y-\eta)^2+\zeta^2]^{3/2}}$$

(B3)

$$\left(\frac{\partial\phi}{\partial y}\right)_p = -2\int_{S_o}^{S}\int_0^\infty \frac{\sigma(S)(y-\eta)d\zeta dS}{[(x-\xi)^2+(y-\eta)^2+\zeta^2]^{3/2}}$$

Since σ is independent of z or ζ, one integration can be performed to give

$$\left(\frac{\partial\phi}{\partial x}\right)_p = \int_{S_o}^{S_l} \frac{\sigma(S)(x-\xi)dS}{(x-\xi)^2+(y-\eta)^2}$$

(B4)

$$\left(\frac{\partial\phi}{\partial y}\right)_p = \int_{S_o}^{S_l} \frac{\sigma(S)(y-\eta)dS}{(x-\xi)^2+(y-\eta)^2}$$

The problem is reduced to one in a single plane, the plane $z = 0$. The continuous boundary curve S is approximated by a series of segments as shown in Figure 25(b). The front, middle, and rear points of a segment are designated by S_{j-1}, S_j, and S_{j+1}. If the source density is assumed constant over each surface element, the preceding equations become

$$\left.\frac{\partial\phi}{\partial x}\right)_p = \sum_{j=1}^{N}\sigma_j \int_{S_{j-1}}^{S_{j+1}} \frac{(x-\xi)dS}{(x-\xi)^2+(y-\eta)^2}$$

(B5)

$$\left.\frac{\partial\phi}{\partial y}\right)_p = \sum_{j=1}^{N}\sigma_j \int_{S_{j-1}}^{S_{j+1}} \frac{(y-\eta)dS}{(x-\xi)^2+(y-\eta)^2}$$

A transformation of the ξ,η variables into S,r_{ij} variables yields (see Fig. 25(b))

$$\left.\frac{\partial\phi}{\partial x}\right)_p = \sum_{j=1}^{N} \sigma_j \int_{S_{j-1}}^{S_{j+1}} \frac{[r_{ij} \sin \alpha_j + (S - S_{ij}) \cos \alpha_j]dS}{r_{ij}^2 + (S - S_{ij})^2}$$

$$\left.\frac{\partial\phi}{\partial y}\right)_p = \sum_{j=1}^{N} \sigma_j \int_{S_{j-1}}^{S_{j+1}} \frac{[-r_{ij} \cos \alpha_j + (S - S_{ij}) \sin \alpha_j]dS}{r_{ij}^2 + (S - S_{ij})^2}$$

(B6)

The quantities in integrals of equation (B6) are functions only of the geometry of the body. If they are identified as X_{ij} and Y_{ij} respectively, the x and y components of velocity become

$$V_x = \left.\frac{\partial\phi}{\partial x}\right)_i = \sum_{j=1}^{N} \sigma_j X_{ij}$$

(B7)

$$V_y = \left.\frac{\partial\phi}{\partial y}\right)_i = \sum_{j=1}^{N} \sigma_j Y_{ij}$$

where i represents an arbitrary point on the body surface. The normal and tangential velocities can be obtained by using the directional derivative formula

$$\left.\frac{\partial\phi}{\partial n}\right)_i = -\left.\frac{\partial\phi}{\partial x}\right)_i \sin \alpha_i + \left.\frac{\partial\phi}{\partial y}\right)_i \cos \alpha_i$$

(B8)

$$\left.\frac{\partial\phi}{\partial s}\right)_i = \left.\frac{\partial\phi}{\partial x}\right)_i \cos \alpha_i + \left.\frac{\partial\phi}{\partial y}\right)_i \sin \alpha_i$$

Then using equation (B7)

$$\left.\frac{\partial\phi}{\partial n}\right)_i = \sum_{j=1}^{N} \sigma_j(-X_{ij}\sin\alpha_i + Y_{ij}\cos\alpha_i)$$

$$\left.\frac{\partial\phi}{\partial s}\right)_i = \sum_{j-1}^{N} \sigma_j(X_{ij}\cos\alpha_i + Y_{ij}\sin\alpha_i) \tag{B9}$$

Letting the terms in the brackets be A_{ij} and B_{ij} respectively, the normal and tangential velocities due to the source contributions become

$$\left.\frac{\partial\phi}{\partial n}\right)_i = \sum_{j=1}^{N} \sigma_j A_{ij}$$

$$\left.\frac{\partial\phi}{\partial s}\right)_i = \sum_{j=1}^{N} \sigma_j B_{ij} \tag{B10}$$

The total velocities are made up of the contribution due to the source-sink distribution and the free stream velocity. The entire normal and tangential velocities on the body become

$$V_{N,i} = \left.\frac{\partial\phi}{\partial n}\right)_i - V_\infty \sin\alpha_i$$

$$V_{t,i} = \left.\frac{\partial\phi}{\partial S}\right)_i + V_\infty \cos\alpha_i \tag{B11}$$

The velocity at any point off the body can be obtained by

$$(\nabla\phi)_k = \sum_{i=1}^{N} (X_{kj}\hat{i} + Y_{kj}\hat{j})\sigma_k \tag{B12}$$

where σ_k is the combined source intensity of the k^{th} element as given by equation (19) of the text, and X_{kj} and Y_{kj} are the effects in the x and y direction, respectively at any point p due to the k^{th} element.

The terms A_{ij}, B_{ij}, X_{kj}, and Y_{kj} are called influence coefficients and all represent velocities at some point that are resolved in a particular direction. These velocities are generated by the j^{th} source element at point p_i (on the body surface) or p_k (off the body surface) and resolved normal and tangent to the body surface (A_{ij}, B_{ij}) or x axis (X_{kj}, Y_{kj}). In terms of complex velocities W_{ij} and W_{kj} the influence coefficients for points on and off the body surface can be expressed as

$$\begin{aligned} B_{ij} + iA_{ij} &= \overline{W}_{ij}\, e^{-i\alpha_i} \\ X_{kj} + iJ_{kj} &= \overline{W}_{kj} \end{aligned} \tag{B13}$$

where the bar indicates the conjugate and α_i is the i^{th} element angular orientation.

The complex potential at z_k for a unit source located at $\zeta(S)$ is expressed as

$$w = \phi + i\psi = \frac{1}{2\pi} \ln\, [z_k - \zeta(S)] \tag{B14}$$

The complex velocity W_{kj} is the influence of element j at the point p_k. Since $W = dw/dz$ the influence coefficient becomes

$$W_{kj} = \frac{1}{2\pi} \int_{j_{elem}} \frac{d}{dz_k} \ln(z_k - \zeta(S))dS \tag{B15}$$

Referring to Figure 26,

$$dS = e^{-i\alpha_j}\, d\zeta \tag{B16}$$

Replacing dS in equation (B15) and evaluating the integral there results

$$W_{kj} = \frac{e^{-\alpha_j}}{2\pi}\int_{\zeta_{1j}}^{\zeta_{2j}} \frac{d}{dz_k}\, \ln[z_k - \zeta(S)]\; d\zeta = \frac{e^{-i\alpha_j}}{2\pi}\, \ln \frac{(z_k - \zeta_{1j})}{(z_k - \zeta_{2j})} \tag{B17}$$

APPENDIX C

COMPUTATION OF FLOW QUANTITIES FOR POTENTIAL FLOW ANALYSIS

APPENDIX C

COMPUTATION OF FLOW QUANTITIES FOR POTENTIAL FLOW ANALYSIS

Once the combined velocities on the body surface are calculated, the pressure distribution and the lift coefficient of the body can be found. The equation of motion for steady, incompressible, inviscid fluid can be expressed as

$$(\vec{V}\cdot\nabla)\vec{V} = -\frac{1}{\rho}\nabla p \tag{C1}$$

For potential (irrotational) flow Bernoulli's equation results

$$\frac{p}{\rho} + \frac{1}{2}V^2 = \text{Constant} \tag{C2}$$

and is applicable everywhere. The pressure coefficient C_p is defined as

$$C_p = \frac{p - p_\infty}{\frac{1}{2}\rho V_\infty^2} \tag{C3}$$

By use of equation (C2)

$$C_p = 1 - \frac{V^2}{V_\infty^2} \tag{C4}$$

The two-dimensional lift coefficient is defined as

$$C_l = \frac{L}{\frac{1}{2}\rho V_\infty^2 C} \tag{C5}$$

This can be obtained by integration of the pressure distribution over the surface of the body. Since $L = \int_S p_i \cos \alpha_i \, dS_i$,

$$C_l = \frac{1}{C} \sum_{i=1}^{N} C_{p,i} \cos \alpha_i \, \Delta S_i \tag{C6}$$

where $C_{p,i}$ represents the pressure coefficient at the control point of the i^{th} element. The thrust coefficient is defined as

$$C_T = \frac{T}{\frac{1}{2} \rho V_\infty^2 C} \tag{C7}$$

where T is the exit thrust of the propulsion system. The exit thrust is obtained from the vertical force on the jet, the jet deflection angle, and the experimental turning efficiency η between the propulsion system exhaust and the trailing edge of the flap. Then

$$T = \frac{F_y}{\eta \sin \theta} \tag{C8}$$

where η is the turning efficiency of the exhaust jet. The vertical force is calculated by integration of the pressures on the jet

$$F_y = \sum_{i=1}^{M} p_i \cos \alpha_i \, \Delta S_i \tag{C9}$$

where α_i is the angular orientation of the i^{th} element.

APPENDIX D

POTENTIAL FLOW COMPUTER PROGRAM

APPENDIX D

POTENTIAL FLOW COMPUTER PROGRAM

Summary

A schematic representation of the main subroutines of the computer program is illustrated in Figure 27. The program is divided up into seven parts. These are called from the main program. Part 1 performs computations with the basic data input. It calculates angular orientation of elements of the body, mid point of elements, rotates the body, etc. Subroutine 22YA generates the initial shape of the exhaust jet of the propulsion system from the input data. Part 2 formulates the matrix including the complex velocity potential for points on and off the body surface. Part 4 solves the above matrix. The influence coefficients A_{ij}, B_{ij}, X_{kj}, and Y_{kj} (see appendix B) are determined in this subroutine. The combination solution is obtained in part 6. Part 7 determines if the jet exhaust is properly orientated. It integrates for the mass flux into the propulsion system and calculates the forces on the exhaust jet.

Input

The inputs required by the program are as follows:

FLG02, FLG03, etc.	- control flags (see comment cards main program)
MON	- controls amount of output desired (see comment cards main program)
CDIM	- total x distance of body including exhaust jet
VINF	- free stream velocity
X_1, Y_1	- point on body at trailing edge of flap (start of jet)
X_2, Y_2	- point of initial location of trailing edge of exhaust jet
BETA	- flap angle
DELT	- thickness of jet
ALF2	- initial jet angle at trailing edge of jet
KKK	- number of elements on jet
POSS	- turning efficiency of exhaust jet
CHORD	- chord length of airfoil
NN	- number of points on body (first time thru DO loop)
THETA	- rotation angle for airfoil
BDN	- one if on body points follow
X(I), X(I + 1), etc.	- coordinates of points on the body surface
Y(I), Y(I + 1), etc.	- coordinates of points off the body surface
NN	- number of off body points (second time thru DO loop)

THETA	- rotation angle for off body points
BDN	- zero if off body points follow
X(I), X(I + 1), etc.	- coordinate of points off the body surface
Y(I), Y(I + 1), etc.	- coordinate of points off the body surface
NTYPE, XP, YR	- equal zero for prescribed velocity normal to surface of body
NUF(I), NUF(I + 1), etc.	- prescribed velocity normal to surface of body (known value for inlet of propulsion system, zero for rest of body)
TUF(I), TUF(I + 1), etc.	- tangential velocity on surface of body, input as zero

Output

The output consist of tangential velocities and pressure coefficients for each element on the body for the basic solutions and the combination solution. It also includes the mass flow rate into the propulsion system, the forces on the exhaust jet, the thrust coefficient of the propulsion system, the lift coefficient of the body, and the basic input data. Also included are the x and y components of velocity and angular orientation of points off the body (in the flow field).

The complete program listing follows:

Complete Program Listing

```
$MAJUND         NOPRINT
$ZERDIV
$IBJOB             NOMAP


$IBFTC B2Y1
CDECK B2Y1                                                              B2Y00040
      COMMON IM,HEDR,CASE,RPI,R2PI,SP,CL,ALPHA,FALPHA,DALFA,CHORD,SUMDS,B2Y00100
     1       XMC,YMC,ADDY,FLG02,FLG03,FLG04,FLG05,FLG06,FLG07,FLG08,    B2Y00110
     2       FLG09,FLG10,FLG11,FLG12,ND,NLF,NER,NT,NB,NCFLG,FLG15,FLG16
      COMMON SUMSIG,VINF,MON,BETA,CDIM,VREF,DELT,FLG13,FLG14,ITER,ALF2
      COMMON /SPACER/DUMMY(10000)
      COMMON /FORCUR/XCURV(200),YCURV(200),KKK
       COMMON / NBSAVE / NBOLD                                          B2Y00140
      DIMENSION  ND(10), NLF(10), SUMDS(10), XMC(8), YMC(8), ADDY(8)    B2Y00080
     1, HEDR(15),CASE(2)                                                B2Y00090
       COMPLEX IM                                                       B2Y00050
       INTEGER FLG02,FLG03,FLG04,FLG05,FLG06,FLG07                      B2Y00060
     1, FLG08, FLG09, FLG10, FLG11, FLG12,FLG13,FLG14,FLG15,FLG16
       DATA KORE/10000/
C  ******  MON=0 IS REGULAR OUTPUT
C  ******  MON=1 IS MINIMUM OUTPUT
C  *****   FLG01=1 ONE BODY
C *******  FLG02=1 DOES OFF BODY POINTS
C  *****   FLG03=1 ALPHA IS INPUT
C  ******  FLG11=1 DOES SUCTION
C  ******  FLG13=1 DOES THE TAIL
C  ******  FLG14=1 COMPUTES THE TAIL WITH A CUBIC
C  ******  FLG15=1 SKIPS INTEGRATING FOR THE MASS FLUX
C  ******  FLG16=1 CACULATES THE FORCE ON THE END OF THE TAIL ONLY
       NBOLD = 0                                                        B2Y00160
       ITER =0
   10 CALL PART1                                                        B2Y00180
      IF ( FLG08 .NE. 0 )  GO TO 60                                     B2Y00190
      CALL PART2                                                        B2Y00200
      CALL PART4                                                        B2Y00220
      CALL SOLVIT (DUMMY, NT, NCFLG, KORE, 1, 2,  8, 3, +100)           B2Y00230
   30 CALL PART5                                                        B2Y00260
   60 CALL PART6                                                        B2Y00270
      IF(FLG13) 80,80,70
   70 CALL PART 7
   80 GO TO 10
      END                                                               B2Y00330


$IBMAP 22YZ
       ENTRY    .UN12.
.UN12. PZE      UNIT12
UNIT12 FILE     ,UT1,INOUT,BIN,BLK=256,NOLIST
       ENTRY    .UN13.
.UN13. PZE      UNIT13
UNIT13 FILE     ,UT3,INOUT,BIN,BLK=256,NOLIST
       END
```

```
$ORIGIN        ALPHA
$IBFTC B2Y2
CDECK B2Y2                                                               B2Y00340
      SUBROUTINE  PART1                                                  B2Y00350
      COMMON IM,HEDR,CASE,RPI,R2PI,SP,CL,ALPHA,FALPHA,DALFA,CHORD,SUMDS, B2Y00460
     1       XMC,YMC,ADDY,FLG02,FLG03,FLG04,FLG05,FLG06,FLG07,FLG08,      B2Y00470
     2       FLG09,FLG10,FLG11,FLG12,ND,NLF,NER,NT,NB,NCFLG,FLG15,FLG16
      COMMON SUMSIG,VINF,MON,BETA,CDIM,VREF,DELT,FLG13,FLG14,ITER,ALF2
      COMMON /FORCUR/XCURV(200),YCURV(200),KKK,POSS
      COMMON /NBS/ KII
      COMMON/ NBSAVE / NBOLD                                             B2Y00360
      DIMENSION  X(300), Y(300), XMP(299), YMP(299),  ALFA( 299),        B2Y00420
     1 RSDS(299), SINA(299), COSA(299), DELS(299), DALF(298), Z(299),    B2Y00430
     2Q(300),HEDR(15),ND(10),NLF(10),SUMDS(10),XMC(8),YMC(8),           B2Y00440
     3ADDY(8),CASE(2),NUF(299),TUF(299)                                  B2Y00450
      DIMENSION RADC(250)
      COMPLEX  IM, Z, Q                                                  B2Y00370
      REAL  MX, MY, NUF                                                  B2Y00380
      INTEGER  BDN, SUBKS, SEQ1, SEQ2                                    B2Y00390
      INTEGER  FLG02, FLG03, FLG04, FLG05, FLG06, FLG07                  B2Y00400
     1, FLG08, FLG09, FLG10, FLG11, FLG12,FLG13,FLG14,FLG15,FLG16
      EQUIVALENCE (NUF, X), (TUF, Y)                                     B2Y00490
      IM = (0., 1.)                                                      B2Y00500
      N = FLG12                                                          B2Y00510
      READ (5,4) HEDR, CASE, NB, FLG02, FLG03, FLG04,     FLG05,FLG06,   B2Y00520
     1 FLG07, FLG08, FLG09, FLG10, FLG11, FLG12,FLG13,FLG14,
     2 FLG15,FLG16,SEQ1,NIN
    4 FORMAT( 15A4, 2X, 2A4/18I1)
      IF( NBOLD .EQ. 0 )        NBOLD = NB                               B2Y00540
      IF( NIN .EQ. 0 )        NIN = 5                                    B2Y00550
      READ (5,6) MON,CDIM,VINF,X1,Y1,X2,Y2,BETA,DELT,VREF,ALF2
      READ (5,7) KKK,POSS
    6 FORMAT (I5,6F10.5,3F5.2/1F10.5)
    7 FORMAT (I5,F10.4)
      READ (5, 8)  SP, CL, ALPHA, FALPHA, DALFA, CHORD, SEQ2             B2Y00570
    8 FORMAT (6F10.0, 16X I4)                                            B2Y00580
      IF ( SEQ2 .GE. SEQ1 )  GO TO 80                                    B2Y00590
   60 WRITE ( 6,9 )                                                      B2Y00600
    9 FORMAT ( 50HODATA OUT OF SEQUENCE. SORT DATA ON 77-80. RELOAD. )   B2Y00610
      STOP                                                               B2Y00620
   80 SEQ1 = SEQ2                                                        B2Y00630
   82 IF ( CHORD .EQ. 0. )  CHORD = 1.                                   B2Y00640
      WRITE (6, 12)  HEDR, CASE, NB, FLG02, FLG03, FLG04, FLG05, FLG06,  B2Y00650
     1 FLG07, FLG08, FLG09, FLG10, FLG11, FLG12,FLG13,FLG14,FLG15,FLG16,
     2 MON,VINF,
     2                                       SP, CL, ALPHA, FALPHA,      B2Y00660
     2 DALFA, CHORD, NIN                                                 B2Y00670
   12 FORMAT (1H1 25X 26HDOUGLAS  AIRCRAFT  COMPANY / 28X 21HLONG  BEACHB2Y00680
     1  DIVISION /// 6X 26HPROGRAM B2YC-- 2-D CASCADE // 11X 29H***** CAB2Y00690
     2SE CONTROL DATA *****,///6X,15A4,4X, 9HCASE NO. ,2A4,//6X,9HBODIESB2Y00700
     3  =I3,20X 9HFLAG 2  =I3/ 6X 9HFLAG 3  =I3,20X 9HFLAG 4  = I3/ 6X   B2Y00710
     4 9HFLAG 5  = I3,20X 9HFLAG 6  = I3/ 6X 9HFLAG 7  = I3,20X 9HFLAG 8B2Y00720
     5  = I3/ 6X 9HFLAG 9  = I3,20X 9HFLAG 10 = I3/ 6X 9HFLAG 11 = I3,   B2Y00730
     620X 9HFLAG 12 =I3/6X 9HFLAG 13 =I3,20X 9HFLAG 14 =I3/6X 9HFLAG 15
     A=I3,20X 9HFLAG 16 = I3,20X 5HMON = I3,20X 6HVINF = F8.2//
     B                  11X 10H SPACING = F13.8/ 16X 5H CL = F13.8/   B2Y00740
     7 13X 8H ALPHA = F13.8/ 7X 14H INLET ALPHA = F13.8/ 7X 14H DELTA ALB2Y00750
     8PHA = F13.8/ 13X 8H CHORD = F13.8/13X,58HINPUT TAPE NO. FOR COORDIB2Y00760
     9NATES AND NON-UNIFORM FLOW ONLY =,  I5  )                          B2Y00770
      IF (FLG08 .EQ. 0)  GO TO 119                                       B2Y00780
```

```
      FLG12 = N                                                         B2Y00790
      RETURN                                                            B2Y00800
  119 NT = 0                                                            B2Y00810
      NCFLG = 2                                                         B2Y00820
      REWIND 4                                                          B2Y00830
      REWIND 9                                                          B2Y00840
      REWIND 12                                                         B2Y00850
      REWIND 13                                                         B2Y00860
      DO 120 I = 1, 10                                                  B2Y00890
      SUMDS(I) = 0.                                                     B2Y00900
      NLF(I) = 0                                                        B2Y00910
  120 ND(I) = 0                                                         B2Y00920
      K2 = NB                                                           B2Y00930
      IF ( FLG02 .NE. 0 )  K2 = NB + 1                                  B2Y00940
      DO 2000 L = 1, K2                                                 B2Y00950
      READ (5, 15)  NN, MX, MY, THETA, ADDX, ADDY(L), SEQ2              B2Y00960
   15 FORMAT (5X I5, 5F10.0, 16X I4 )                                   B2Y00970
      IF ( SEQ2 .LT. SEQ1 )  GO TO 60                                   B2Y00980
      SEQ1 = SEQ2                                                       B2Y00990
  122 READ (5,16) BDN,SUBKS,NLFF,XMC(L),YMC(L),ELPSTH,SEQ2
   16 FORMAT (3(5X I5),3F10.0,16X,I4)                                   B2Y01010
      IF ( SEQ2 .LT. SEQ1 )  GO TO 60                                   B2Y01020
      SEQ1 = SEQ2                                                       B2Y01030
  124 ND(L)=NN
      JJ=ND(1)
      II=ND(1)-KKK+1
      KII=ND(1)
      M = NN - 1                                                        B2Y01050
      NLF(L) = NLFF                                                     B2Y01060
      NT = NT + NN                                                      B2Y01070
       IF( NLFF .EQ. 0  .AND.  BDN .NE. 0 )      NCFLG = NCFLG + 1      B2Y01080
      IF ( SUBKS .EQ. 0 ) GO TO 140                                     B2Y01090
       IF( L .NE. K2 )       GO TO 145                                  B2Y01100
       NTIMES = NBOLD - NB                                              B2Y01110
       IF( NTIMES .LE. 0 )       GO TO 145                              B2Y01120
      GO TO 145                                                         B2Y01180
  140 ELPSTH = ABS(ELPSTH)                                              B2Y01190
      IF (ELPSTH .LE. 0.0) GO TO 139                                    B2Y01200
      DANGLE = 6.2831853E0 / FLOAT (M)                                  B2Y01210
      ANGLE = 0.0                                                       B2Y01220
      X(1) = 1.0                                                        B2Y01230
      X(NN) = 1.0                                                       B2Y01240
      Y(1) = 0.0                                                        B2Y01250
      Y(NN) = 0.0                                                       B2Y01260
      N = M - 1                                                         B2Y01270
      DO 141 I = 1,N                                                    B2Y01280
      ANGLE = ANGLE - DANGLE                                            B2Y01290
      X(I+1) = COS (ANGLE)                                              B2Y01300
  141 Y(I+1) = ELPSTH * SIN (ANGLE)                                     B2Y01310
      GO TO 145
  139 DO 142 I = 1,NN,6                                                 B2Y01330
      READ (NIN,20) X(I), X(I+1), X(I+2), X(I+3), X(I+4), X(I+5), SEQ2  B2Y01340
   20 FORMAT (6F10.0, 16X I4)                                           B2Y01350
      IF ( SEQ2 .LT. SEQ1 )  GO TO 60                                   B2Y01360
  142 SEQ1 = SEQ2                                                       B2Y01370
      DO 144 I = 1, NN, 6                                               B2Y01380
      READ (NIN,20) Y(I), Y(I+1), Y(I+2), Y(I+3), Y(I+4), Y(I+5), SEQ2  B2Y01390
      IF ( SEQ2 .LT. SEQ1 )  GO TO 60                                   B2Y01400
  144 SEQ1 = SEQ2                                                       B2Y01410
      THETA=THETA/57.2957795E0
```

```
      IF ( THETA .EQ. 0. )  GO TO 300
      CSTHT = COS( THETA )
      SNTHT = SIN( THETA )
      DO 290 I = 1, NN
      T1 = X(I)
      X(I) = T1*CSTHT + Y(I)*SNTHT
  290 Y(I) = Y(I)*CSTHT - T1*SNTHT
  300 CONTINUE
  145 IF (FLG12 .GT. 0)  GO TO 150
      IF(FLG14 .EQ. 0) GO TO 148
      IF (BDN.NE.1) GO TO 148
      T1=X1
      X1=T1*COS(THETA)+Y1*SIN(THETA)
      Y1=Y1*COS(THETA)-T1*SIN(THETA)
      T2=X2
      X2=T2*COS(THETA)+Y2*SIN(THETA)
      Y2=Y2*COS(THETA)-T2*SIN(THETA)
      X3=X2+9.72
      Y3=Y2-1.32
      THETA=THETA*57.2957795E0
      ALF=BETA+THETA
      CALL SUBCUR(X1,Y1,X2,Y2,X3,Y3,ALF,ALF2,DELT)
      MMM=KKK
      NNN=1
  143 DO 147 I=NNN,MMM
      X(I)=XCURV(I)
  147 Y(I)=YCURV(I)
      IF (NNN-II) 146,148,148
  146 NNN=II
      MMM=JJ
      GO TO 143
  148 WRITE (13) (X(I),I=1,NN)
      WRITE (13) (Y(I),I=1,NN)
  150 IF ( BDN .EQ. 0 )  GO TO 200
      IF (FLG12 .GT. 0)  GO TO 163
      DO 160 I = 1, M
      XMP(I) = ( X(I+1) + X(I) ) / 2.
  160 YMP(I) = ( Y(I+1) + Y(I) ) / 2.
      WRITE (13) ( XMP(I), I = 1, M )
      WRITE (13) ( YMP(I), I = 1, M )
      GO TO 200
  163 SUMS = 0.0
      DO 164 I = 1,M
      XMP(I) = ( X(I+1)+X(I) )/2.
      YMP(I) = ( Y(I+1)+Y(I) )/2.
      T1 = X(I+1)-X(I)
      T2 = Y(I+1)-Y(I)
      DELS(I) = SQRT( T1*T1+T2*T2)
      SUMS = SUMS + DELS(I)
      RSDS(I) = SUMS
  164 ALFA(I) = ATAN2(T2,T1)
      MM = NN-2
      DO 165 I = 1, MM
  165 DALF(I) = (ALFA(I+1)-ALFA(I))*57.2957795E0
  200 WRITE (6, 24)  HEDR, NN, NLF(L), MX, MY, THETA, ADDX, ADDY(L),
     1 XMC(L), YMC(L)
   24 FORMAT (1H  25X 26HDOUGLAS  AIRCRAFT  COMPANY / 28X 21HLONG  BEACH
     1  DIVISION,///5X,15A4,// 5X,4HNN =,I4,4X,5HNLF =, I4,5X,4HMX =,
     2 F13.8, 4X 4HMY = F13.8 / 5X 7HTHETA = F13.8, 4X 6HADDX = F13.8,
     3 2X 6HADDY = F13.8 / 7X 5HXMC = F13.8, 5X 5HYMC = F13.8 )
```

```
      IF (MON-1) 27,240,240
   27 IF ( BDN .EQ. 0 )  GO TO 220                                      B2Y01740
      IF (FLG12.LE.0) WRITE (6,25)                                      B2Y01750
      IF (FLG12.GT.0) WRITE (6,26)                                      B2Y01760
   25 FORMAT (1H0 4X 33HON-BODY CCORDINATES (TRANSFORMED) )            B2Y01770
   26 FORMAT (1H0 4X 35HON-BODY CCORDINATES (UNTRANSFORMED) )          B2Y01780
      WRITE (6,28) BDN                                                  B2Y01790
   28 FORMAT(9H BODY NO.I3//12X1HX13X1HY11X7HDELTA S 7X 5HSUMDS 8X     B2Y01800
     1        7HD ALPHA //)                                             B2Y01810
      GO TO 230                                                         B2Y01820
  220 IF (FLG12.LE.0) WRITE (6,31)                                      B2Y01830
   31 FORMAT (1H0 4X 34HOFF-BODY COORDINATES (TRANSFORMED) // 10X      B2Y01840
     1        5HX-OFF 9X 5HY-OFF //)                                    B2Y01850
      IF (FLG12.GT.0) WRITE (6,32)                                      B2Y01860
   32 FORMAT (1H0 4X 36HOFF-BODY COORDINATES (UNTRANSFORMED) // 10X    B2Y01870
     1        5HX-OFF 9X 5HY-OFF // )                                   B2Y01880
  230 IF (FLG12.LE.0) GO TO 240                                         B2Y01890
      IF (BDN.LE.0) GO TO 235                                           B2Y01900
      WRITE (6,36) X(1),Y(1),XMP(1),YMP(1),DELS(1),RSDS(1)              B2Y01910
      WRITE (6,40) ( I, X(I), Y(I), DALF(I-1), XMP(I), YMP( I),         B2Y01920
     1               DELS(I), RSDS(I), I = 2, M )                       B2Y01930
      WRITE (6,44) NN, X(NN), Y(NN)                                     B2Y01940
      GO TO 240                                                         B2Y01950
  235 WRITE (6,48) (I, X(I), Y(I), I = 1, NN)                           B2Y01960
  240 IF ( MX .EQ. 0. )  GO TO 260                                      B2Y01970
      DO 250 I = 1, NN                                                  B2Y01980
  250 X(I) = X(I) * MX                                                  B2Y01990
      XMC(L) = XMC(L) * MX                                              B2Y02000
  260 IF ( MY .EQ. 0. )  GO TO 280                                      B2Y02010
      DO 270 I = 1, NN                                                  B2Y02020
  270 Y(I) = Y(I) * MY                                                  B2Y02030
      YMC(L) = YMC(L) * MY                                              B2Y02040
  280 IF ( ADDX .EQ. 0. ) GO TO 320
      DO 310 I = 1, NN                                                  B2Y02170
  310 X(I) = X(I) + ADDX                                                B2Y02180
      XMC(L) = XMC(L) + ADDX                                            B2Y02190
  320 T1 = ADDY(L)                                                      B2Y02200
      IF ( T1 .EQ. 0. )  GO TO 340                                      B2Y02210
      DO 330 I = 1, NN                                                  B2Y02220
  330 Y(I) = Y(I) + T1                                                  B2Y02230
      YMC(L) = YMC(L) + T1                                              B2Y02240
  340 IF ( CHORD .EQ. 1. )  GO TO 360                                   B2Y02250
      DO 350 I = 1, NN                                                  B2Y02260
      X(I) = X(I)/CHORD                                                 B2Y02270
  350 Y(I) = Y(I)/CHORD                                                 B2Y02280
      XMC(L) = XMC(L)/CHORD                                             B2Y02290
      YMC(L) = YMC(L)/CHORD                                             B2Y02300
  360 IF ( BDN .EQ. 0 )  GO TO 500                                      B2Y02310
      SUMS = 0.                                                         B2Y02320
      DO 400 I = 1, M                                                   B2Y02330
      T1 = X(I+1) - X(I)                                                B2Y02340
      T2 = Y(I+1) - Y(I)                                                B2Y02350
      XMP(I) = (X(I+1) + X(I)) / 2.                                     B2Y02360
      YMP(I) = (Y(I+1) + Y(I)) / 2.                                     B2Y02370
      TDS = SQRT ( T1*T1 + T2*T2 )                                      B2Y02380
      DELS(I) = TDS                                                     B2Y02390
      SUMS = SUMS + TDS                                                 B2Y02400
      RSDS(I) = SUMS                                                    B2Y02410
      COSA(I) = T1 / TDS                                                B2Y02420
      SINA(I) = T2 / TDS                                                B2Y02430
```

```
      ALFA(I) = ATAN2 (T2, T1)                                          B2Y02440
      Z(I) = CMPLX ( XMP(I), YMP(I) )                                   B2Y02450
  400 Q(I) = CMPLX ( X(I), Y(I) )                                       B2Y02460
      Q(NN) = CMPLX ( X(NN), Y(NN) )                                    B2Y02470
      SUMDS(L) = RSDS(M)                                                B2Y02480
      WRITE (12) ( XMP(I), I = 1, M )                                   B2Y02490
      WRITE (12) ( YMP(I), I = 1, M )                                   B2Y02500
      WRITE (12) ( DELS(I), I = 1, M )                                  B2Y02510
      IF (FLG12.GT.0) GO TO 450                                         B2Y02520
      M = NN - 2                                                        B2Y02530
      DO 420 I = 1, M                                                   B2Y02540
      DALF(I) = ( ALFA(I+1)-ALFA(I) ) * 57.2957795
      IF (ABS(DALF(I)).GT.270.)  DALF(I)=360.)-ABS(DALF(I))
  420 CONTINUE
      IF (MON.GE.1) GO TO 600
      WRITE (6, 36)  X(1), Y(1), XMP(1), YMP(1), DELS(1), RSDS(1)       B2Y02560
   36 FORMAT (1H  3H  1  2F14.8,  / 4X  4F14.8 )                        B2Y02570
      M = NN - 1                                                        B2Y02580
      WRITE (6, 40) ( I, X(I), Y(I), DALF(I-1), XMP(I), YMP(I), DELS(I) B2Y02590
     1 , RSDS(I), I = 2, M )                                            B2Y02600
   40 FORMAT (1H   I3, 2F14.8, 28X F14.8 / 4X  4F14.8 )                 B2Y02610
      WRITE (6, 44)  NN, X(NN), Y(NN)                                   B2Y02620
   44 FORMAT (1H  I3, 2F14.8 )                                          B2Y02630
      GO TO 600                                                         B2Y02640
  450 WRITE (13) (X(I),I=1,NN)                                          B2Y02650
      WRITE (13) (Y(I),I=1,NN)                                          B2Y02660
      M = NN-1                                                          B2Y02670
      WRITE (13) (XMP(I), I=1,M)                                        B2Y02680
      WRITE (13) (YMP(I), I=1,M)                                        B2Y02690
      GO TO 600                                                         B2Y02700
  500 IF (MON.GE.1) GO TO 501
      IF (FLG12 .LE. 0)  WRITE (6,48) (I, X(I), Y(I), I = 1, NN)        B2Y02710
   48 FORMAT (1H  I3, 2F14.8 )                                          B2Y02720
  501 M=NN
      IF (FLG12 .LE. 0)  GO TO 530                                      B2Y02740
      WRITE (13) (X(I), I=1,NN)                                         B2Y02750
      WRITE (13) (Y(I), I=1,NN)                                         B2Y02760
  530 DO 550 I = 1, NN                                                  B2Y02770
  550 Z(I) = CMPLX( X(I), Y(I) )                                        B2Y02780
  600 WRITE (9) ( Z(I), I = 1, NN )                                     B2Y02790
      IF ( BDN .EQ. 0 )  GO TO 2000                                     B2Y02800
      M=NN-1
      WRITE (9) ( SINA(I), I = 1, M )                                   B2Y02810
      WRITE (4) ( SINA(I), I = 1, M )                                   B2Y02820
      WRITE (9) ( COSA(I) , I = 1, M )                                  B2Y02830
      WRITE (4) ( COSA(I) , I = 1, M )                                  B2Y02840
      WRITE (9) ( Q(I), I = 1, NN )                                     B2Y02850
 2000 CONTINUE                                                          B2Y02860
      NT = NT - NB - ND(NB+1)                                           B2Y02870
C     NT = TOTAL NO. OF ELEMENTS                                        B2Y02880
      IF (FLG11.EQ.0) RETURN                                            B2Y02890
      REWIND 12                                                         B2Y02900
      REWIND 4                                                          B2Y02910
      M = 1                                                             B2Y02920
      N = ND(1)-1                                                       B2Y02930
      DO 2050 J = 1, NB                                                 B2Y02940
      READ (12) (XMP(I),I=M,N)                                          B2Y02950
      READ (4) (SINA(I),I=M,N)                                          B2Y02960
      READ (12) (YMP(I),I=M,N)                                          B2Y02970
      READ (4) (COSA(I),I=M,N)                                          B2Y02980
```

```
      READ (12)                                                          B2Y02990
      M = N+1                                                            B2Y03000
 2050 N = N+ND(J+1)-1                                                    B2Y03010
      IF (FLG11.LE.8) GO TO 2100                                         B2Y03020
      WRITE (6,56)                                                       B2Y03030
   56 FORMAT (1H1 5X 37HNUMBER OF NON-UNIFORM FLOWS EXCEEDS 8 //         B2Y03040
     1        6X 18HPROGRAM TERMINATED )                                 B2Y03050
      STOP                                                               B2Y03060
 2100  NCFLG = NCFLG + FLG11
      DO 4000 K = 1, FLG11                                               B2Y03080
      READ (5,64) NTYPE,XR,YR,SEQ2                                       B2Y03090
   64 FORMAT (I1, 9X 2F10.0, 46X I4)                                     B2Y03100
      IF (SEQ2.LT.SEQ1) GO TO 60                                         B2Y03110
      SEQ1 = SEQ2                                                        B2Y03120
      IF (NTYPE.GT.1) GO TO 2400                                         B2Y03130
      DO 2200 I = 1, NT, 6                                               B2Y03140
      READ(NIN,20)NUF(I),NUF(I+1),NUF(I+2),NUF(I+3),NUF(I+4),NUF(I+5),   B2Y03150
     1            SEQ2                                                   B2Y03160
 2200 SEQ1 = SEQ2                                                        B2Y03180
 2160 DO 2300 I = 1, NT, 6
      READ(NIN,20)TUF(I),TUF(I+1),TUF(I+2),TUF(I+3),TUF(I+4),TUF(I+5),   B2Y03200
     1            SEQ2                                                   B2Y03210
 2300 SEQ1 = SEQ2                                                        B2Y03230
 2260 IF (NTYPE) 3000,3000,2800
 2400 IF (NTYPE.EQ.3) GO TO 2600                                         B2Y03250
      DO 2500 I = 1, NT                                                  B2Y03260
      T1 = (XMP(I)-XR)**2 + (YMP(I)-YR)**2                               B2Y03270
      NUF(I) = (YMP(I)-YR)/T1                                            B2Y03280
 2500 TUF(I) = (XR-XMP(I))/T1                                            B2Y03290
      GO TO 2800                                                         B2Y03300
 2600 DO 2700 I = 1, NT                                                  B2Y03310
      NUF(I) = YMP(I)-YR                                                 B2Y03320
 2700 TUF(I) = XR-XMP(I)                                                 B2Y03330
 2800 DO 2900 I = 1, NT                                                  B2Y03340
      T1 = NUF(I)                                                        B2Y03350
      NUF(I) =-T1*SINA(I)+TUF(I)*COSA(I)                                 B2Y03360
 2900 TUF(I) = T1*COSA(I)+TUF(I)*SINA(I)                                 B2Y03370
 3000 WRITE (4) (NUF(I),I=1,NT)                                          B2Y03380
      WRITE (4) (TUF(I),I=1,NT)                                          B2Y03390
      WRITE (6,68) HEDR, K, (I,NUF(I),NUF(I+1),NUF(I+2),NUF(I+3),
     1 NUF(I+4),NUF(I+5),I=1,NT,6)
   68  FORMAT(1H1,6X,15A4,//7X,20HNON-UNIFORM FLOW NO.,I3,//12X,2HNG,    B2Y03410
     1        11X 2HTG // (1X I5, 6F13.2) )
 4000 CONTINUE                                                           B2Y03430
      RETURN                                                             B2Y03440
      END                                                                B2Y03450
```

```
$IBFTC 22YAA
      SUBROUTINE SUBCUR(X1,Y1,X2,Y2,X3,Y3,ALF,ALF2,DELT)
      COMMON /FORCUR/XCURV(200),YCURV(200),KKK
      COMMON /NBS/ KII
      COMMON XD(50),YD(50)
      COMMON /FNC/ B,C,D
      DIMENSION XS(50), X(50), Y(50), XL(50), YL(50),ND(10)
      DATA RAD/.01745329/
```

```
      DATA TOL/1.E-6/
      EXTERNAL FUNC
      WRITE (6,23) X2,Y2,X3,Y3,ALF,DELT ,ALF2,X1,Y1
   23 FORMAT (9F10.4)
      ALF2=ALF2*RAD
      X3=X2+9.72*COS(ALF2)-DELT/2.0*SIN(ALF2)
      Y3=Y2-DELT/2.0*COS(ALF2)-9.72*SIN(ALF2)
      ALF2=-ALF2
      ALF = -ALF * RAD
      X2MX1= (X2-X1)
      X2PX1= X2+X1
      X1TX2= X1 * X2
      Y2MY1= Y2-Y1
      X1S= X1 *X1
      X2S= X2*X2
      DET = -1.0 * (X2MX1) **3
      ALF = SIN(ALF)/COS(ALF)
      ALF2=SIN(ALF2)/COS(ALF2)
      A =(X2S*(X2MX1*X1*ALF +Y1*(3.0*X1-X2))+X1S*(Y2*(X1-3.0*X2)+ALF2*X2*
     1X2MX1))/DET
      B =(X2*(6.0*X1*Y2MY1+ALF*(2.0*X1S-X1TX2-X2S))+ALF2*X1*(X1S+X1TX2-2.
     10*X2S))/DET
      C =(-3.0*Y2MY1*X2PX1+3.0*ALF*(X2S-X1S)+(ALF2-ALF)*(X2S+X1TX2-2.0*X1
     1S))/DET
      D=(2.0*Y2MY1-2.0*X2MX1*ALF-(ALF2-ALF)*X2MX1)/ DET
      SC = SIMPS1(X1,X2,FUNC,K)
      S= SC + DSQRT(  (X3-X2)**2 + (Y3-Y2)**2)
      JJ=KKK+1
      KK=KKK-1
      DS=S/FLOAT(KK)
      DO 1 I=1,KKK
      AY = I-1
    1 XS(I)= AY *DS
      XG=(X2MX1)/FLOAT(KK)+X1
      X(1)= X1
      Y(1)= Y1
      DO 2 I=2,KK
      I1 = I
    3  GNUM = XS(I) - SIMPS1(X1,XG,FUNC,K) + XG * FUNC(XG)
      DENOM = FUNC(XG)
      XN = GNUM/DENOM
      REL = ABS (( XG-XN)/XN)
      XG = XN
      IF (REL .GT. TOL) GO TO 3
      IF(XG .GE. X2) GO TO 4
      X(I)= XG
      Y(I)= A + XG *(B+XG*(C+D*XG))
      YP = B + X(I) *(2.0*C+3.0* D  *X(I))
      YP = -1.0/YP
      THET = ATAN(YP)
      IF(YP .LT. 0.0) GO TO 10
      DY =-DELT * SIN(THET)
      DX=-DELT * COS(THET)
      GO TO 11
   10 DY = DELT * SIN(THET)
      DX = DELT * COS(THET)
   11 XL(I)= X(I) + DX
    2 YL(I)= Y(I) + DY
      GO TO 5
    4 IK= I1
```

```
      SLOP = (Y3-Y2)/(X3-X2)
      THET = ATAN(SLOP)
      SLOPL= (Y3-(Y2-DELT))/(X3-X2)
    6 XG = XS(I1) - SC
      DY = XG * SIN(THET)
      DX = XG * COS(THET)
      X(I1) = X2 + DX
      Y(I1)= Y2 + DY
      IF(ALF2 .NE. 0.0) GO TO 20
      YL(I1)= SLOPL * (X(I1)-X2) + (Y2 - DELT)
      XL(I1)= X(I1)
      GO TO 21
   20 DELTG = (1.0 - XG/(S-SC)) * DELT
      SLOPL = -1.0/ALF2
      SLOPL = ATAN(SLOPL)
      DYL = -DELTG * SIN(SLOPL)
      DYX = -DELTG * COS(SLOPL)
      YL(I1) = Y(I1) + DYL
      XL(I1) = X(I1) + DXL
   21 I1 = I1 + 1
      IF(I1 .EQ. KKK) GO TO 5
      GO TO 6
    5 X(KKK)=X3
      XL(KKK)=X3
      Y(KKK)=Y3
      YL(KKK)=Y3
      YP = -1.0/ALF
      THET = ATAN(YP)
      DY = -DELT * SIN(THET)
      DX = -DELT * COS(THET)
      XL(1)= X1 + DX
      YL(1)= Y1 + DY
      DO 7 I=1,KKK
      J=JJ-I
      XCURV(I)= XL(J)
      YCURV(I)= YL(J)
      K=KII-KKK+I
      XCURV(K)= X(I)
    7 YCURV(K)= Y(I)
      RETURN
      END


$IBFTC FXYZ
      FUNCTION FUNC(X)
      COMMON /FNC/ B,C,D
      FUNC= SQRT(1.0 + (B+2.0 * C*X+3.0*D*X*X)
     1**2)
      RETURN
      END




$ORIGIN        ALPHA
$IBFTC B2Y3
CDECK B2Y3                                                              B2Y03460
      SUBROUTINE  PART2                                                 B2Y03470
```

```
C **  MATRIX FORMATION SUBROUTINE **                                        B2Y03480
      COMPLEX  IM, Z, Q, W1, W2, TF, T2, T1, CLOG, CSINH                    B2Y03490
      INTEGER  FLG02, FLG03, FLG04, FLG05, FLG06, FLG07                     B2Y03500
     1, FLG08, FLG09, FLG10, FLG11, FLG12                                   B2Y03510
      DIMENSION  Z(299), Q(300), SINA(299), COSA(300), ND(10),              B2Y03520
     1 VNS(400 ), VTS(400 ), A(299), B(299), SUMDS(10), NLF(10)             B2Y03530
      DIMENSION VNST(10),HEDR(15),CASE(2),XMC(8),YMC(8),ADDY(8)             B2Y03540
      COMMON IM,HEDR,CASE,RPI,R2PI,SP,CL,ALPHA,FALPHA,DALFA,CHORD,SUMDS,B2Y03550
     1        XMC,YMC,ADDY,FLG02,FLG03,FLG04,FLG05,FLG06,FLG07,FLG08,       B2Y03560
     2        FLG09,FLG10,FLG11,FLG12,ND,NLF,NER,NT,NB,NCFLG                B2Y03570
      RPI = 0.31830989E0                                                    B2Y03580
      R2PI = 0.15915494E0                                                   B2Y03590
      REWIND  9                                                             B2Y03600
      REWIND 10                                                             B2Y03610
      REWIND 8
      M = 1                                                                 B2Y03630
      N = ND(1) - 1                                                         B2Y03640
      M1 = 1                                                                B2Y03650
      N1 = ND(1)                                                            B2Y03660
      DO 100 L = 1, NB                                                      B2Y03670
      READ (9) (Z(I), I = M, N)                                             B2Y03680
      READ (9) (SINA(I), I = M, N)                                          B2Y03690
      READ (9) (COSA(I), I = M, N)                                          B2Y03700
      READ (9) (Q(I), I = M1, N1)                                           B2Y03710
      M = N + 1                                                             B2Y03720
      N = N + ND(L+1) - 1                                                   B2Y03730
      M1 = N1 + 1                                                           B2Y03740
  100 N1 = N1 + ND(L+1)                                                     B2Y03750
      K = NB * NT                                                           B2Y03760
      DO 200 I = 1, K                                                       B2Y03770
      VNS(I) = 0.                                                           B2Y03780
  200 VTS(I) = 0.                                                           B2Y03790
      ASSIGN 850 TO N50                                                     B2Y03800
      ASSIGN 1050 TO N51                                                    B2Y03810
      IF (FLG11.LE.0) GO TO 400                                             B2Y03820
      REWIND 4                                                              B2Y03830
C
C
      M1 = 2*NB                                                             B2Y03860
      DO 250 K = 1, M1                                                      B2Y03870
  250 READ (4)                                                              B2Y03880
      M1=NT+1
      N1=2*NT
      DO 300 K = 1, FLG11                                                   B2Y03910
      READ (4) (VNS(I), I = M1, N1)                                         B2Y03920
      READ(4)                                                               B2Y03930
      M1 = M1 + NT                                                          B2Y03940
  300 N1 = N1 + NT                                                          B2Y03950
  400 NPFLG = 0                                                             B2Y03960
      A2 = 0.                                                               B2Y03970
      B2 = 0.                                                               B2Y03980
      L = NT                                                                B2Y03990
  500 DO 1500 J = 1, L                                                      B2Y04000
      M1 = 1                                                                B2Y04010
      N1 = ND(1) - 1                                                        B2Y04020
      J1 = J - L                                                            B2Y04030
      J2 = 0                                                                B2Y04040
      J4 = 0                                                                B2Y04050
      T1 = CMPLX( COSA(J), -SINA(J) )                                       B2Y04060
      DO 1200 I = 1, NB                                                     B2Y04070
```

```
      J1 = J1 + L                                                       B2Y04080
      J4 = J4 + 1                                                       B2Y04090
C     IF (SP .NE. 0.0) TF = CSINH(3.14159265E)*(Z(J)-Q(M1))/SP)         B2Y04100
      DO 1000 K = M1, N1                                                B2Y04110
      J2 = J2 + 1                                                       B2Y04120
      CALL FORM1 ( J, K, J2, Z, Q, SINA, COSA, W1 )                     B2Y04140
  700 IF ( NPFLG .NE. 0 )  GO TO 750                                    B2Y04260
  720 T2 = CONJG(W1) * T1                                               B2Y04270
      A1 = AIMAG( T2 )                                                  B2Y04280
      IF (J .EQ. J2)  A1 = ABS( A1 )                                    B2Y04290
      B1 = REAL( T2 )                                                   B2Y04300
      GO TO 800                                                         B2Y04310
  750 A1 = - AIMAG( W1 )                                                B2Y04320
      B1 = REAL( W1 )                                                   B2Y04330
  800 GO TO N50,(850,900)                                               B2Y04340
  850 VNS(J1) = VNS(J1) - B1 + B2                                       B2Y04350
      VTS(J1) = VTS(J1) + A1 - A2                                       B2Y04360
  900 A(J2) = A1 + A2                                                   B2Y04370
 1000 B(J2) = B1 + B2                                                   B2Y04380
      GO TO N51,(1050,1100)                                             B2Y04390
 1050 VNS(J1) = VNS(J1) / SUMDS(J4)                                     B2Y04400
      VTS(J1) = VTS(J1) / SUMDS(J4)                                     B2Y04410
 1100 M1 = N1 + 2                                                       B2Y04420
 1200 N1 = N1 + ND(I+1)                                                 B2Y04430
      VNST(1) = - SINA(J)                                               B2Y04440
      VNST(2) =   COSA(J)                                               B2Y04450
       IF( FLG11 .LT. 1 )       GO TO 1275                              B2Y04460
      KL = J - L                                                        B2Y04470
      DO 1250 I = 3, NCFLG                                              B2Y04480
      KL = KL + L                                                       B2Y04490
 1250 VNST(I) =    VNS(KL)                                              B2Y04500
 1275 WRITE (10) ( A(I), I = 1, NT), ( VNST(KL), KL = 1, NCFLG )        B2Y04510
      WRITE (10) ( B(I), I = 1, NT )                                    B2Y04520
      IF ( FLG07 .EQ. 0 )  GO TO 1300                                   B2Y04530
      WRITE (6, 5) J, (A(I), I = 1, NT)                                 B2Y04540
    5 FORMAT (1H0 12H   AJK   ROW I4 // (6F15.8) )                      B2Y04550
      WRITE (6, 10)J, (B(I), I = 1, NT)                                 B2Y04560
   10 FORMAT (1H0 12H   BJK   ROW  I4 // (6F15.8) )                     B2Y04570
 1300 WRITE ( 8) ( A(I), I = 1, NT )                                    B2Y04580
      WRITE ( 8) ( B(I), I = 1, NT )
 1500 CONTINUE                                                          B2Y04600
C
      M = 1                                                             B2Y04620
      N = L                                                             B2Y04630
      DO 2000 J = 1, NB                                                 B2Y04640
      IF ( NLF(J) .NE. 0 ) GO TO 1800                                   B2Y04650
      WRITE (4) (VNS(I), I = M, N )                                     B2Y04660
      WRITE (4) (VTS(I), I = M, N )                                     B2Y04670
 1800 M = N + 1                                                         B2Y04680
 2000 N = N + L                                                         B2Y04690
      IF ( FLG07 .EQ. 0 )  GO TO 3000                                   B2Y04700
      N = NB * L                                                        B2Y04710
      WRITE (6, 15) ( VNS(I), I = 1, N )                                B2Y04720
      WRITE (6, 20) ( VTS(I), I = 1, N )                                B2Y04730
   15 FORMAT (1H0/10X 3HVNS /// (6F15.8) )                              B2Y04740
   20 FORMAT (1H0 / 10X 3HVTS /// (6F15.8) )                            B2Y04750
 3000 IF ( FLG02 .EQ. 0 .OR. NPFLG .NE. 0 )  RETURN                     B2Y04760
      NPFLG = 1                                                         B2Y04770
      L = ND(NB+1)                                                      B2Y04780
      READ (9) ( Z(I), I = 1, L )                                       B2Y04790
```

```
      K = NB * L                                                        B2Y04800
      DO 3100 I = 1, K                                                  B2Y04810
      VNS(I) = 0.                                                       B2Y04820
 3100 VTS(I) = 0.                                                       B2Y04830
      ASSIGN 850 TO N50                                                 B2Y04840
      ASSIGN 1050 TO N51                                                B2Y04850
      GO TO 500                                                         B2Y04860
      END                                                               B2Y04870


$IBFTC B2Y4
CDECK B2Y4                                                              B2Y04880
      SUBROUTINE  FORM1  ( J, K, J2, Z, Q, SINA, COSA, W )              B2Y04890
      COMPLEX  IM, Z, Q, W, CLOG                                        B2Y04900
      COMMON IM,HEDR,CASE,RPI,R2PI,SP,CL,ALPHA,FALPHA,NER,NT,NB,NCFLG   B2Y04910
      DIMENSION   Z(299), Q(300), SINA(299), COSA(299)                  B2Y04920
      DIMENSION HEDR(15),CASE(2)                                        B2Y04930
      W = CLOG ( (Z(J)-Q(K)) / (Z(J)-Q(K+1)) )                          B2Y04940
      W = ( COSA(J2) - IM*SINA(J2) ) * R2PI * W                         B2Y04950
      RETURN                                                            B2Y04960
      END                                                               B2Y04970


$ORIGIN       ALPHA
$IBFTC B2Y9
CDECK B2Y9                                                              B2Y06110
      SUBROUTINE  PART4                                                 B2Y06120
      COMPLEX  IM                                                       B2Y06130
      INTEGER  FLG02, FLG03, FLG04, FLG05, FLG06, FLG07                 B2Y06140
     1, FLG08, FLG09, FLG10, FLG11, FLG12                               B2Y06150
      DIMENSION  A(300    ), R(300, 5), ND(10), NLF(10)                 B2Y06160
      DIMENSION HEDR(15),CASE(2),SUMDS(10),XMC(8),YMC(8),ADDY(8)        B2Y06170
      COMMON IM,HEDR,CASE,RPI,R2PI,SP,CL,ALPHA,FALPHA,DALFA,CHORD,SUMDS,B2Y06180
     1      XMC,YMC,ADDY,FLG02,FLG03,FLG04,FLG05,FLG06,FLG07,FLG08,     B2Y06190
     2      FLG09,FLG10,FLG11,FLG12,ND,NLF,NER,NT,NB,NCFLG              B2Y06200
       REWIND 1                                                         B2Y06210
      REWIND  3                                                         B2Y06220
      REWIND  4                                                         B2Y06230
      REWIND 10                                                         B2Y06240
      M = 1                                                             B2Y06250
      N = ND(1) - 1                                                     B2Y06260
      DO 100 K = 1, NB                                                  B2Y06270
      READ (4) ( R(I,1), I = M, N )                                     B2Y06280
      READ (4) ( R(I,2), I = M, N )                                     B2Y06290
      M = N + 1                                                         B2Y06300
  100 N = N + ND(K+1) - 1                                               B2Y06310
C     PRECEDING READS IN SINES, COSINES. ONSET FLOWS NEXT ( IF ANY).    B2Y06320
      IF ( NCFLG .LE. 2 )  GO TO 180                                    B2Y06330
      DO 150 J = 3, NCFLG                                               B2Y06340
      READ (4) ( R(I,J), I = 1, NT )                                    B2Y06350
  150 READ (4)                                                          B2Y06360
  180 DO 200 J = 2, NCFLG                                               B2Y06370
      DO 200 I = 1, NT                                                  B2Y06380
  200 R(I, J) = -R(I, J)                                                B2Y06390
  250 DO 300 I = 1, NT                                                  B2Y06400
      READ (10) ( A( J ), J = 1, NT )                                   B2Y06410
      READ (10)                                                         B2Y06420
  300 WRITE(1) (A(J), J=1, NT),(R(I, J), J=1, NCFLG)                    B2Y06430
```

```
      END FILE 1                                                        B2Y06440
      REWIND 1                                                          B2Y06450
      RETURN                                                            B2Y06460
      END                                                               B2Y06470
```

```
$ORIGIN        ALPHA
$IBFTC C20X9
C20X9                                                                   B2Y06480
      SUBROUTINE  SOLVIT (A, ND, MD, KD, NI, MM, NO, NW, *)             B2Y06490
      DIMENSION  A ( KD )                                               B2Y06620
C                                                                       B2Y06630
      LOGICAL  LAST                                                     B2Y06640
C                                                                       B2Y06650
      N = ND                                                            B2Y06680
      M = MD                                                            B2Y06690
      KORE = KD                                                         B2Y06700
      NPM = N + M                                                       B2Y06710
      IF (MAX0(3 * NPM, M * N) .GT. KORE) RETURN 1                      B2Y06720
      MT = MM                                                           B2Y06730
      REWIND MT                                                         B2Y06740
      NIN = NI                                                          B2Y06750
      REWIND NIN                                                        B2Y06760
      NOUT = NO                                                         B2Y06770
      REWIND NOUT                                                       B2Y06780
      MP1 = M + 1                                                       B2Y06790
      NN = N                                                            B2Y06800
      NEL = NPM                                                         B2Y06810
C                                                                       B2Y06820
C - - CALCULATE THE MAXIMUM NO. OF ROWS, 'K'                            B2Y06830
C                                                                       B2Y06840
   10 K = (KORE - NEL) / NEL                                            B2Y06850
C                                                                       B2Y06860
C - - TEST TO SEE IF THE REST OF THE MATRIX WILL FIT IN CORE            B2Y06870
C                                                                       B2Y06880
      LAST = K .GE. NN                                                  B2Y06890
      IF (LAST) K = NN                                                  B2Y06900
C                                                                       B2Y06910
C - - READ 'K' ROWS OF THE AUGMENTED 'A' MATRIX                         B2Y06920
C                                                                       B2Y06930
   30 NT = 0                                                            B2Y06940
      DO 40 IB = 1, K                                                   B2Y06950
      NS = NT + 1                                                       B2Y06960
      NT = NT + NEL                                                     B2Y06970
   40 READ (NIN) (A(IO), IO = NS, NT)                                   B2Y06980
C                                                                       B2Y06990
C - - CHECK TO SEE IF WE WERE UNLUCKY ENOUGH TO END UP WITH ONLY ONE ROWB2Y07000
C                                                                       B2Y07010
      IF (K .EQ. 1) GO TO 90                                            B2Y07020
C                                                                       B2Y07030
C - - 'K' IS GREATER THAN '1' SO WE CAN START THE TRIANGULARIZATION     B2Y07040
C                                                                       B2Y07050
      NELP1 = NEL + 1                                                   B2Y07060
      NS = - NEL                                                        B2Y07070
      NELP2 = NELP1 + 1                                                 B2Y07080
C                                                                       B2Y07090
```

```
C - - FORM THE 'TRAPEZOIDAL' ARRAY  (8)                               B2Y07100
C                                                                     B2Y07110
      DO 50 IB = 2, K                                                 B2Y07120
      NP = NELP2 - IB                                                 B2Y07130
      NS = NS + NELP1                                                 B2Y07140
      NT = NS                                                         B2Y07150
      DO 50 IO = IB, K                                                B2Y07160
      NT = NT + NEL                                                   B2Y07170
      MN = NT                                                         B2Y07180
      NB = NS                                                         B2Y07190
      A(NT) = (-A(NT)) / A(NS)                                        B2Y07200
      DO 50 NF = 2, NP                                                B2Y07210
      MN = MN + 1                                                     B2Y07220
      NB = NB + 1                                                     B2Y07230
   50 A(MN) = A(MN) + A(NT) * A(NB)                                   B2Y07240
      IF (LAST) GO TO 90                                              B2Y07250
C                                                                     B2Y07260
C - - WRITE THE 'TRAPEZOIDAL' MATRIX ON TAPE                          B2Y07270
C                                                                     B2Y07280
      NT = 0                                                          B2Y07290
      NP = NEL                                                        B2Y07300
      NS = - NEL                                                      B2Y07310
      DO 60 IO = 1, K                                                 B2Y07320
      NS = NS + NELP1                                                 B2Y07330
      NT = NT + NEL                                                   B2Y07340
      WRITE (MT) NP, (A(IB), IB = NS, NT)                             B2Y07350
   60 NP = NP - 1                                                     B2Y07360
      NP = NP - M                                                     B2Y07370
      NS = KORE - NEL + 1                                             B2Y07380
C                                                                     B2Y07390
C - - READ ANOTHER ROW                                                B2Y07400
C                                                                     B2Y07410
      DO 80 IO = 1, NP                                                B2Y07420
      READ (NIN) (A(IB), IB = NS, KORE)                               B2Y07430
C                                                                     B2Y07440
C - - MODIFY THIS ROW BY THE 'TRAPEZOIDAL' ARRAY                      B2Y07450
C                                                                     B2Y07460
      NT = 1                                                          B2Y07470
      MN = NS                                                         B2Y07480
      DO 70 IB = 1, K                                                 B2Y07490
      NB = NT                                                         B2Y07500
      NF = MN + 1                                                     B2Y07510
      A(MN) = (-A(MN)) / A(NT)                                        B2Y07520
      DO 65 NN = NF, KORE                                             B2Y07530
      NB = NB + 1                                                     B2Y07540
   65 A(NN) = A(NN) + A(MN) * A(NB)                                   B2Y07550
      MN = NF                                                         B2Y07560
   70 NT = NT + NELP1                                                 B2Y07570
C                                                                     B2Y07580
C - - WRITE THE MODIFIED ROW ON TAPE                                  B2Y07590
C                                                                     B2Y07600
   80 WRITE (NOUT)      (A(NT), NT = MN, KORE)                        B2Y07610
      REWIND NOUT                                                     B2Y07620
      REWIND NIN                                                      B2Y07630
C                                                                     B2Y07640
C - - SWITCH THE TAPES                                                B2Y07650
C                                                                     B2Y07660
      NT = NIN                                                        B2Y07670
      NIN = NOUT                                                      B2Y07680
      NOUT = NT                                                       B2Y07690
```

```
C
C - - RE-CALCULATE ROW LENGTH AND LOOP BACK
C
      NEL = NEL - K
      NN = NEL - M
      GO TO 10
C
C - - REWIND ALL TAPES
C
   90 REWIND MT
      REWIND NIN
      REWIND NOUT
C
C - - CONDENSE THE MATRIX
C
      NN = NEL
      NL = NELP1
      IF (K .EQ. 1) GO TO 105
      NS = 1
      NT = NEL
      DO 100 IB = 2, K
      NS = NS + NELP1
      NT = NT + NEL
      DO 100 IO = NS, NT
      A(NL) = A(IO)
  100 NL = NL + 1
  105 N1 = KORE - K * M + 1
C
C - - THERE, NOW WE CAN START THE BACK-SOLUTION
C * * NOTE..THE FIRST AVAILABLE LOCATION FOR THE SOLUTIONS IS A(N1)
C
      NREM = N
      NEL = NPM
      LAST = K .EQ. N
      NPASS = 0
C
C - - SOLVE FOR THE ANSWERS CORRESPONDING TO 'K' ROWS
C
  110 KM1 = K - 1
      KP1 = K + 1
      NS = NL - MP1
      NPASS = NPASS + 1
      DO 130 MN = 1, M
      NF = NS + MN
      A(NF) = A(NF) / A(NS)
      NT = NS
      IF (KM1 .EQ. 0) GO  TO 130
      DO 125 IB = 1, KM1
      NF = NF - IB - M
      NT = NT - MP1 - IB
      SUM = 0.0
      NP = NF
      N2 = MP1 + IB
      DO 120 IO = 1, IB
      NN = NT + IO
      NP = NP + N2 - IO
  120 SUM = SUM + A(NN) * A(NP)
  125 A(NF) = (A(NF) - SUM) / A(NT)
  130 CONTINUE
C
```

```
C - - MOVE THE SOLUTIONS TO CONTIGUOUS LOCATIONS STARTING AT A(N1)
C
      N1 = KORE + 1
      DO 140 NN = 1, K
      DO 135 MN = 1, M
      NL = NL - 1
      N1 = N1 - 1
  135 A(N1) = A(NL)
  140 NL = NL - NN
C
C - - WRITE THE SOLUTIONS ON TAPE
C
      WRITE (NIN) K
      NS = N1 - 1
      DO 145 MN = 1, M
      NT = NS + MN
  145 WRITE ( NIN ) (A(IO), IO = NT, KORE, M)
C
C - - TEST IF THIS IS THE LAST PASS
C
      IF (LAST) GO TO 200
C
C - - WE MUST NOW MODIFY THE TRIANGULAR MATRIX TO REFLECT THE EFFECT OF
C     THE SOLUTIONS OBTAINED SO FAR  (EQ 21)
C * * NOTE..LOCATIONS A(1) TO A(N1-1) ARE NOW FREE TO USE
C
C - - CALCULATE THE NEXT VALUES OF 'NEL' AND 'NREM'
C
      NELOLD = NEL
      KOLD = K
      NEL = NEL - K
      NREM = NREM - K
C
C - - NOW APPLY THE INCREDIBLE FORMULA FOR THE NEW 'K'
C
      K = (-4 * M - 1) / 2 + IFIX(SQRT(0.25 + FLOAT((4 * M + 2) * M +
     1 2 * (KORE - NELOLD))))
      NROW = NREM - K + 1
      IF (K .LT. NREM) GO TO 150
      LAST = .TRUE.
      NROW = 1
      K = NREM
  150 NS = 1
      NT = NELOLD + 1
C
C - - READ IN THE ROWS TO BE MODIFIED
C
      DO 190 IB = 1, NREM
      NT = NT - 1
      IF (IB .LE. NROW) GO TO 160
      NS = NS + NN
      NT = NT + NN
  160 READ ( MT ) NN, (A(IO), IO = NS, NT)
      NP = N1 - 1
      NF = NT - M - KM1
      NN = NN - KOLD
      DO 170 MN = 1, M
      N2 = NF
      NA = NP + MN
      NB = NA
```

```
      SUM = 0.0
      DO 165 IO = 1, KOLD
      SUM. = SUM + A(N2) * A(NA)
      N2 = N2 + 1
  165 NA = NA + M
      N2 = N2 + MN - 1
  170 A(N2) = A(N2) - SUM
C
C - - WRITE THE MODIFIED ROW ON TAPE OR CONDENSE THE ROW
C
      NL = NT - M + 1
      IF (IB .GE. NROW) GO TO 175
      NF = NL - KP1
      WRITE (NOUT) NN, (A(IO), IO = NS, NF), (A(IO), IO = NL, NT)
      GO TO 190
  175 NF = NL - KOLD
      DO 180 MN = NL, NT
      A(NF) = A(MN)
  180 NF = NF + 1
  190 CONTINUE
      REWIND MT
      REWIND NOUT
C
C - - SWITCH THE TAPES
C
      NT = MT
      MT = NOUT
      NOUT = NT
C
C - - LOOP BACK THRU THE SOLUTION
C
      NL = NF
      GO TO 110
C
C - - START TO WRAP IT UP
C
  200 REWIND NIN
      N2 = N
C
C * * NOTE.. AT THIS POINT ALL LOCATIONS A(1) THRU A(KORE) ARE FREE
C
      DO 220 IB = 1, NPASS
      READ (NIN) K
      N1 = N2 - K + 1
      NS = N1
      NT = N2
C
C - - READ IN THE SOLUTIONS
C
      DO 210 IO = 1, M
      READ (NIN) (A(NN), NN = NS, NT)
      NT = NT + N
  210 NS = NS + N
  220 N2 = N1 - 1
C
C - - WRITE THE SOLUTIONS ON TAPE
C
      NT = 0
      DO 230 IO = 1, M
      NS = NT + 1
```

```
      NT = NT + N                                                       B2Y09500
  230 WRITE (NW) (A(NN), NN = NS, NT)                                   B2Y09510
C                                                                       B2Y09520
      RETURN                                                            B2Y09580
      END                                                               B2Y09590




$ORIGIN        ALPHA
$IBFTC B2YE
CDECK B2YE                                                              B2Y10740
      SUBROUTINE  PART5                                                 B2Y10750
      COMPLEX  IM                                                       B2Y10760
      INTEGER  FLG02, FLG03, FLG04, FLG05, FLG06, FLG07                 B2Y10770
     1, FLG08, FLG09, FLG10, FLG11, FLG12                               B2Y10780
      DIMENSION  B(299), VT(299, 5), SIG(299, 5), T(299, 5), CP(299, 6) B2Y10790
     1, ND(10), NLF(10), X(300), Y(300), XMP(299), YMP(299),CASE(2)     B2Y10800
     2, SUMDS(10), XMC(8), YMC(8), ADDY(8),HEDR(15), VELID(10),VID(2)   B2Y10810
      COMMON IM,HEDR,CASE,RPI,R2PI,SP,CL,ALPHA,FALPHA,DALFA,CHORD,SUMDS,B2Y10820
     1       XMC,YMC,ADDY,FLG02,FLG03,FLG04,FLG05,FLG06,FLG07,FLG08,    B2Y10830
     2       FLG09,FLG10,FLG11,FLG12,ND,NLF,NER,NT,NB,NCFLG,FLG15,FLG16
      COMMON SUMSIG,VINF,MON,BETA,CDIM,VREF,DELT,FLG13,FLG14,ITER,ALF2
      EQUIVALENCE  ( T, CP )                                            B2Y10850
      DATA VELID / 3H V0, 4H V90, 3H V1, 3H V2, 3H V3, 3H V4, 3H V5,    B2Y10860
     1 3H V6, 3H V7, 3H V8 /,BLANK/1H /                                 B2Y10870
      REWIND  3                                                         B2Y10880
      REWIND  4                                                         B2Y10890
      REWIND 10                                                         B2Y10900
      REWIND 8
      REWIND 12                                                         B2Y10920
      REWIND 13                                                         B2Y10930
      M = 1                                                             B2Y10940
      N = ND(1) - 1                                                     B2Y10950
      DO 100 K = 1, NB                                                  B2Y10960
      READ (4) ( T(I,2), I = M, N )                                     B2Y10970
      READ (4) ( T(I,1), I = M, N )                                     B2Y10980
C     READS IN SINES AND COSINES                                        B2Y10990
      M = N + 1                                                         B2Y11000
  100 N = N + ND(K+1) - 1                                               B2Y11010
      IF ( NCFLG .LE. 2 )  GO TO 200                                    B2Y11020
      DO 150 J = 3, NCFLG                                               B2Y11030
      READ (4)                                                          B2Y11040
  150 READ (4) ( T(I,J), I = 1, NT )                                    B2Y11050
  200 DO 250 J = 1, NCFLG                                               B2Y11060
  250 READ (3) ( SIG(I,J), I = 1, NT )                                  B2Y11070
      DO 400 I = 1, NT                                                  B2Y11080
      READ (10)                                                         B2Y11090
      READ (10) ( B(L), L = 1, NT )                                     B2Y11100
      DO 400 J = 1, NCFLG                                               B2Y11110
      PR = 0.                                                           B2Y11120
      DO 300 L = 1, NT                                                  B2Y11130
  300 PR = PR + B(L)*SIG(L,J)                                           B2Y11140
      VT(I,J) = PR + T(I,J)                                             B2Y11150
  400 CP(I,J) = 1. - VT(I,J)**2                                         B2Y11160
      DO 500 J = 1, NCFLG                                               B2Y11170
  500 WRITE ( 8) ( VT(I,J), I = 1, NT )
      IF (MON-1) 510,520,520
```

```
  510 M = 1                                                              B2Y11190
      N = ND(1)                                                          B2Y11200
      M1 = 1                                                             B2Y11210
      N1 = ND(1) - 1                                                     B2Y11220
      DO 700 J = 1, NB                                                   B2Y11230
      READ (13) ( X(I), I = M, N )                                       B2Y11240
      READ (13) ( Y(I), I = M, N )                                       B2Y11250
      READ (13) ( XMP(I), I = M1, N1 )                                   B2Y11260
      READ (13) ( YMP(I), I = M1, N1 )                                   B2Y11270
      M = N + 1                                                          B2Y11280
      N = N + ND(J+1)                                                    B2Y11290
      M1 = N1 + 1                                                        B2Y11300
  700 N1 = N1 + ND(J+1) - 1                                              B2Y11310
      DO 2500 L = 1, NCFLG                                               B2Y11320
      I = 1                                                              B2Y11330
      J = 1                                                              B2Y11340
      M = 1                                                              B2Y11350
      N = ND(1)                                                          B2Y11360
      LCTR = 220
      K = L - 2                                                          B2Y11380
      IF (FLG10 .LT. 2) GO TO 1000                                       B2Y11390
 1000 WRITE (6, 1100)  HEDR, CASE                                        B2Y11440
 1100 FORMAT (1H1 25X 26HDOUGLAS  AIRCRAFT  COMPANY / 28X 21HLONG  BEACHB2Y11450
     1  DIVISION //// 5X,15A4,// 6H CASE ,2A4)                           B2Y11460
       IF( K )  1150, 1300, 1500                                         B2Y11470
 1150 WRITE (6, 1200)                                                    B2Y11480
 1200 FORMAT (1H 19HSTREAMFLOW SOLUTION )                                B2Y11490
      GO TO 1700                                                         B2Y11500
 1300 WRITE (6, 1400)                                                    B2Y11510
 1400 FORMAT (1H 23H90-DEGREE FLOW SOLUTION )                            B2Y11520
      GO TO 1700                                                         B2Y11530
 1500 WRITE (6, 1600)  K                                                 B2Y11540
 1600 FORMAT (1H 35HNON-UNIFORM ONSET FLOW SOLUTION NO. I3 )             B2Y11550
 1700 IF (FLG12.LE.0) WRITE (6,1800)                                     B2Y11560
 1800 FORMAT (1H 25HUNTRANSFORMED COORDINATES // )                       B2Y11570
      IF (FLG12.GT.0) WRITE (6,1900)                                     B2Y11580
 1900 FORMAT (1H 23HTRANSFORMED COORDINATES // )                         B2Y11590
      WRITE (6,1950)                                                     B2Y11600
 1950 FORMAT (12X 1HX 13X 1HY 14X 1HV 12X 2HCP 11X 5HSIGMA // )          B2Y11610
 2000 WRITE (6, 2100) I, X(I), Y(I), XMP(J), YMP(J), VT(J,L)             B2Y11620
     1, CP(J,L), SIG(J,L)                                                B2Y11630
 2100 FORMAT (1H  I3, 2F14.8 / 4X 5F14.8 )                               B2Y11640
      I = I + 1                                                          B2Y11650
      J = J + 1                                                          B2Y11660
      IF ( I .EQ. N )  GO TO 2200                                        B2Y11670
      IF ( I .LE. LCTR)  GO TO 2000                                      B2Y11680
      LCTR = LCTR + 22                                                   B2Y11690
      GO TO 1000                                                         B2Y11700
 2200 M = M + 1                                                          B2Y11710
      N = N + ND(M)                                                      B2Y11720
      WRITE (6, 2300)  I, X(I), Y(I)                                     B2Y11730
 2300 FORMAT (1H  I3, 2F14.8 // )                                        B2Y11740
      I = I + 1                                                          B2Y11750
      IF ( J .GE. NT )  GO TO 2500                                       B2Y11760
      GO TO 2000                                                         B2Y11770
 2500 CONTINUE                                                           B2Y11780
  520 RETURN                                                             B2Y11790
      END                                                                B2Y11800
```

```
$ORIGIN        ALPHA
$IBFTC B2YF
CDECK B2YF                                                              B2Y11810
      SLBROUTINE  PART6                                                 B2Y11820
      COMPLEX  IM                                                       B2Y11830
      INTEGER  FLG02, FLG03, FLG04, FLG05, FLG06, FLG07                 B2Y11840
     1, FLG08, FLG09, FLG10, FLG11, FLG12                               B2Y11850
       DIMENSION SIGMA(299, 4), SUMA(300, 4), SUMB(300, 4)
      DIMENSION THETV(299)
      DIMENSION  VC(299), X(300), Y(300), XMP(299), YMP(299), XM(299)   B2Y11870
     1, YM(299), SINA(299), COSA(299), CP(299), DELS(299), ND(10)       B2Y11880
     2, NLF(10), SUMDS(10), GAM(9), XMC(8), YMC(8), HEDR(15),ADDY(8)    B2Y1189
     4, YTEMP(1500), VXL(299), VYL(299), XIJ(299), YIJ(299), DVA(9,8)   B2Y11910
     3, DVT(9,10),DV(9,9),DELSUT(299),SIGT(299), XTEMP(1500)            B2Y11900
     5, DVX(9,10), ZTEMP(300),VCID(2),VXID(2),VYID(2),GAMT(8),CASE(2)   B2Y11920
      DIMENSION PRES(299),XN(299),YN(299)
       DIMENSION XID(2), YID(2), XIDOFF(2), YIDOFF(2)                   B2Y11930
      COMMON IM,HEDR,CASE,RPI,R2PI,SP,CL,ALPHA,FALPHA,DALFA,CHORD,SUMDS,B2Y11940
     1       XMC,YMC,ADDY,FLG02,FLG03,FLG04,FLG05,FLG06,FLG07,FLG08,    B2Y11950
     2       FLG09,FLG10,FLG11,FLG12,ND,NLF,NER,NT,NB,NCFLG,FLG15,FLG16
      COMMON SUMSIG,VINF,MON,BETA,CDIM,VREF,DELT,FLG13,FLG14,ITER,ALF2
      EQUIVALENCE  (GAM, DVT), (DV, DVT(10)), (DVA, DVT(19))            B2Y11970
     1, (VXL, XMP), (VYL, YMP), (SIGT, XM), (XIJ, SINA), (YIJ, COSA)    B2Y11980
     2, (ZTEMP, XTEMP(300))
      DATA VCID,VXID,VYID/4H    V,1HC,4H    V,1HX,4H    V,1HY/          B2Y12000
       DATA XID /6H  XM5 ,1HP/,YID/6H  YM  ,1HP/                        B2Y12010
       DATA XIDOFF /4H XO ,3HFFB/,YIDOFF/4H  YO,3HFFB/                  B2Y12020
      SPP = SP                                                          B2Y12030
C      I( 'S77 .E8. 0.0)  SPP = 1.0 E6                                  + Y  040
      IF (FLG08 .EQ. 0  .OR.  FLG02 .EQ. 0)  GO TO 40                   B2Y12050
      REWIND 10                                                         B2Y12060
      J = 2 * NT                                                        B2Y12070
      DO 30 I = 1, J                                                    B2Y12080
   30 READ (10)                                                         B2Y12090
C **  LOOP SKIPS BOTH ON-BODY MATRICES                                  B2Y12100
   40 NER = 0                                                           B2Y12110
      DET = 1.                                                          B2Y12120
      K = NCFLG - 2                                                     B2Y12130
      REWIND 7
      REWIND  3                                                         B2Y12140
      REWIND  4                                                         B2Y12150
      REWIND 8
      REWIND 12                                                         B2Y12170
      REWIND 13                                                         B2Y12180
      DO 50 J = 1, 10                                                   B2Y12190
      DO 50 I = 1, 9                                                    B2Y12200
      DVX(I,J) = 0.                                                     B2Y12210
   50 DVT(I,J) = 0.                                                     B2Y12220
      IF ( FLG04 .NE. 0 )  ALPHA = DALFA                                B2Y12240
      IF ( FLG06 .NE. 0 )  ALPHA = 0.                                   B2Y12250
      ALPHA = ALPHA / 57.2957795E0                                      B2Y12260
      CSALF = COS(ALPHA)                                                B2Y12270
      SNALF = SIN(ALPHA)                                                B2Y12280
      READ ( 8) ( XTEMP(I), I = 1, NT )
      READ ( 8) ( YTEMP(I), I = 1, NT )
      M = 1                                                             B2Y12310
```

```
      N = ND(1) - 1                                                     B2Y12320
      DO 100 I = 1, NB                                                  B2Y12330
      GAM(I) = (XTEMP(M) + XTEMP(N))*CSALF                              B2Y12340
      GAM(I) = - ( GAM(I) + (YTEMP(M)+YTEMP(N)) *SNALF )                B2Y12350
      M = N+1                                                           B2Y12360
  100 N = N + ND(I+1) - 1                                               B2Y12370
      IF ( K .EQ. 0 )  GO TO 160                                        B2Y12380
      DO 150 J = 1, K                                                   B2Y12390
      READ ( 8) ( ZTEMP(I), I = 1, NT )
      M = 1                                                             B2Y12410
      N = ND(1) - 1                                                     B2Y12420
      DO 150 I = 1, NB                                                  B2Y12430
      DVA(I,J) = ZTEMP(M) + ZTEMP(N)                                    B2Y12440
  150 DVX(I,J) = DVA(I,J)                                               B2Y12450
  160 REWIND  8
      GAM(1)=(GAM(1)-DVA(1,1)) /DVA(1,2)
 5040 READ ( 8) ( XTEMP(I), I = 1, NT )
      SNALF = SIN( ALPHA )                                              B2Y13870
      READ ( 8) ( YTEMP(I), I = 1, NT )
      DO 5070 I = 1, NT                                                 B2Y13890
 5070 VC(I) = XTEMP(I)*CSALF + YTEMP(I)*SNALF                           B2Y13900
      READ ( 8) ( XTEMP(I), I = 1, NT )
      DO 5100 I = 1, NT                                                 B2Y13940
 5100 VC(I) = VC(I) + XTEMP(I)
      IF(NLF(1).NE.0) GO TO 5150
      READ(8) (XTEMP(I),I=1,NT)
      DO 5125 I=1,NT
 5125 VC(I)=VC(I)+XTEMP(I)*GAM(1)
 5150 DO 5200 I = 1, NT                                                 B2Y13960
 5200 CP(I) = 1. - VC(I)*VC(I)                                          B2Y13970
      M = 1                                                             B2Y13980
      N = ND(1) - 1                                                     B2Y13990
      M1 = 1                                                            B2Y14000
      N1 = ND(1)                                                        B2Y14010
      DO 5250 J = 1, NB                                                 B2Y14020
      READ (4) ( SINA(I), I = M, N )                                    B2Y14030
      READ (13) ( X(I), I = M1, N1 )                                    B2Y14040
      READ (4) ( COSA(I), I = M, N )                                    B2Y14050
      READ (13) ( Y(I), I = M1, N1 )                                    B2Y14060
      READ (13) ( XMP(I), I = M, N )                                    B2Y14070
      READ (13) ( YMP(I), I = M, N )                                    B2Y14080
      READ (12) ( XM(I), I = M, N )                                     B2Y14090
      READ (12) ( YM(I), I = M, N )                                     B2Y14100
      READ (12) ( DELS(I), I = M, N )                                   B2Y14110
      M1 = N1 + 1                                                       B2Y14120
      N1 = N1 + ND(J+1)                                                 B2Y14130
      M = N + 1                                                         B2Y14140
 5250 N = N + ND(J+1) - 1                                               B2Y14150
       M=1
      N=ND(1)-1
      DO 5210 I=M,N
      XN(I+1)=(X(I)+X(I+1))/2.0
      YN(I+1)=(Y(I)+Y(I+1))/2.0
 5210 PRES(I+1)=CP(I)
      WRITE (7) (PRES(I+1),I=M,N)
      WRITE (7) (CP (I),I=M,N)
      WRITE (7) (XN(I+1),I=M,N)
      WRITE (7) (YN(I+1),I=M,N)
      IF (MON-2) 5220,5230,5230
 5220 PUNCH 5551, L,ALPHA
```

```
 5551 FORMAT (I5,F10.5)
      CALL BCDUMP (XMP(M),XMP(N))                                              2
      CALL BCDUMP (YMP(M),YMP(N))
      CALL BCDUMP (VC (M),VC (N))
 5230 IF (FLG12 .LE. 0)  GO TO 5252
      DO 5251 I = 1,NT                                                  B2Y14170
 5251 DELSUT(I) = DELS(I)                                               B2Y14180
      GO TO 5301                                                        B2Y14190
 5252 DO 5300 I = 1,NT                                                  B2Y14200
 5300 DELSUT(I) = SQRT( (X(I+1)-X(I))**2 + (Y(I+1)-Y(I))**2 )           B2Y14210
 5301 GT = 0.0                                                          B2Y14220
      DO 5350 I = 1, 1
 5350 GT = GT + GAM(I)                                                  B2Y14240
      T=0.0
C     T = .5 * GT / SPP                                                 B2Y14250
      IF ( FLG05 .EQ. 0 ) FALPHA= ATAN2 (SNALF+T , CSALF)               B2Y14260
      ALFEX = ATAN2 (SNALF - T, CSALF)                                  B2Y14270
      ALFEX = ALFEX * 57.2957795E0                                      B2Y14280
      FALPHA = FALPHA * 57.2957795E0                                    B2Y14290
      ALPHA = ALPHA * 57.2957795E0                                      B2Y14300
      IF ( FLG04 .EQ. 0 )  DALFA = FALPHA - ALFEX                       B2Y14310
      VIN = SQRT ( 1. + 2.*SNALF*T + T*T )                              B2Y14320
      VEX = SQRT ( 1. - 2.*SNALF*T + T*T )                              B2Y14330
 5375 J = 1                                                             B2Y14340
      K1 = 1                                                            B2Y14350
      M = 1                                                             B2Y14360
      N = ND(1) - 1                                                     B2Y14370
      DO 5800 L = 1, NB                                                 B2Y14380
      LCTR = 190
      CL = 0.0                                                          B2Y14400
      CD = 0.0                                                          B2Y14410
      CM = 0.0                                                          B2Y14420
      DO 5400 I = M, N                                                  B2Y14430
      T = CP(I) * DELS(I)                                               B2Y14440
      CL = CL - T*COSA(I)                                               B2Y14450
      CD = CD + T*SINA(I)                                               B2Y14460
 5400 CM = CM + T*(COSA(I)*(XM(I)-XMC(L)) + SINA(I)*(YM(I)-YMC(L)) )    B2Y14470
      AAA=CHORD/CDIM
      CL=CL*AAA
      I = 1                                                             B2Y14480
      K2 = ND(L)                                                        B2Y14490
 5500 WRITE (6, 5550)  HEDR, SP, ALPHA, DALFA, FALPHA, VIN, XMC(L),     B2Y14500
     1 ALFEX, VEX, YMC(L), CASE                                         B2Y14510
 5550 FORMAT (1H1 25X 26HDOUGLAS  AIRCRAFT  COMPANY / 28X 21HLONG  BEACHB2Y14520
     1  DIVISION /// 5X 15A4// 5X 9HSPACING = F13.8, 5X 7HALPHA = F13.8 B2Y14530
     2, 5X 13HDELTA ALPHA = F13.8 // 14H INLET  ALPHA =  F13.8, 3X      B2Y14540
     3 5HV INLET = F13.8, 13X 5HXMC = F13.8 // 2X 12HEXIT ALPHA = F13.8,B2Y14550
     4 4X 8HV EXIT = F13.8, 13X 5HYMC = F13.8 // 6H CASE 2A4,22H   COMBIB2Y14560
     5NED VELOCITIES )                                                  B2Y14570
      IF (FLG12.LE.0) WRITE (6,5560) L                                  B2Y14580
 5560 FORMAT (10H  BODY NO.I3,27H  UNTRANSFORMED COORDINATES // )       B2Y14590
      IF (FLG12.GT.0) WRITE (6,5570) L                                  B2Y14600
 5570 FORMAT (10H  BODY NO. I3, 25H TRANSFORMED COORDINATES // )        B2Y14610
      WRITE (6,5580)                                                    B2Y14620
 5580 FORMAT (11X 1HX 13X 1HY 13X 2HVC 12X 2HCP 10X 7HDELTA S // )      B2Y14630
 5600 WRITE (6, 5650) I, X(J), Y(J), XMP(K1), YMP(K1), VC(K1), CP(K1)   B2Y14640
     1 ,DELSUT(K1)                                                      B2Y14650
 5650 FORMAT (1H  I3, 2F14.8 / 4X 5F14.8 )                              B2Y14660
      I = I + 1                                                         B2Y14670
      J = J + 1                                                         B2Y14680
```

```
      K1 = K1 + 1                                                       B2Y14690
      IF ( I .EQ. K2 )  GO TO 5700                                      B2Y14700
      IF ( I .LE. LCTR )  GO TO 5600                                    B2Y14710
      LCTR = LCTR + 19                                                  B2Y14720
      GO TO 5500                                                        B2Y14730
 5700 WRITE (6, 5650)  I, X(J), Y(J)                                    B2Y14740
      J = J + 1                                                         B2Y14750
      WRITE (6, 5750)  CL
 5750 FORMAT (1H0 / 5X 4HCY = F13.8)
      M = N + 1                                                         B2Y14780
 5800 N = N + ND(L+1) - 1                                               B2Y14790
C     K = NCFLG-2 = NUMBER OF GAMMAS                                    B2Y14800
      CL=2.*GT*AAA
      IF (FLG10 .LT. 2) GO TO 5830                                      B2Y14820
 5830 WRITE (6, 5840)  CL                                               B2Y14890
 5840 FORMAT (1H0 4X 4HCL = F13.8 )                                     B2Y14900
 5850 IF (FLG02 .EQ. 0 .OR. FLG10 .EQ. 1 .OR. FLG10 .EQ. 2)  GO TO 6700 B2Y14910
      N = ND(NB+1)                                                      B2Y14920
      K2 = K + 2                                                        B2Y14930
      DO 6100 J=1,K2                                                    B2Y14940
      READ(3) (SIGMA(I,J),I=1,NT)                                       B2Y14950
 6100 CONTINUE                                                          B2Y14960
C     NOW ALL SIGMAS ARE IN CORE. ORDER = 0,90,1,2,ETC.                 B2Y14970
      DO 6110 I=1,NT                                                    B2Y14980
 6110 SIGT(I)= SIGMA(I,1)*CSALF + SIGMA(I,2)*SNALF +SIGMA(I,3)
      IF(K.EQ.0) GO TO 6150                                             B2Y15000
      DO 6120 J = 1,1
      READ(4)                                                           B2Y15020
      READ(4)                                                           B2Y15030
      DO 6120 I = 1,NT                                                  B2Y15040
 6120 SIGT(I) = SIGT(I) + SIGMA(I,J+3)*GAM(J)                           B
      M = 1                                                             B2Y15060
      M1 = N                                                            B2Y15070
      DO 6130 J = 1,K                                                   B2Y15080
       IF( J .LE. FLG11 )       GO TO 6122                              B2Y15090
      READ(4) (XTEMP(I),I=M,M1)                                         B2Y15100
      READ(4) (YTEMP(I),I=M,M1)                                         B2Y15110
       GO TO 6125                                                       B2Y15120
 6122  DO 6123 I = M, M1                                                B2Y15130
       XTEMP(I) = 0.0                                                   B2Y15140
 6123  YTEMP(I) = 0.0                                                   B2Y15150
      IF(NLF(1).NE.0) GO TO 6125
      READ (4)
      READ (4)
 6125  M = 1
 6130 M1 = N
 6150 READ(13)(X(I),I=1,N)                                              B2Y15180
      READ(13)(Y(I),I=1,N)                                              B2Y15190
      IF (MON-1) 6152,6155,6155
 6152 CONTINUE
       WRITE ( 6,6151 )  HEDR, SP, ALPHA
 6151 FORMAT(1H1,25X,26HDOUGLAS  AIRCRAFT  COMPANY / 28X,21HLONG  BEACH B2Y15210
     1 DIVISION     ///5X,15A4//5X,9HSPACING = ,F13.8,4X,7HALPHA =,F13.8  B2Y15220
     2///39H  OFF-BODY POINT COMPONENT VELOCITIES.  / 75H  ORDER OF PRINB2Y15230
     4TOUT IS STREAMFLOW,90-DEGREE FLOW,NON-UNIFORM FLOW 1, ETC.   //   B2Y15240
     513X,1HX,20X,1HY,18X,3HVXL,17X,3HVYL,17X,3HVXL,17X,3HVYL //)       B2Y15250
 6155 DO 6400 J = 1,N                                                   B2Y15260
      READ(10) (YIJ(I),I=1,NT)                                          B2Y15270
      READ(10) (XIJ(I),I=1,NT)                                          B2Y15280
      SUM1 =0.                                                          B2Y15290
```

```
      SUM2 =0.                                                          B2Y15300
      DO 6210 I = 1,K2                                                  B2Y15310
       SUMA(J,I) = 0.0                                                  B2Y15320
 6210  SUMB(J,I) = 0.0                                                  B2Y15330
      DO 6200 I = 1,NT                                                  B2Y15340
      T = SIGT(I)                                                       B2Y15350
      SUM1 = SUM1 + T*XIJ(I)                                            B2Y15360
 6200 SUM2 = SUM2 + T*YIJ(I)                                            B2Y15370
      IF(K.EQ.0) GO TO 6300                                             B2Y15380
      N1 = J                                                            B2Y15390
      DO 6250 I = 1,1
      T = GAM(I)                                                        B2Y15410
      SUM1 = SUM1 + T*YTEMP(N1)                                         B2Y15420
      SUM2 = SUM2 + T*XTEMP(N1)                                         B2Y15430
 6250 N1 = N1 +N                                                        B2Y15440
 6300 VXL(J) = SUM1 + CSALF                                             B2Y15450
      VYL(J) = SUM2 + SNALF                                             B2Y15460
      IF(MON-1) 6305,6400,6400
 6305 DO 6370 I = 1,K2                                                  B2Y15470
      DO 6310 LSD = 1,NT                                                B2Y15480
      T = SIGMA(LSD,I)                                                  B2Y15490
       SUMA(J,I) = SUMA(J,I) + T*XIJ(LSD)                               B2Y15500
 6310  SUMB(J,I) = SUMB(J,I) + T*YIJ(LSD)                               B2Y15510
      IF (I.LE.2 ) GO TO 6355                                           B2Y15520
      N1 = J                                                            B2Y15530
      DO 6350 LSD=1,1
      IF(LSD+2.NE.I) GO TO 6350                                         B2Y15550
      SUMA(J,I) = SUMA(J,I) + YTEMP(N1)                                 B2Y15560
      SUMB(J,I) = SUMB(J,I) + XTEMP(N1)                                 B2Y15570
 6350 N1 = N1 + N                                                       B2Y15580
      GO TO 6370                                                        B2Y15590
 6355 IF ( I.EQ.2 ) GO TO 6360                                          B2Y15600
C***   ***I = 1 MEANS AXISYMMETRIC FLOW                                 B2Y15610
      SUMA(J,I) = SUMA(J,I) + 1.0                                       B2Y15620
      GO TO 6370                                                        B2Y15630
C***   ***I = 2 MEANS 90 DEGREE FLOW                                    B2Y15640
 6360 SUMB(J,I) = SUMB(J,I) + 1.0                                       B2Y15650
 6370 CONTINUE                                                          B2Y15660
       WRITE( 6,6371 ) J, X(J), Y(J), (SUMA(J,I),SUMB(J,I), I=1,K2)     B2Y15670
 6371 FORMAT(1H ,I3,6F20.8 / (44X,4F20.8))                              B2Y15680
 6400 THETV(J)=ATAN2(VYL(J),VXL(J))*57.2957795
      WRITE (7) (VXL(I),I=1,N)
      WRITE (7) (VYL(I),I=1,N)
      IF (MON-2) 6420,6430,6430
 6420 CALL BCDUMP (X(1),X(N))
      CALL BCDUMP(Y(1),Y(N))
      CALL BCDUMP (VXL(1),VXL(N))
      CALL BCDUMP (VYL(1),VYL(N))
 6430 LCTR = 45                                                         B2Y15700
      I = 1                                                             B2Y15710
      IF (FLG10 .LT. 2) GO TO 6500                                      B2Y15720
 6500 WRITE (6, 6550)  HEDR, SP, ALPHA                                  B2Y15860
 6550 FORMAT (1H1 25X 26HDOUGLAS  AIRCRAFT  COMPANY / 28X 21HLONG  BEACHB2Y15870
     1  DIVISION ///5X 15A4 // 5X 9HSPACING = F13.8, 4X 7HALPHA = F13.8 B2Y15880
     2 ///28H    OFF-BODY POINT VELOCITIES // 11X 1HX 13X 1HY 12X 3HVXL  B2Y15890
     3 11X 3HVYL    10X  5HTHETA//)
 6600 WRITE (6, 6650)  I, X(I), Y(I), VXL(I), VYL(I)  , THETV(I)
 6650 FORMAT (1H  I3, 5F14.8 )
      I = I + 1                                                         B2Y15930
      IF (I .GT. N)  GO TO 7000                                         B2Y15940
```

```
      IF ( I .LE. LCTR )  GO TO 6600                                    B2Y15950
      LCTR = LCTR + 45                                                  B2Y15960
      GO TO 6500                                                        B2Y15970
 6700 IF (FLG10 .EQ. 0 .OR. FLG10 .EQ. 3)  GO TO 7000                   B2Y15980
      FLG10 = 3 * FLG10 - 3                                             B2Y15990
      IF ( FLG02 .NE. 0 ) WRITE (6, 6750)                               B2Y16000
 6750 FORMAT (32H1FLAG 10 IS NON-ZERO -- OFF-BODY /                     B2Y16010
     1        30H VELOCITIES CANNOT BE COMPUTED )                       B2Y16020
      FLG02 = 0                                                         B2Y16030
      READ (5, 6800) (XTEMP(I), I = 1, NT)                              B2Y16040
 6800 FORMAT (6F10.0)                                                   B2Y16050
      DO 6900 I = 1, NT                                                 B2Y16060
      VC(I) = VC(I)*XTEMP(I)                                            B2Y16070
 6900 CP(I) = 1. - VC(I)*VC(I)                                          B2Y16080
      GO TO 5375                                                        B2Y16090
 7000 DO 7100 I = 1,NB                                                  B2Y16100
 7100 GAMT(I) = GAM(I)                                                  B2Y16110
      RETURN                                                            B2Y16120
      END                                                               B2Y16130
```

```
$ORIGIN        ALPHA
$IBFTC 22YP
      SUBROUTINE PART 7
C
C          THIS SUBROUTINE INTEGRATES FOR THE MASS FLUX AND IS USED TO
C                DETERMINE IF THE JET STREAM IS PROPERLY ORIENTED
C
      COMMON IM,HEDR,CASE,RPI,R2PI,SP,CL,ALPHA,FALPHA,DALFA,CHORD,SUMDS,
     1       XMC,YMC,ADDY,FLG02,FLG03,FLG04,FLG05,FLG06,FLG07,FLG08,
     2       FLG09,FLG10,FLG11,FLG12,ND,NLF,NER,NT,NB,NCFLG,FLG15,FLG16
      COMMON SUMSIG,VINF,MON,BETA,CDIM,VREF,DELT,FLG13,FLG14,ITER,ALF2
      COMMON /FORCUR/XCURV(200),YCURV(200),KKK,POSS
      COMPLEX  IM
      INTEGER FLG15,FLG16,FLG02
      DIMENSION  X(300), Y(300), HEDR(15),CASE(2),ADDY(8),
     2              ND(10), NLF(10), SUMDS(10), XMC(8), YMC(8)
C    1 RSDS(499), SINA(499), COSA(499), DELS(499), DALF(498), Z(499),     7
      DIMENSION  RADC(250),PRES(250),VXL(250),VYL(250),XN(250),YN(250),
     1   CP(250),DPRES(50),V(50),PTOT(50),RADCCL(50),XCL(50),YCL(50)
      DIMENSION VSPEC(4) ,XB(500),YB(500)
      REWIND 13
      REWIND 7
      M=ND(1)
      READ (13)  (XB(I),I=1,M)
      READ (13)(YB(I),I=1,M)
      READ (13)
      READ (13)
      M=NT
      M1=NT-3
      N=ND(2)
      KK=KKK-1
      JJ=ND(1)
      II=ND(1)-KKK+1
      READ (13)  (X(I),I=1,N)
      READ (13)  (Y(I),I=1,N)
```

```
      READ(7) (PRES(I+1),I=1,M)
      READ (7) (CP(I),I=1,M)
      READ (7) (XN(I+1),I=1,M)
      READ (7) (YN(I+1),I=1,M)
      READ (7) (VXL(I),I=1,N)
      READ (7) (VYL(I),I=1,N)
      DO 30  I=1,NT
   30 PRES(I)=CP(I)*0.00119*VINF**2
      TMASS=0.0
      M=1
      N=36
      DO 100 I=M,N
      VXL(I)=(VXL(I)+VXL(I+1))/2.0
      VYL(I)=(VYL(I)+VYL(I+1))/2.0
      DELY=Y(I+1)-Y(I)
      DELX=X(I+1)-X(I)
      DMASS=-VXL(I)*DELY
      DMASSY=DELX*VYL(I)
  100 TMASS= TMASS+DMASS+DMASSY
      VAVG=TMASS/3.61
      TMASS=TMASS*0.00238*VINF*32.2/12.0*4.5
C
C         TMASS IS THE MASS FLOW INTO THE FANS FOUND BY INTEGRATION
C
      WRITE (6,1000) TMASS,VINF,VAVG
 1000 FORMAT (1H1/23H THE INTEGRATED MASS  =,F10.4,7H LB/SEC/23H FREE ST
     1REAM VELOCITY =,F10.4,4H FPS/,23H THE AVERAGE VELOCITY =,F10.4//)
      IF (VINF-300.) 200,200,999
  200 WRITE (6,1006)
 1004 FORMAT (1H ,2F10.4,6F15.8////)
 1006 FORMAT (1H1//8X1HX,9X,1HY,8X,8HPRESSURE)
  645 M=2
      N=KKK
      MM=II+2
  650 DO 700 I=M,N
  700 WRITE (6,1004) XN(I),YN(I),PRES(I-1)
      IF (N-MM) 750,800,800
  750 M=II
      N=JJ
      GO TO 650
  800 TFY=0.0
      TFX=0.0
      IF (FLG16.EQ.1) GO TO 840
      N=1
      M=KK
      GO TO 850
  840 N=1
      M=10
      JJJ=1
  850 DO 900 I=N,M
      T1=XB(I+1)-XB(I)
      T2=YB(I+1)-YB(I)
      TDS=SQRT(T1*T1+T2*T2)
      COSAL=T1/TDS
      SINAL=T2/TDS
      IF (FLG16.EQ.1) GO TO 860
      DFX=PRES(I)  *TDS*SINAL*4.5/12.0
      DFY=-PRES(I)  *TDS*COSAL*4.5/12.0
      GO TO 870
  860 SLOP=-T2/T1
```

```
      AL1=ATAN(SLOP)
      AL2MAL=-ALF2-AL1
      CJJJ= JJJ
      DFY= PRES(I)*TDS*COS(AL2MAL)*CJJJ
      TFY=TFY+DFY
      GO TO 900
  870 TFX=TFX+DFX
      TFY=TFY+DFY
  900 CONTINUE
      IF (N-II) 950,975,975
  950 IF (FLG16.EQ.1) GO TO 960
      N=II
      M=JJ-1
      GO TO 850
  960 N=ND(1)-10
      M=ND(1)-1
      JJJ=-1
      GO TO 850
  975 WRITE(6,1008) TFX,TFY
 1008 FORMAT ( 1H ,//,48H THE TOTAL FORCE ON THE JET IN THE X-DIRECTION
     1=,F10.4/48H THE TOTAL FORCE ON THE JET IN THE Y-DIRECTION =,F10.4)
      IF (FLG16.EQ.0) GO TO 980
      FLG16=0
       GO TO 800
  980 BETA=BETA*3.14159/180.
      THRUST =TFY/(SIN(BETA)*POSS)
      CMU=THRUST*12./(0.00119*4.5*CDIM*VINF**2)
      WRITE (6,1010) THRUST,CMU
 1010 FORMAT (1H ,//,9H THRUST =,F10.4,3H LB//23H CMU FOR THE JET FLAP =
     1,F10.4)
      TPA=THRUST*12.0/(4.5*DELT)
      PRATIO=((TPA-40.)*0.2/760.+1.0)*2116./(2116.+.00119*VINF**2)
      WRITE (6,1020) PRATIO
 1020 FORMAT(1H ,9H PRATIO =,F10.4)
  999 RETURN
      END
```

APPENDIX E

SYMBOLS FOR BOUNDARY LAYER ANALYSIS

APPENDIX E

SYMBOLS FOR BOUNDARY LAYER ANALYSIS

$b_1 \cdots b_5$	coefficients in linearized momentum equation (43)
c	airfoil chord
$c_1 \cdots c_4$	coefficients in equation (41)
C_f	coefficient of skin friction, $\tau_w \Big/ \left(\frac{1}{2} \rho U^2\right)$
C_L	three-dimensional lift coefficient
f'	velocity defect variable, $(U - \overline{u})/U$
H	shape factor, δ^*/θ
K	curvature
L	distance along airfoil surface from stagnation point to trailing edge
p	static pressure
P	parameter in equation (31)
Q	parameter in equation (31)
Re_x	Reynolds number based on x, xU/ν
Re_{δ^*}	Reynolds number based on δ^*, $\delta^* U/\nu$
Re_θ	Reynolds number based on θ, $\theta U/\nu$
t	thickness of airfoil
T	non-dimensional effective viscosity (see eq. (38))
$\overline{u}, \overline{v}$	time average velocities in the x and y directions, respectively

U	velocity at the outer edge of the boundary layer (potential flow velocity)
$\overline{u'v'}$	Reynolds stress
$\overline{v}_w$	wall transpiration velocity
x	streamwise coordinate (see Fig. (16))
y	coordinate normal to wall (see Fig. (16))
α	angle of attack
β	the Clauser equilibrium pressure gradient, $\delta^*(dp/dx)/\tau_w$
δ	boundary layer thickness
δ^*	displacement thickness, $\int_0^\infty (U - \overline{u})/U \, dy$
η	non-dimensional coordinate normal to wall, y/δ^*
θ	momentum thickness, $\int_0^\infty \overline{u}(U - \overline{u})/U^2 \, dy$
κ	von Karman constant in the effective viscosity function (taken here to be 0.41)
ν	molecular kinematic viscosity
ν_e	effective kinematic viscosity
ρ	density
$\overline{\tau}$	local shear stress
τ_b'	non-dimensional shear stress gradient (see eq. (42))
ϕ,Φ	wall and defect effective kinematic viscosity functions
χ,X	wall and defect layer variables for the effective kinematic viscosity function

Subscripts:

i	index of variable in the x direction
w	evaluated at wall
x	differentiation with respect to x
∞	evaluated at edge of the boundary layer

Superscripts:

$\overline{(\ )}$	used with functions of x only, denotes average value, $[(\ )_{i+1} + (\ )_i]/2$
$(\ )'$	differentiation with respect to η

APPENDIX F

DERIVATION OF THE TRANSFORMED BOUNDARY LAYER EQUATION OF MOTION

APPENDIX F

DERIVATION OF THE TRANSFORMED BOUNDARY LAYER EQUATION OF MOTION

The transformed boundary layer equation of motion is obtained by making a coordinate transformation to the standard continuity and momentum equations for two-dimensional, incompressible flow. The momentum equation as given by equation (25) of the text is:

$$\bar{u}\,\frac{\partial \bar{u}}{\partial x} + \bar{v}\,\frac{\partial \bar{u}}{\partial y} = U\,\frac{dU}{dx} + \frac{\partial}{\partial y}\left(\nu_e\,\frac{\partial \bar{u}}{\partial y}\right) \tag{F1}$$

or

$$\frac{\bar{u}}{U}\,\frac{\partial \bar{u}}{\partial x} + \frac{\bar{v}}{U}\,\frac{\partial \bar{u}}{\partial y} = \frac{dU}{dx} + \frac{\partial}{\partial y}\left(\frac{\nu_e}{U}\,\frac{\partial \bar{u}}{\partial y}\right) \tag{F2}$$

Transform variables from (x,y) to (ξ,η) where $\xi = x$ and $\eta = y/\delta^*$, and utilizing Mellor's transformation,

$$\frac{\bar{u}}{U} = 1 - f' \quad \text{or} \quad \bar{u} = (1 - f')U \tag{F3}$$

where $f' = \partial f/\partial \eta$. Then

$$\frac{\partial \bar{u}}{\partial x} = (1 - f')\,\frac{dU}{dx} - U\,\frac{\partial f'}{\partial x} \tag{F4}$$

Here

$$f' = f'(\xi,\eta) \tag{F5}$$

Then

$$\left(\frac{\partial f'}{\partial x}\right)_y = \frac{\partial f'}{\partial \xi}\frac{\partial \xi}{\partial x} + \frac{\partial f'}{\partial \eta}\frac{\partial \eta}{\partial x} \tag{F6}$$

The following conventional notation will be used:

$$\frac{\partial f'}{\partial \eta} = f'' \tag{F7}$$

It follows that

$$\frac{\partial \eta}{\partial x} = \frac{\partial}{\partial x}\left(\frac{y}{\delta^*}\right) = \frac{\delta^* \frac{\partial y}{\partial x} - y \frac{\partial \delta^*}{\partial x}}{(\delta^*)^2} = - \frac{\eta \frac{d\delta^*}{dx}}{\delta^*} \tag{F8}$$

Hence, using equation (F7) and (F8), equation (F6) becomes

$$\left(\frac{\partial f'}{\partial x}\right)_y = \frac{\partial f'}{\partial \xi} - \frac{f'' \eta \frac{d\delta^*}{dx}}{\delta^*} \tag{F9}$$

Substituting equation (F9) into (F4) yields

$$\frac{\partial \overline{u}}{\partial x} = (1 - f')\frac{dU}{dx} - U\frac{\partial f'}{\partial \xi} + \frac{U f'' \eta \, d\delta^*/dx}{\delta^*} \tag{F10}$$

Also

$$\frac{\partial \overline{u}}{\partial y} = U \frac{\partial}{\partial y}(1 - f') = - U \frac{\partial f'}{\partial y}$$

$$= - U \frac{\partial f'}{\partial \eta}\frac{\partial \eta}{\partial y} = - Uf'' \frac{\partial}{\partial y}\left(\frac{y}{\delta^*}\right) \tag{F11}$$

or

$$\frac{\partial \overline{u}}{\partial y} = - \frac{Uf''}{\delta^*} \tag{F12}$$

The continuity equation

$$\frac{\partial \bar{u}}{\partial x} + \frac{\partial \bar{v}}{\partial y} = 0. \qquad \text{(F13)}$$

is used to obtain $\bar{v}$, and $\partial\bar{v}/\partial x$ which are inserted into the momentum equation. Integrating each term of the continuity equation yields:

$$\int_0^y \frac{\partial \bar{v}}{\partial y'} dy' = \int_{\bar{v}(x,0)}^{\bar{v}(x,y)} d\bar{v}' = \bar{v} - \bar{v}_w = -\int_0^y \frac{\partial \bar{u}}{\partial x} dy' \qquad \text{(F14)}$$

Let

$$y' = \eta^+ \delta^* \qquad \text{(F15a)}$$

and

$$dy' = \delta^* d\eta^+ \qquad \text{(F15b)}$$

where $'$ and $+$ denote dummy variables for integration purposes, and substitute equation (F10) into equation (F14) to obtain

$$\bar{v} = \bar{v}_w - \frac{dU}{dx}\delta^* \int_0^\eta (1-f')d\eta^+ + U\delta^* \int_0^\eta \frac{\partial f'}{\partial \xi} d\eta^+ - U\frac{d\delta^*}{dx}\int_0^\eta f''\eta^+ d\eta^+ \qquad \text{(F16)}$$

or

$$\frac{\bar{v}}{U} = \frac{\bar{v}_w}{U} - \frac{\delta^* \frac{dU}{dx}}{U} \int_0^\eta (1-f')d\eta^+ + \delta^* \int_0^\eta \frac{\partial f'}{\partial \xi} d\eta^+ - \frac{d\delta^*}{dx}\int_0^\eta f''\eta^+ d\eta^+ \qquad \text{(F17)}$$

Introduce

$$P = \frac{\delta^* \frac{dU}{dx}}{U}, \quad Q = \frac{\frac{d}{dx}(\delta^* U)}{U} = \frac{\delta^* \frac{dU}{dx}}{U} + \frac{d\delta^*}{dx} \qquad \text{(F18)}$$

so that

$$\frac{d\delta^*}{dx} = Q - P \tag{F19}$$

Using the above expressions in equation (F17) yields

$$\frac{\bar{v}}{U} = \frac{\bar{v}_w}{U} - P \int_0^{\eta} (1 - f')d\eta^+ + \delta^* \int_0^{\eta} \frac{\partial f'}{\partial \xi}\, d\eta^+$$

$$- (Q - P) \int_0^{\eta} f''\eta^+ d\eta^+ \tag{F20}$$

Then, it follows that

$$\int_0^{\eta} d\eta^+ = \eta \tag{F20a}$$

$$\int_0^{\eta} f'd\eta^+ = \int_0^{\eta} \frac{\partial f}{\partial \eta^+}\, d\eta^+ = \int_0^{\eta} df^+ = f \tag{F20b}$$

$$\int_0^{\eta} \frac{\partial f'}{\partial \xi}\, d\eta^+ = \frac{\partial}{\partial \xi} \int_0^{\eta} f'd\eta^+ = \frac{\partial f}{\partial \xi} \tag{F20c}$$

$$\int_0^{\eta} \eta^+ f''d\eta^+ = \int_0^{\eta} \eta^+ \frac{\partial f'}{\partial \eta^+}\, d\eta^+ = \eta f' - \int_0^{\eta} f'd\eta^+ = \eta f' - f \tag{F20d}$$

Hence, equation (F20) becomes

$$\frac{\bar{v}}{U} = \frac{\bar{v}_w}{U} - P(\eta - f) + \delta^* \frac{\partial f}{\partial \xi} - (Q - P)(\eta f' - f) \quad . \tag{F21}$$

or

$$\frac{\overline{v}}{U} = \frac{\overline{v}_w}{U} - Q(\eta - f) + \delta^* \frac{\partial f}{\partial \xi} + (Q - P)(1 - f')\eta \tag{F22}$$

Substituting equations (F3), (F10), (F12), and (F22) into the momentum equation (F2) gives:

$$(1 - f')^2 \frac{dU}{dx} - (1 - f')U \frac{\partial f'}{\partial \xi} + \frac{(1 - f')f''\eta \frac{d\delta}{dx} U}{\delta^*} - \frac{\overline{v}_w}{U} \frac{Uf''}{\delta^*}$$

$$+ Q(\eta - f) \frac{Uf''}{\delta^*} - \frac{(Q - P)(1 - f')\eta Uf''}{\delta^*} - \frac{\delta^* \frac{\partial f}{\partial \xi} Uf''}{\delta^*}$$

$$= \frac{dU}{dx} + \frac{1}{\delta^*} (- TUf'')' \tag{F23}$$

where

$$T = \nu_e/U\delta^*$$

Using

$$(1 - f')^2 \frac{\frac{dU}{dx} \delta^*}{U} - \frac{\frac{dU}{dx} \delta^*}{U} = P(1 - 2f' + f'^2 - 1) = P(f' - 2)f' \tag{F24}$$

and

$$(1 - f') \frac{f''\eta U \frac{d\delta^*}{dx}}{U} = (Q - P)(1 - f')f''\eta \tag{F25}$$

The transformed boundary layer equation of motion becomes

$$(Tf'')' + [Q(\eta - f) - \overline{v}_w/U]f'' + P(f' - 2)f'$$

$$= \delta^*(1 - f') \frac{\partial f'}{\partial x} + \delta^* f'' \frac{\partial f}{\partial x} \tag{F26}$$

where

$$Q = \frac{\frac{d}{dx}(\delta^* U)}{U}, \quad P = \frac{\delta^* dU/dx}{U}, \quad T = \frac{\nu_e}{U\delta^*}$$

and x has been substituted for ξ. The independent variables are then x and η.

REFERENCES

REFERENCES

1. Koenig, David G.; Corsiglia, Victor R.; and Morelli, Joseph P.: Aerodynamic Characteristics of a Large-Scale Model with an Unswept Wing and Augmented Jet Flap. NASA TN D-4610, 1968.

2. Campbell, John P.; and Johnson, Joseph L., Jr.: Wind Tunnel Investigation of an External-Flow Jet Augmented Slotted Flap Suitable for Application to Airplanes with Pod-Mounted Jet Engines. NACA TN 3898. 1956.

3. Parlett, Lysle P.; and Freeman, Delma C., Jr.; and Smith, Charles C., Jr.: Wind Tunnel Investigation of a Jet Transport Airplane Configuration with High Thrust-Weight Ratio and an External-Flow Jet Flap. NASA TN D-6058, 1970.

4. Gartshore, I. S.: Prediction of the Blowing Required to Suppress Separation from High-Lift Aerofoils. Paper no. 70-872, AIAA, July 1970.

5. Thwaites, Bryan, ed.: Incompressible Aerodynamics. Clarendon Press, Oxford, 1960.

6. Weber, J.: The Calculation of the Pressure Distribution over the Surface of Two-Dimensional and Swept Wings with Symmetrical Aerofoil Sections. Rep. R & M 2918, Aeronautical Research Council, Gt. Britain, 1956.

7. Goldstein, S.: Approximate Two-Dimensional Airfoil Theory. Parts I-VI. Aeronautical Research Council, Gt. Britain, Reps. CP-68 to CP-73, 1952.

8. Anon: A Direct Iteration Method for the Calculation of the Velocity Distribution of Bodies of Revolution and Symmetrical Profiles. Rep. ARL/RI/G/HY/12/2, Admiralty Research Laboratory, Gt. Britain, August 1951.

9. Jacob, K.: Some Programs for Incompressible Aerodynamic Flow Calculations. Tech. Rep. 122, Calif. Inst. Technology Computing Center, 1960.

10. Davenport, F. J.: Singularity Solutions to General Potential-Flow Airfoil Problems. Rep. D6-7202, Rev., Boeing Co., 1963.

11. Spence, D. A.: The Lift Coefficient of a Thin, Jet-Flapped Wing. Proc. Roy Soc. (London), Ser. A, vol. 238, December 4, 1956, pp. 46-68.

12. Spence, D. A.: The Lift on a Thin Aerofoil with a Jet-Augmented Flap. Aeron. Quart., vol. 9, August 1958, pp. 287-299.

13. Smith, A. M. O.; and Pierce, J.: Exact Solution of the Neumann Problem. Calculation of Noncirculatory Plane and Axially Symmetric Flows about or Within Arbitrary Boundaries. Rep. ES-26988-V, Douglas Aircraft, Apr. 25, 1968.

14. Giesing, Joseph P.: Extension of the Doublas Neumann Program to Problems of Lifting Infinite Cascades. Rep. LB-31653, Douglas Aircraft Co., July 2, 1964. (Available from DDC as AD-605207.)

15. Giesing, Joseph P.: Potential Flow About Two-Dimensional Airfoils. Part I: A Summary of Two-Dimensional Airfoil Methods. Part II: Solution of the Flow Field About One or More Airfoils of Arbitrary Share in Uniform or Non-uniform Flows by the Douglas Neumann Method. Rep. LB-31946, Douglas Aircraft Co., Dec. 1, 1965.

16. Cohen, Clarence B.; and Reshotko, Eli: The Compressible Laminar Boundary Layer with Heat Transfer and Arbitrary Pressure Gradient. NACA TR 1294, 1956.

17. Sasman, Philip K.; and Cresci, Robert J.: Compressible Turbulent Boundary Layer with Pressure Gradient and Heat Transfer. AIAA J., vol. 4, no. 1, Jan. 1966, pp. 19-25.

18. McNally, William D.: Fortran Program for Calculating Compressible Laminar and Turbulent Boundary Layers in Arbitrary Pressure Gradients. NASA TN D-5681, May 1970.

19. Bennett, J. A.; and Goradia, S. H.: Methods for Analysis of Two-Dimensional Airfoils with Subsonic and Transonic Applications. Rep. ER-8591, Lockheed-Georgia Co., July 1966.

20. Crank, J.; and Nicolson, P.: A Practical Method for Numerical Evaluation of Solutions of Partial Differential Equations of the Heat-Conduction Type. Proc. Cambridge Phil. Soc., vol. 43, 1947, pp. 50-67.

21. Flügge-Lotz, I.: The Computation of the Laminar Compressible Boundary Layer. Dept. Mech. Eng., Stanford Univ., Rep. R-352-30-7, 1954, or Office of Scientific Research, Tech. Note 54-144, 1954.

22. Bradshaw, P.; Ferriss, D. H.; and Atwell, N. P.: Calculation of Boundary Layer Development Using the Turbulent Energy Equation. J. Fluid Mech., Vol. 28, pt. 3, 1967, pp. 953-616.

23. Patankar, S. V.; Spalding, D. B.; and Ng, K. H.: The Hydrodynamic Turbulent Boundary Layer on a Smooth Wall, Calculated by a Finite Difference Method. Proc. Conf. on Computation of Turbulent Boundary Layer Prediction, Stanford University, 1968, pp. 356-365.

24. Cebeci, T.; and Smith, A. M. O.: A Finite-Difference Solution of the Incompressible Turbulent Boundary Layer Equations by an Eddy-Viscosity Concept. Proc. Conf. on Computation of Turbulent Boundary Layer Prediction, Stanford University, 1968, pp. 346-355.

25. Smith, A. M. O.; and Cebeci, T.: Numerical Solution of the Turbulent Boundary Layer Equations. Rep. DAG 33725, Douglas Aircraft Co., 1967.

26. Herring, H. J.; and Mellor, G. L.: Computer Program to Calculate Incompressible Laminar and Turbulent Boundary Layer Development. NASA CR-1564, 1970.

27. Patankar, S. V.; and Spalding, D. B.: Heat and Mass Transfer in Boundary Layers. C. R. C. Press, 1968.

28. Mellor, G. L.; and Gibson, D. M.: Equilibrium Turbulent Boundary Layers. J. Fluid Mec., v. 24, pt. 1, 1966, pp. 225-253.

29. Mellor, G. L.: The Effects of Pressure Gradients on Turbulent Flow Near a Smooth Wall. J. Fluid Mech., v. 24, pt. 2, 1966, pp. 254-274.

30. Mellor, G. L.; and Herring, H. J.: Two Methods of Calculating Turbulent Boundary Layer Behavior Based on Numerical Solutions of the Equations of Motion. Proc. Conf. on Computation of Turbulent Boundary Layer Prediction, Stanford University, 1968, pp. 331-345.

31. Kellogg, Oliver D.: Foundations of Potential Theory. Dover Publi., Inc., 1953.

32. Purcell, E. W.: The Vector Method of Solving Simultaneous Linear Equations. Math. Phys., vol. 32, 1953, pp. 180-183.

33. Stockman, Norbert O.: Potential Flow Solutions for Inlets of VTOL Lift Fans and Engines. Analytic Methods in Aircraft Aerodynamics, NASA SP-228, 1970, pp. 659-681.

34. Emslie, K.: Wind Tunnel Test on Models of V. T. O. Aircraft. Aircraft Eng., vol. 38, no. 6, June 1966, pp. 8-13.

35. Williams, J.; Butler, F. J.; and Wood, M. N.: The Aerodynamics of Jet Flaps. Rep. R & M 3304, Aeronautical Research Council, Gt. Britain, 1963.

36. Goldstein, S.: Modern Developments in Fluids Dynamics, vol. 1, Dover Pub., 1965, p. 119.

37. Massey, B. S.; and Clayton, B. R.: Some Properties of Laminar Boundary Layers on Curved Surfaces. Journal of Basic Engineering, June 1968, pp. 301-312.

38. Schlichting, H.: Boundary Layer Theory. McGraw Hill Book Co., 1968.

39. Hartree, D. R.; and Womersley, J. R.: A Method for the Numerical or Mechanical Solution of Certain Types of Partial Differential Equations. Proc. Roy. So. (London), Series A, vol. 161, no. 906, Aug. 1937, p. 353-366.

40. Clauser, F. H.: The Turbulent Boundary Layer. Advances in Applied Mechanics, vol. IV, Academic Press, Inc., 1956, pp. 2-51.

41. Mellor, G. L.: Turbulent Boundary Layers with Arbitrary Pressure Gradients on Convergent Cross Flows. AIAA Journal, 1967, pp. 1570-1578.

42. Laufer, J.: The Structure of Turbulence in Fully Developed Pipe Flow. NACA TR 1174, 1954.

43. Van Dyke, M.: Perturbation Methods in Fluid Mechanics. Academic Press, New York, 1964.

44. Hildebrand, F. B.: Advanced Calculus for Engineers. Prentice-Hall, 1958.

45. McCracken, D. D.; and Dorn, W. S.: Numerical Methods and Fortran Programming. John Wiley and Sons, Inc., 1965.

46. Crabtree, L. F.: Prediction of Transition in the Boundary Layer on an Aerofoil. Royal Aircraft Establishment, London, Technical Note Aero. 2491, Jan. 1957.

47. Michel, R.: Determination of Transition Point and Calculation of Drag of Airfoils in Incompressible Flow. Publication no. 58, O. N. E. R. A. (France), 1952.

48. Granville, Paul S.: The Calculation of Viscous Drag of Bodies of Revolution Navy Department. Rep. no. 849, David Taylor Model Basin, 1953.

49. Hancock, G. J.: Problems of Aircraft Behavior at High Angles of Attack. AGARD 136, April 1969.

50. Chappell, P. D.: Flow Separation and Stall Characteristics of Plane, Constant-Section Wings in Subcritical Flow. The Aeronautical Journal of the Royal Aeronautical Society. Vol. 72, Jan. 1968, pp. 82-90.

ILLUSTRATIONS

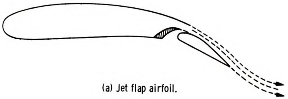

(a) Jet flap airfoil.

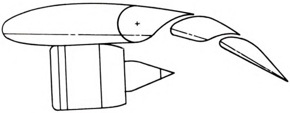

(b-1) 30^{0} flap deflection.

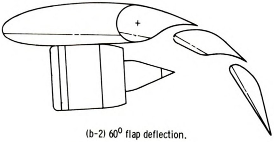

(b-2) 60^{0} flap deflection.

(b) Externally blown flap wing section.

Figure 1. - Types of wing flap systems considered.

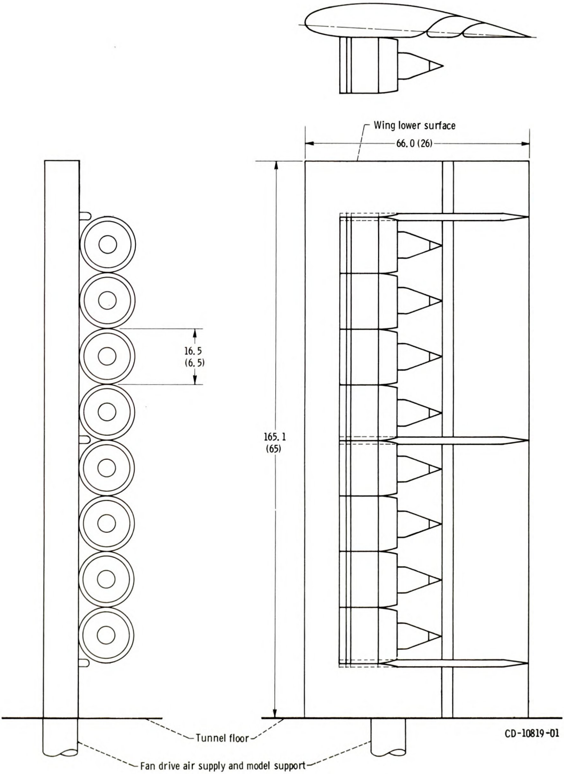

(a) Schematic of model. (Dimensions are in cm (in.).)

Figure 2. - Lewis wind tunnel model of multiple-fan, blown flap, wing propulsion system.

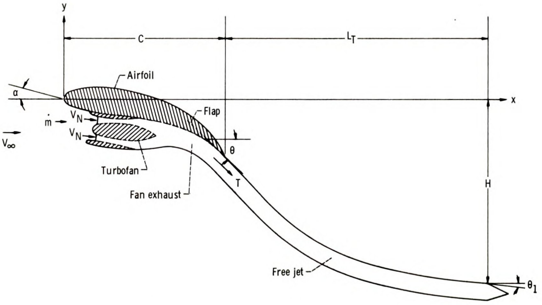

(b) Two-dimensional representation of wing propulsion system.

Figure 2. - Concluded.

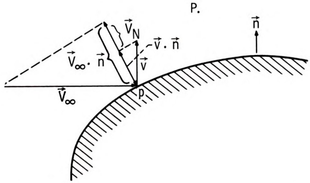

Figure 3. - Representation of boundary condition on body surface.

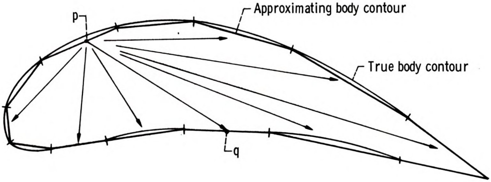

Figure 4. - Finite-element approximation to body surface.

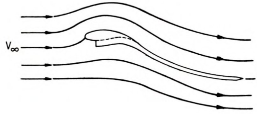

(a) 0° uniform flow solution, V_0.

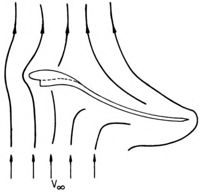

(b) 90° uniform flow solution, V_{90}.

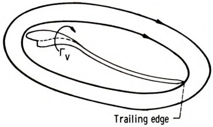

(c) Vortex solution, V_V. ($V_\infty = 0.$)

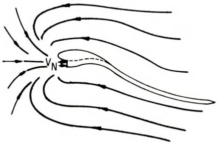

(d) Suction solution, V_S. ($V_\infty = 0.$)

Figure 5. - Basic solutions of potential flow.

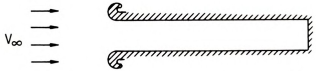

(a) 0^{0} solution with duct closed, $\vec{V}_1$.

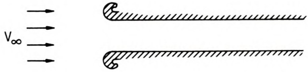

(b) 0^{0} solution with duct open, $\vec{V}_2$.

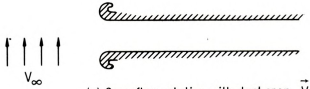

(c) Crossflow solution with duct open, $\vec{V}_3$.

Figure 6. - Basic solutions for inlet.

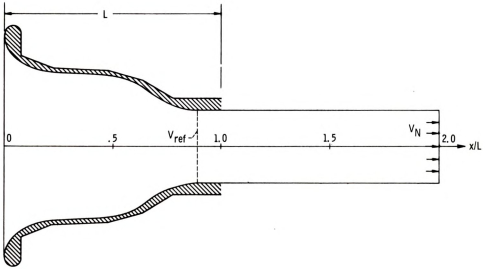

Figure 7. - Two-dimensional inlet configuration.

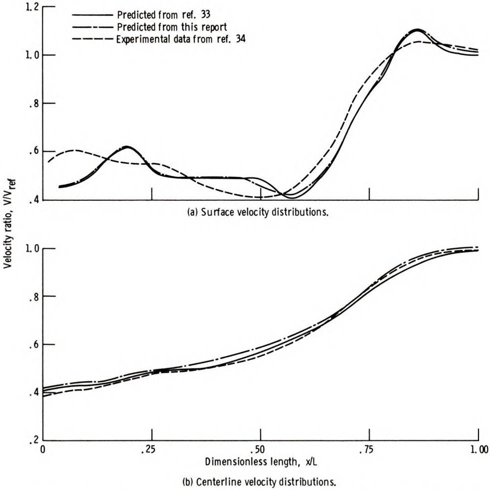

Figure 8. - Comparison of theoretical velocity distributions with experimental data for two-dimensional inlet.

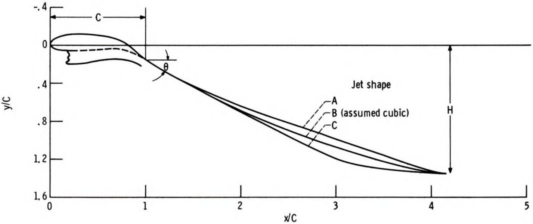

(a) Illustration of jet shapes.

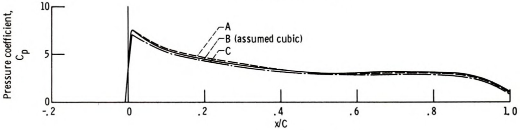

(b) Upper-surface pressure distributions.

Figure 9. - Effect of jet shapes on upper-surface pressure distribution. Flap angle, 30°; wing angle of attack, 0°.

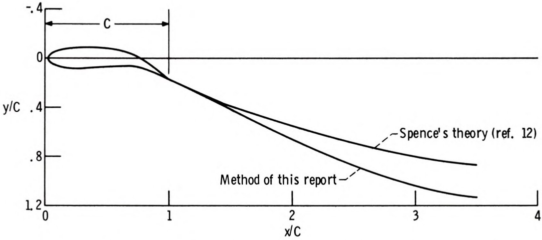

Figure 10. - Comparison of theoretical nondimensional jet shapes. Flap angle, 30°; thrust coefficient, 3.

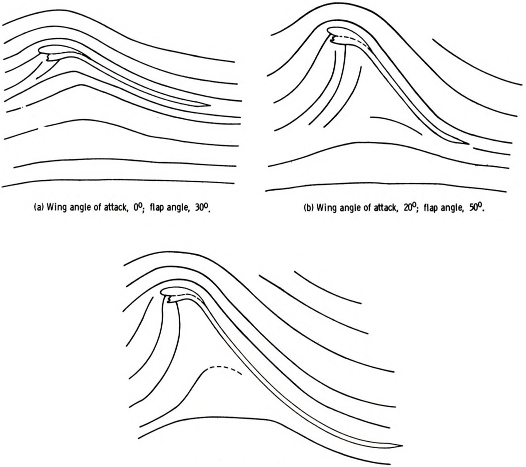

(a) Wing angle of attack, 0°; flap angle, 30°.

(b) Wing angle of attack, 20°; flap angle, 50°.

(c) Wing angle of attack, 0°; flap angle, 60°.

Figure 11. - Flow field for externally blown flap, wing propulsion system. Mass flow coefficient, 0.38; thrust coefficient, 3.

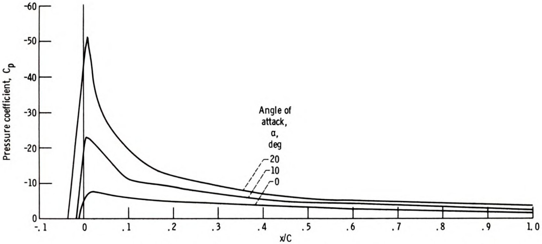

Figure 12. - Calculated pressure distributions on upper surface for fan-wing combination for various angles of attack. Flap angle, 30°; mass flow coefficient, 0.38; thrust coefficient, 3.

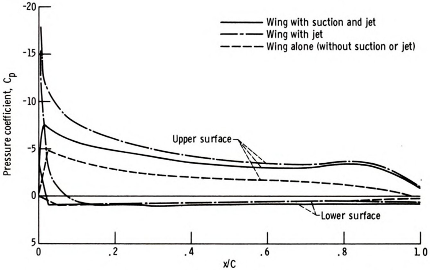

Figure 13. - Effect of suction and jet on pressure distribution. Flap angle, 30°; angle of attack, 0°.

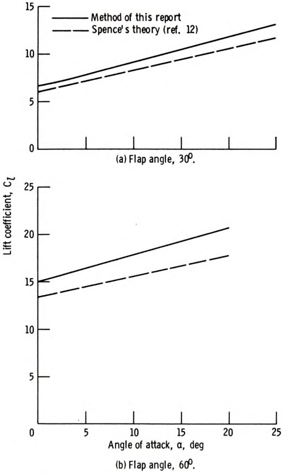

Figure 14. - Comparison of theoretical two-dimensional lift coefficients for blown flap. Thrust coefficient, 3.

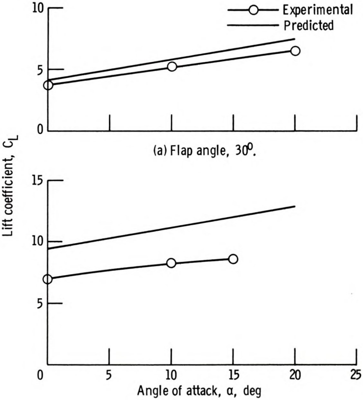

(a) Flap angle, 30°.

(b) Flap angle, 60°.

Figure 15. - Comparison of calculated and experimental three-dimensional lift coefficients for blown flap. Thrust coefficient, 3.

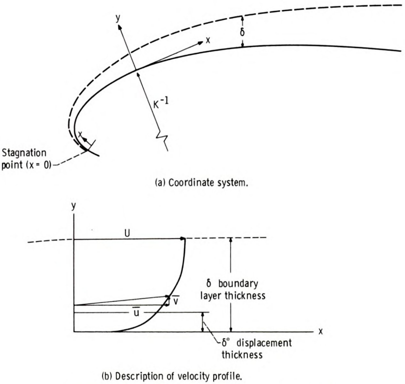

Figure 16. - Illustration of notation for boundary layer analysis.

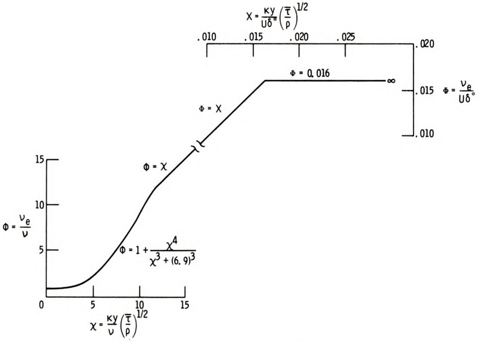

Figure 17. - The turbulent effective viscosity hypothesis.

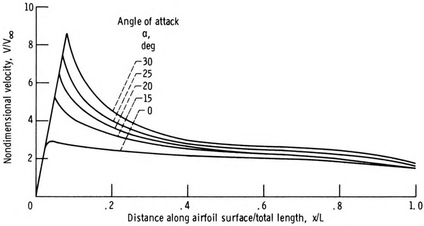

Figure 18. - Calculated velocity distributions for fan-wing combination for various angles of attack. Flap angle, 30^0; mass flow coefficient, 0.38; thrust coefficient, 3.

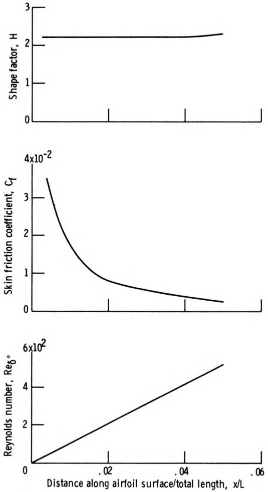

Figure 19. - Laminar boundary layer parameters on the airfoil of a blown flap wing propulsion system. Wing angle of attack, 15°.

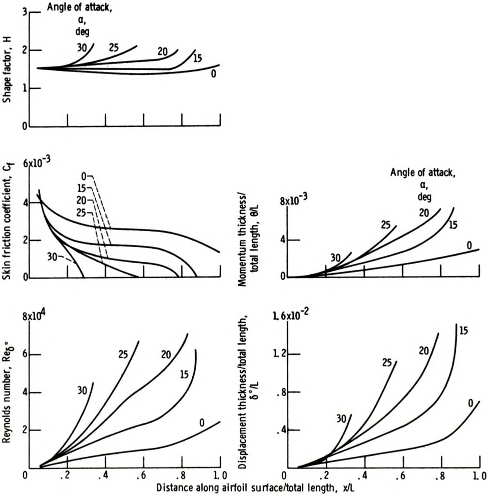

Figure 20. - Turbulent boundary layer parameters on the airfoil of a blown flap wing propulsion system at various angles of attack.

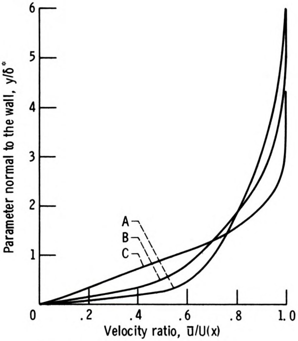

Figure 21. - Velocity profiles at start of turbulent boundary layer growth.

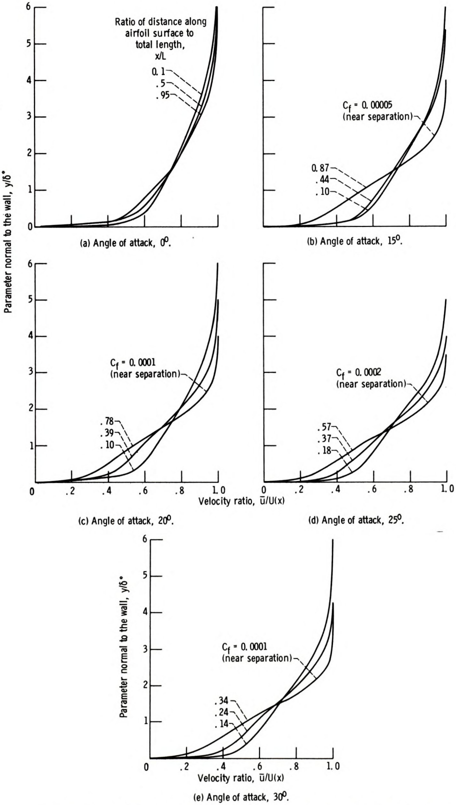

Figure 22. - Turbulent boundary layer velocity profiles on the airfoil of a blown flap wing propulsion system at various angles of attack.

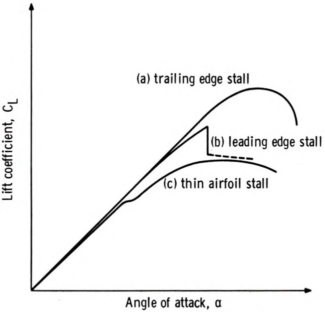

Figure 23. - The stalling characteristics of airfoils.

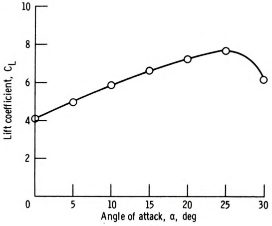

(a) Experimental lift curve.

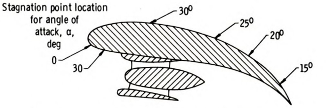

(b) Location of separation point for various angles of attack.

Figure 24. - The stalling characteristics of a blown flap wing propulsion system.

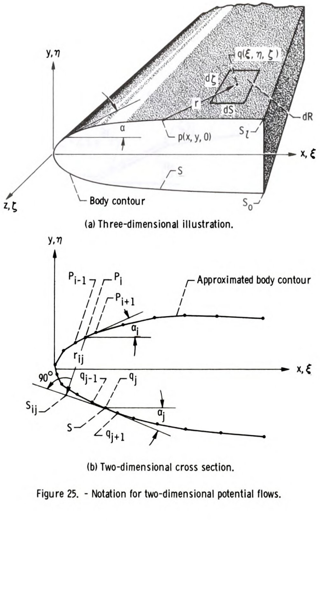

(a) Three-dimensional illustration.

(b) Two-dimensional cross section.

Figure 25. - Notation for two-dimensional potential flows.

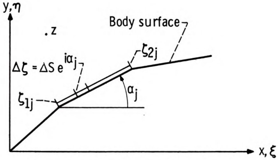

Figure 26. - Element of body surface.

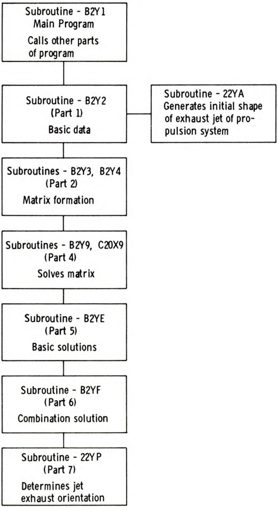

Figure 27. - Schematic representation of computer program.